UNIVERSITY OF SALERNO

Department of Pharmacy

INTERNATIONAL RESEARCH DOCTORATE PROGRAM IN MOLECULAR PHYSIOPATHOLOGY, DIAGNOSIS AND THERAPY OF METABOLIC DISEASES

Coordinator: Prof. Maurizio Bifulco

XII cycle NS

2010–2013

NOVEL INSIGHTS INTO THE BIOLOGICAL EFFECTS OF THE ISOPRENOID DERIVATIVE N6-ISOPENTENYLADENOSINE: INVOLVEMENT OF THE METABOLIC SENSOR AMPK IN ANGIOGENESIS INHIBITION

Tutor

Prof. Patrizia Gazzerro

PhD Student

Paola Picardi

This dissertation is based upon the following articles:

Picardi P, Pisanti S, Ciaglia E, Margarucci L, Ronca R, Giacomini A, Malfitano AM, Casapullo A, Laezza C, Gazzerro P, Bifulco M. Antiangiogenic effects of N6-isopentenyladenosine, an endogenous isoprenoid end product, mediated by AMPK activation. *FASEB J*. **2013**. [Epub ahead of print] PubMed PMID: 24265487.

Ciaglia E, Pisanti S, **Picardi P**, Laezza C, Malfitano AM, D'Alessandro A, Gazzerro P, Vitale M, Carbone E, Bifulco M. N6-isopentenyladenosine, an endogenous isoprenoid end product, directly affects cytotoxic and regulatory functions of human NK cells through FDPS modulation. *J Leukoc Biol*. **2013**. 94:1207-19

Καὶ μικροὶ καιροὶ μεγάλων πραγμάτων αἴτιοι γίγνονται

Δημοσθένης, Περὶ συντάξεως

TABLE OF CONTENTS

LIST OF PUBLICATIONS

1) **Picardi P**, Pisanti S, Ciaglia E, Margarucci L, Ronca R, Giacomini A, Malfitano AM, Casapullo A, Laezza C, Gazzerro P, Bifulco M. Antiangiogenic effects of N6-isopentenyladenosine, an endogenous isoprenoid end product, mediated by AMPK activation. *FASEB J.* **2013**. [Epub ahead of print] PubMed PMID: 24265487.

2) Ciaglia E, Pisanti S, **Picardi P**, Laezza C, Malfitano AM, D'Alessandro A, Gazzerro P, Vitale M, Carbone E, Bifulco M. N6-isopentenyladenosine, an endogenous isoprenoid end product, directly affects cytotoxic and regulatory functions of human NK cells through FDPS modulation. *J Leukoc Biol.* **2013**; 94:1207-19.

3) Pisanti S, **Picardi P**, D'Alessandro A, Laezza C, Bifulco M. The endocannabinoid signaling system in cancer. *Trends Pharmacol Sci.* **2013**; 34(5):273-82.

4) Pisanti S, **Picardi P,** Prota L, Proto MC, Laezza C, McGuire PG, Morbidelli L, Gazzerro P, Ziche M, Das A, Bifulco M. Genetic and pharmacological inactivation of cannabinoid CB1 receptor inhibits angiogenesis. *Blood.* **2011**; 117(20):5541-50.

LIST OF ABBREVIATIONS

5-Itu = 5-iodotubercidin

ADK = adenosine kinase

AICAR = 5-aminoimidazole-4-carboxamide riboside

AMP = adenosine monophosphate

AMPK = AMP-activated protein kinase

AO = acridin orange

APC = antigen presenting cell

Atg = autophagy-related gene

ATP = adenosine triphosphate

CCL = chemokine (C-C motif) ligand

CFSE = carboxyfluorescein diacetate succinimidyl ester

CTL = cytotoxic T lymphocyte

DC = dendritic cell

DMAPP = dimethylallyl pyrophosphate

EHNA = erythro-9 (2-hydroxy-3-nonyl)-adenine

eNOS = endothelial nitric oxide synthase

FDPS = farnesyl diphosphate synthase

Hif = hypoxia-inducible factor

HLA = human leukocyte antigen

HO-1 = heme oxygenase 1

HUVEC = human umbilical vein endothelial cell

IFN-γ = interferon-γ

IL-2 = interleukin-2

iPA = N6-isopentenyladenosine

iPAMP = N6-isopentenyladenosine 5'-monophosphate

IPP = isopentenyl pyrophosphate

IPT = isopentenyl transferase

LC3 = microtubule-associated protein light chain 3

LC-MS/MS = liquid chromatography–coupled tandem mass spectrometry

LKB1 = liver kinase B1

MAPK = mitogen-activated protein kinases

MMP = matrix metalloproteinase

MFI = mean fluorescence intensity

mTOR = mammalian target of rapamycin

NK = natural killer

PARP = poly(ADP-ribose) polymerase

pATM = phospho-ataxia telangiectasia mutated

pATR = phospho-ATM and Rad3-related

PBMC = peripheral blood mononucleated cell

pChk1 = phospho-checkpoint kinase 1

PI = propidium iodide

SRM = selected-reaction monitoring

TNF-α = tumor necrosis factor-α

VEGF = vascular endothelial growth factor

ZMP = 5-amino-4-imidazolecarboxamide ribotide

ABSTRACT

N6-isopentenyladenosine (iPA) is a modified adenosine characterized by an isopentenyl chain derived by dimethylallyl pyrophosphate (DMAPP), an intermediate of the metabolic pathway of mevalonate, that is known to be deregulated in cancer.

iPA is an endogenous isoprenoid-derived product present in mammalian cells as a free nucleoside in the cytoplasm, or in a tRNA-bound form, displaying well established pleiotropic biological effects, including a direct anti-tumor activity against several cancers. However, the precise mechanism of action of iPA in inhibiting cancer cell proliferation remains to be clarified.

In this work, we investigated whether iPA could directly interfere with the angiogenic process, fundamental to cancer growth and progression, and if the growth and proliferation of human melanoma cells, known for their highly angiogenic phenotype, could be affected by the treatment with iPA. Finally, we investigated if iPA could have an immunomodulatory role targeting directly human natural killer (NK) cells, components of innate immunity that participate in immunity against neoplastic cells, in order to provide a cooperative and multifactorial mode of action of iPA to arrest cancer growth. To evaluate the potential involvement of iPA in angiogenesis, we employed human umbilical vein endothelial cells (HUVECs) as a suitable *in vitro* model of angiogenesis, by evaluating the viability, proliferation, migration, invasion, tube formation, and molecular mechanisms involved. Data were corroborated in mice by using a gel plug assay. iPA dose- and time-dependently inhibited all the neoangiogenesis stages, with an IC50 of 0.98 µM. We demonstrated for the first time that iPA was monophosphorylated into iPA 5'-monophosphate (iPAMP) by adenosine kinase (ADK) inside the cells. iPAMP is the active form that

inhibits angiogenesis through the direct activation of AMP-kinase (AMPK). Indeed, all effects were completely reversed by pre-treatment with 5-iodotubercidin (5-Itu), an ADK inhibitor. The isoprenoid intermediate isopentenyl pyrophosphate (IPP), which shares the isopentenyl moiety with iPA, was ineffective in the inhibition of angiogenesis, thus showing that the iPA structure is specific for the observed effects. Thus, iPA is a novel AMPK activator and could represent a useful tool for the treatment of diseases where excessive neoangiogenesis is the underlying pathology**.**

The activation of AMPK seems to be the mechanism by which iPA exerts also its anticancer effects in A375 human melanoma cells. Indeed, in order to evaluate if iPA could be a useful agent able to inhibit tumor angiogenesis, we tested *in vitro* the ability of iPA to arrest the proliferation and the growth of melanoma, a tumor known for its highly angiogenic phenotype. In particular, we performed co-cultures of HUVEC and A375 cells, and we evaluated melanoma cells vitality to delucidate their cell fate following iPA-treatment. Moreover, the molecular mechanism elicited by iPA in this cancer model was analyzed. According with endothelial cells, iPA (from 2.5 to 10 μM) was able to inhibit melanoma cell growth, inducing autophagy and subsequently apoptosis, through AMPK activation, acting as an AMP mimetic.

In the last part of this work, we analyzed a possible role of iPA in immune regulation. In analogy to the unique specificity for phosphoantigens like IPP, shown by human Vγ9Vδ2 T cells, we report for the first time the ability of iPA to selectively expand and directly target human NK cells. Interestingly, at submicromolar concentrations, iPA stimulated resting human NK cells and synergized with IL-2 to induce a robust *ex vivo* activation with significant secretion of CCL5 and CCL3 and a large increase in TNF-α and IFN-γ production when compared with IL-2 single

cytokine treatment. Moreover, iPA was able to promote NK cell proliferation, upregulating the expression of specific NK cell activating receptors, as well as CD69 and CD107a expression. Cytotoxic activity of NK cells against tumor targets was due to a selective potent activation of MAPK signaling intermediaries downstream IL-2 receptor. The effect resulted at least in part from the fine modulation of the farnesyl diphosphate synthase (FDPS) activity, the same enzyme implicated in the stimulation of the human γδ T cells. The iPA-driven modulation of FDPS can cause an enhancement of post-translational prenylation essential for the biological activity of key proteins in NK signaling and effector functions, such as Ras. These unanticipated properties of iPA provide additional piece of evidence of the immunoregulatory role of the intermediates of the mevalonate pathway and open novel therapeutic perspectives for this molecule as an immune-modulatory drug.

Taken together, these results highlight a sinergic mode of action of iPA as antitumor agent, interfering with neovascularization and hence blood supply to nourish cancer cells, inducing autophagy and apoptosis directly in tumor cells and stimulating the immune response to attack neoplastic cells.

.

ABSTRACT

1. BACKGROUND

1.1 N6-isopentenyladenosine, an endogenous isoprenoid end-product, from plants..

N6-isopentenyladenosine (iPA) is a modified adenosine characterized by an isopentenyl chain linked to the nitrogen at position 6 of the purine base (Fig. 1).

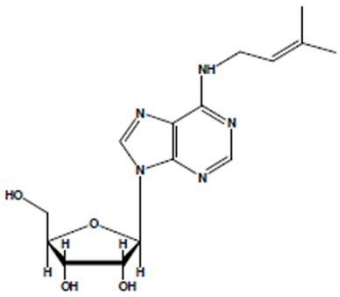

Figure 1. **Chemical structure of iPA**

iPA belongs to a class of substances known as cytokinins, which are important purine derivatives that serve as hormones that control many processes in plants (Bifulco et al., 2008). Cytokinin literally means stimulus of cell movement (cytokinesis) but it is also used in terms of cell division. They were discovered as factors promoting cell division in tobacco tissue cultures (Skoog et al., 1965) and have been shown to regulate several other developmental events, such as *de novo* bud formation, release of buds from apical dominance, leaf expansion, delay of senescence, promotion of seed germination, and chloroplast formation (Mok and Mok, 2001). Thus, cytokinins are plant growth regulators defined by their ability to promote cell division in tissue cultured in presence of auxin (Astot et al., 2000). The discovery of auxin, the first

organic substance defined as hormone of the plants, led to the discovery of other chemical substances regulating the plant growth. As in the animal world, it was unlikely that plant growth and development depended on the control of a unique hormone. Indeed, it was found a growth factor derived from DNA degradation that stimulated the growth of plant tissues *in vitro* (Skoog et al., 1965). This substance was named kinetin and the class of regulators was named cytokinins. The general term "kinin" was created to describe chemicals that promote cell division, but it was subsequently replaced by "cytokinin" for confusion with the term kinin from the realm of zoology (Oka, 2003). In 1963 the first cytokinin in plants was discovered from the immature cariosside of corn (*Zea mais*): the substance was named zeatin (Oka, 2003). iPA is one of the cytokinins isolated from plants and its ribosides, ribotide and 2- methyltioderivate are known (Bifulco et al., 2008). Many studies suggest that cytokinins are mainly generated in the radical system and transported to the aerial part through the xilematic flux. The metabolism of cytokinins seems to occur in various tissues of the plant, either by elimination of the side chain through cytokinins oxidases or by ribosylation. Glucosylation seems to occur in the leaves: glucosides could store hormones which, when required, are transported in specific organs. All the known cytokinins present adenine substitution on position N6, with an isoprenoid or an aromatic group (Bifulco et al., 2008).

1.2 ..to mammals

iPA was found in transfer RNA (tRNA) of many eukaryotic and prokaryotic cells (Burns et al., 1976) and it is the only known cytokinin existing in animal tRNAs, specifically at position 37 of the tRNA molecules that bind codons starting with uridine (Persson et al., 1994). It is

a rare component of some ribosomal RNA and was isolated from yeast through the hydrolysis of the serine of tRNA. Free iPA, not linked to tRNA, was found in cell extracts of *Saccharomyces cerevisiae* and *Schizosaccharomyces pombe* (Laten and Zahareas-Doktor, 1985). However, the cell levels of free iPA are not decreased in yeast strains having mutations that result in reduced amounts of isopentenylated tRNA (Faust and Dice, 1991). This result demonstrates that free iPA is derived from a biosynthetic pathway independent from isopentenyl tRNA degradation and probably related to modifications of monophosphate adenosine.

The adenosine is generated through the classic biosynthetic pathway of nucleosides, while the isoprenoid chain derives from a product of the mevalonate pathway and, more specifically, from dimethylallyl pyrophosphate (DMAPP), which is in equilibrium with its isomer isopentenyl pyrophosphate (IPP) (Faust and Dice, 1991). iPA is typically found next to the 3' of the tRNA anticodon that binds to codons containing uracile as first base ($tRNA^{Leu}$, $tRNA^{Phe}$, $tRNA^{Ser}$, $tRNA^{Trp}$, $tRNA^{Tyr}$): this site suggests a role in the process of transduction. The tRNA containing iPA binds more efficiently the ribosome than the unmodified analogous nucleoside, thus demonstrating that the absence of isopentenyladenosine decreases the efficacy of transduction *in vitro* and *in vivo* (Warner et al., 2000; Moustafa et al., 2001; Bifulco et al., 2008).

It was previously believed that the RNA degradation was the main source of free cytokinins, including iPA. Nevertheless, calculation on the rate of RNA turnover demonstrated that a *de novo* biosynthetic pathway independent from tRNA should be present in plants; a further step was the discovery of an enzyme for cytokinin biosynthesis in *Dictiostelum discoideum*. Cell extracts from this organism can convert adenosine 5'-monophosphate (AMP) and DMAPP in cytokinins: N6-

isopentenyladenosine-5'-monophosphate (iPAMP) and the correspondent nucleoside iPA (Fig. 2). Moreover, in 1984 it was shown that the product of the T-DNA gene4 (*ipt*) of the crown gall-forming bacterium, *Agrobacterium tumefacien,* was an isopentenyl transferase, IPT (Bifulco et al., 2008). IPTs are a family of enzymes, conserved from microorganisms to mammals, that catalyze the addition of iPA on residue 37 of tRNA molecules using DMAPP as donor of the isopentenyl group. IPT is also involved in the synthetic pathway independent of isopentenylated tRNA degradation (Golovko et al., 2000; Spinola et al., 2005).

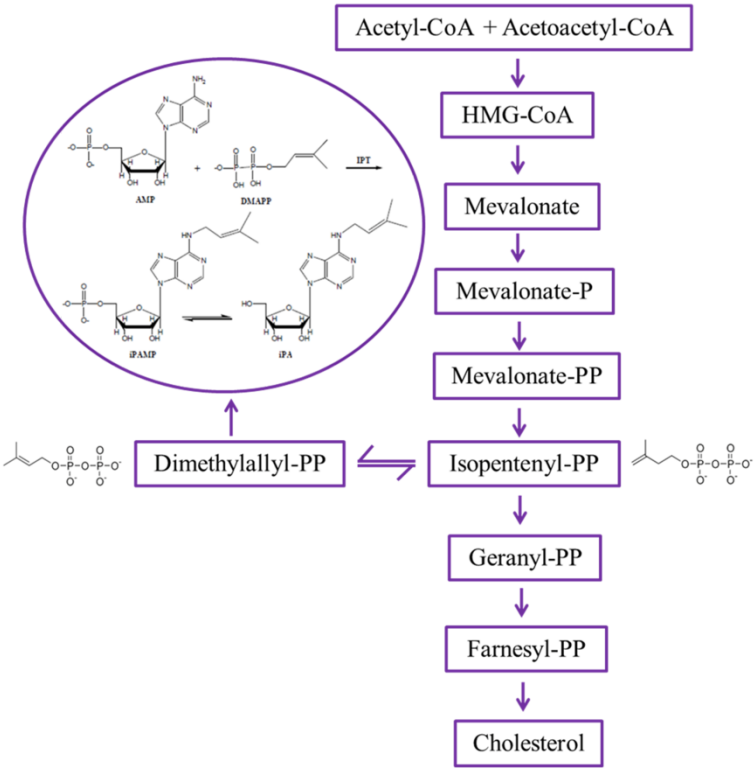

Figure 2. Proposed biosynthesis of iPA in plants

Astot and coworkers provided then evidence for an alternative iPAMP independent cytokinin biosynthetic pathway both in *Arabidopsis thaliana* expressing the *Arabidopsis tumefaciens ipt* gene and as part of normal

wild-type plant metabolism (Astot et al., 2000). Sequence analysis shows the homology between the human and *Saccharomyces cerevisiae* and *Escherichia coli* IPT aminoacid sequence. All well-conserved motifs present in tRNA-IPT can be found in the deduced human protein sequence (Golovko et al., 2000). The full-length TRIT1 transcript is able to complement the yeast tRNA-IPT biochemical activity, producing amounts of iPA-tRNA similar to those produced by the yeast gene. In mammalian cells, iPA is found in selenocysteine (Sec) tRNA that decodes UGA stop codons and inserts Sec residues into nascent peptides. The ability to decode UGA as a Sec codon is affected when the $tRNA^{Sec}$ lacks iPA at position 37 as demonstrated in *Xenopus* (Spinola et al., 2005). iPA is therefore the only cytokinin modified tRNA species found in animals. However, biosynthesis of iPA in mammals has not been fully disclosed.

1.3 Biological effects of N6-isopentenyladenosine

It has been proved that in plants cytokinins are able to induce callus (clusters of dedifferentiated plant cells that proliferate indefinitely in a disorganized manner) to re-differentiate into adventitious buds, just like human cancer cells. Because of these similarities, cytokinins may also affect the differentiation of human cancer cells through mechanisms of action that could involve common signal events of the signal transduction (Bifulco et al., 2008). Indeed, whilst iPA biosynthesis in mammals has not been fully disclosed, some of its biological effects are known, including anti-tumour action on human and murine cells.

More than forty years ago, it has been shown by Gallo and colleagues that iPA can exert a promoting or inhibitory effect on human cell growth, on the bases of used concentration and the cell cycle phase. They reported a biphasic effect of iPA: an inhibitory action at high μM concentrations and

a stimulatory effect at lower concentrations (0.1-1.0 μM). Moreover, they demonstrated that the addition of iPA 12 hours after phytohemagglutinin stimulation determined a decrease of mitotic figures, suggesting that iPA effects depend on the phase of cell cycle. It was also demonstrated that the effects on DNA synthesis are preceded by the inhibition of RNA and protein synthesis. The mechanism of RNA inhibition could be the result of the competition of iPA with the adenosine-3'-phosphate, adenosine or 2'-deoxyadenosine 5'-triphosphate during RNA synthesis. However, the addition of such substances, even at higher concentrations of iPA, did not decrease its inhibitory effect (Gallo et al., 1969). Inhibitory effect of iPA has been demonstrated also on the growth of sarcoma cells at very high concentration (22 and 100 μM). Studies from these cell extracts demonstrated *in silico* that iPA may be a potential substrate for adenosine kinase, and also a weak inhibitor of adenosine deaminase, glucose-6-phosphate-dehydrogenase and methylase of mammalian tRNAs. iPA acts also as potent inhibitor of the uptake of purine and pirimidine nucleosides. The authors suggest that iPA cytotoxicity for these cells might be due to its conversion in 5'-monophosphate even if they don't definitively prove it. This derivative molecule from iPA, at high intracellular levels, could be cytotoxic since it affects the enzymes involved in purine metabolism (Divekar et al., 1973).

More recent studies demonstrated that iPA exerts a significant apoptotic effect on viable human lymphocytes. The capacity of the modified ribonucleosides to induce apoptosis was studied also in several human cell lines and it was observed that iPA was the most active cytokinin. The cancer cell lines Caco-2 and HL-60 were more reactive to an apoptotic stimulation than non-malignant human peripheral blood lymphocytes (Meisel et al., 1998). In a thyroid cell system iPA was able to influence cAMP dependent organization of the microfilaments. The effects of iPA

were exerted both on the synthesis of cAMP and on its activity, probably due to the substitution on the nitrogen 6 of adenosine (Laezza et al., 1997). Of note, iPA is the only adenosine substituted on nitrogen 6 with physiologic relevance. Then, the same research group investigated the anti-proliferative effect of iPA, highlighting a dose-dependent arrest of the G1 cell phase transition associated with a reduction of cells in the S phase through the inhibition of farnesyl diphosphate synthase (FDPS) and protein prenylation. Interestingly, iPA effect was not mediated by the adenosine receptors but was due to a direct modulation of FDPS enzyme activity as a result of its uptake inside the cells (Laezza et al., 2006). The antiproliferative activity of iPA was confirmed also in 9 human epithelial cancer cell lines derived from different types of malignant tissues (Spinola et al., 2007): it was observed a complete suppression of clonogenic activity in 8 of the cell lines after exposure to iPA at a concentration of 10 μM. The observed effects appeared to reflect a block in DNA synthesis, not involving a FDPS down-regulation in lung cells model. These findings are consistent with the reported inhibition of proliferation of rat thyroid tumor cells induced by iPA. Although iPA has been reported to induce apoptosis as well as differentiation in a human myeloid leukemia cell line (Ishii et al., 2002), any pro-apoptotic effect has been reported in thyroid and epithelial cancer cells (Laezza et al., 2006; Spinola et al., 2007). Moreover, iPA was able to cause a pronounced change in cell morphology, associated to a disorganization of actin fibers in the cytoplasm, suggestive of a cell stress condition. Antiproliferative effects of iPA was confirmed also on human colon cancer cells, through inhibition of DNA synthesis and induction of apoptosis (Laezza et al., 2009).

There are some evidence of the activity of iPA also in patients. A far away work described a clinical study on the therapeutic use of iPA on twenty leukaemia patients who were treated daily with intravenous infusion of

iPA. Patients received the substance drug orally or intravenous, showing transient and short lasting effects of the therapy probably due to iPA instability (Mittelman et al., 1975). Other researchers had already reported that iPA inhibited the growth of various cancers, but iPA LD50 was different and dependent on the way of administration and species (from ca. 200 to 800 mg/Kg). However, they focused particularly on toxic effects (hepatotoxicity, pancreatic atrophy and antiproliferative effects in lymphoid tissue) of iPA in rats and dogs and did not gain further insights into the observed antitumour effects (Suk et al., 1970).

No additional example of *in vivo* anticancer activity has been reported for humans or, in general, mammalians up to the present. Only in 2006, the successful inhibition of a rat tumour by iPA injected in a nude mouse directly at the tumour site has been reported, without detectable toxic or hypolocomotor effects on the treated animals (Laezza et al., 2006). Later, Colombo and colleagues have shown no significant *in vivo* activity of iPA injected intraperitoneally into nude mice inoculated with ovarian-carcinoma cells, suggesting that the pharmacokinetics of the compound do not allow to reach efficacious concentrations. The lack of activity might rest in the rapid clearance and short half-life *in vivo* of circulating nucleosides and, most likely, of circulating iPA (Colombo et al., 2009).

Taken together, these data suggest that this isoprenoid end product might be used for antineoplastic therapy, representing a potential new anticancer drug. However, it would be necessary to increase knowledge about the exact biological role of iPA inside mammalian cells even in the sense of its ability to control cancer cell growth (Bifulco et al., 2008).

1.4 Basic aspects of angiogenesis

The term ‘‘angiogenesis’’ is commonly used to reference the development of new blood vessels growth from preexisting vasculature. It plays an important role in physiologic conditions, including development, reproduction, wound healing and bone morphogenesis, and in pathologic ones as cancer, intraocular neovascular disorders, rheumatoid arthritis, psoriasis and others. The entire process, that consists in localized enzymatic degradation of basal membrane, migration and proliferation of endothelial cells, and lumen formation of the new capillary (Fig. 3), is finely controlled by a tuned balance between positive and negative effectors (Carmeliet, 2003). In the embryo, new vessels form *de novo* via the assembly of mesoderm-derived endothelial precursors (angioblasts) that differentiate into a primitive vascular labyrinth (vasculogenesis) (Swift and Weinstein, 2009). Subsequent vessel sprouting (angiogenesis) creates a network that finally remodels into arteries and veins (Adams and Alitalo, 2007). Recruitment of pericytes and vascular smooth muscle cells that enwrap nascent endothelial cell tubules provides stability and regulates perfusion (arteriogenesis) (Jain, 2003). In the adult, vessels are quiescent and rarely form new branches.

Vessels can also grow through other mechanisms, such as the splitting of pre-existing vessels through intussusception or the stimulation of vessel expansion by circulating precursor cells (Fang and Salven, 2011; Makanya et al., 2009).

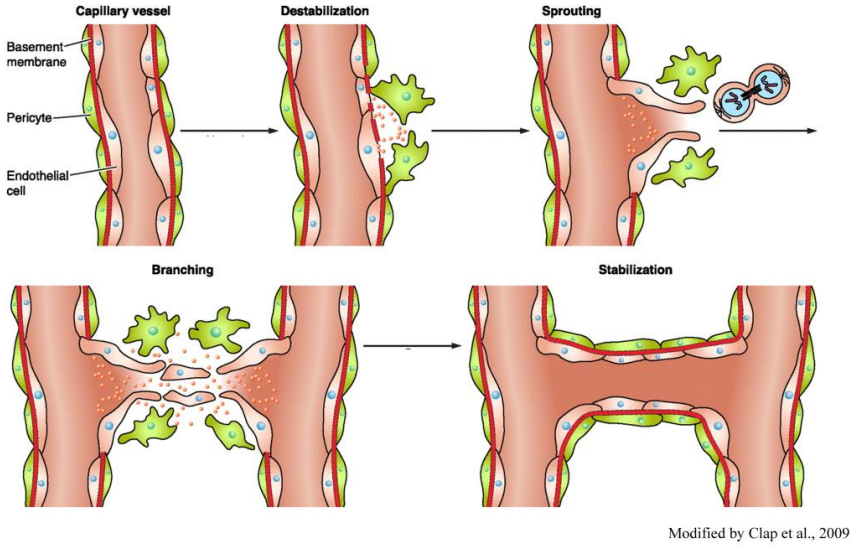

Figure 3. **The cellular steps involved in angiogenesis**

Blood vessels supply oxygen and nutrients and provide gateways for immune surveillance. As this network nourishes all tissues, it is not surprising that structural or functional vessel abnormalities contribute to many diseases. Inadequate vessel maintenance or growth causes ischemia in diseases such as myocardial infarction, stroke, and neurodegenerative or obesity-associated disorders, whereas excessive vascular growth or abnormal remodeling promotes many ailments including cancer as routes for tumor cells to metastasize, inflammatory disorders, and eye diseases (Carmeliet, 2003; Folkman, 2007).

1.5 Angiogenesis in cancer

Angiogenesis is widely considered as an essential process to nourish the growing tumor and to remove metabolic waste products (Folkman, 1971). Intratumoral hypoxia leads to the stabilization and expression of the pro-tumorigenic hypoxia-inducible factor (Hif)α transcription factors. Under

normal oxygen levels, Hif-1α and Hif-2α are short-lived because prolyl hydroxylase (PHD) proteins mediate their degradation (Fong and Takeda, 2008). During hypoxia, PHD proteins show reduced activity, which results in the formation of heterodimerization by Hif-1α and Hif-2α with Hif-1β. This complex is able to trigger the expression of genes containing hypoxia-responsive elements, including the gene encoding vascular endothelial growth factor (VEGF) (Qing and Simon, 2009). Under hypoxic conditions, pericytes are able to secrete VEGF which can act in a paracrine manner on endothelial cell proliferation (Reynolds et al., 2000). In consequence, the quiescent vascular network is getting disturbed and activated (Fig. 4).

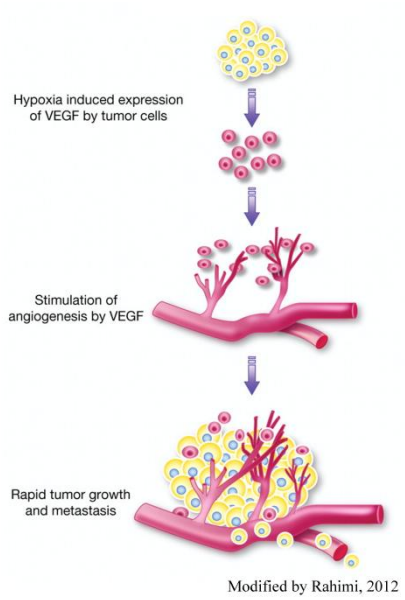

Figure 4. **Tumor associated-angiogenesis**

Whereas blood vessel growth is tightly controlled under physiological conditions, tumor progression is highly associated with the acquisition of an angiogenic phenotype based on a transition from the avascular to the vascular phase (Folkman et al., 1989). This process is called the "angiogenic switch", in which the balance of pro- and anti-angiogenic

molecules leads toward angiogenic inducers (Folkman and Hanahan, 1991). Tumor vasculature is often characterized by the presence of poorly developed so called "immature" vessels with multiple branch-points and deregulated vessel sprouting which contributes to tumor hypoxia. In particular, tumor vessels display abnormal structure and function with seemingly chaotic organization. Endothelial cells lack a cobblestone appearance, are poorly interconnected and occasionally multilayered. Also, arterio-venous identity is ill defined and shunting compromises flow. The basement membrane is irregular in thickness and composition, and fewer, more loosely attached hypocontractile mural cells cover tumor vessels, though tumor-type-specific differences exist. The resulting irregular perfusion impairs oxygen, nutrient and drug delivery (Goel et al., 2011). Neovascularization enhances tumor cell proliferation, local invasion and hematogenous metastasis. However, the abnormalities of tumor vessels provide the potential for targeting these vessels without destroying the normal vasculature (Arap et al., 2002).

Vessel leakiness, together with growing tumor mass, increases the interstitial pressure and thereby impedes nutrient and drug distribution. The loosely assembled vessel wall also facilitates tumor cell intravasation and dissemination. As a consequence of poor oxygen, nutrient and growth factor supply, tumor cells further stimulate angiogenesis in an effort to compensate for the poor functioning of the existing ones. However, this excess of proangiogenic molecules only leads to additional disorganization as the angiogenic burst is nonproductive, further aggravating tumor hypoperfusion in a vicious cycle.

Nowadays anti-angiogenetic pharmacological approaches are approved for several advanced metastatic cancers, in combination with validated chemotherapy or cytokine therapy, aimed at blocking vessel growth targeting VEGF (Potente at al., 2011). The hypoxic and acidic tumor

milieu constitutes a hostile microenvironment that is believed to drive selection of more malignant tumor cell clones and further promotes tumor cell dissemination. The uneven delivery of chemotherapeutics, together with a reduced efficacy of radiotherapy owing to the lower intratumoral oxygen levels, limit the success of conventional anticancer treatments. Moreover, tumors would be able to switch mechanisms of vascular growth and some of these mechanisms rely less on VEGF, so they would possess the means to escape from treatment with VEGF receptor inhibitors. Identifying the molecular basis of these alternative modes of vessel growth will thus be critical to improve the efficacy of antiangiogenic treatment (Potente et al., 2011).

Despite efforts to stimulate angiogenesis therapeutically by proangiogenic factors, most trials failed to meet these expectations. Alternative strategies, based on pro-angiogenic cell therapies or targeting of microRNAs, offer new opportunities but are in (pre)clinical development (Bonauer et al., 2010). Nonetheless, only a fraction of cancer patients show benefit as tumors evolve mechanisms of resistance or are refractory toward VEGF receptor inhibitors. Conflicting results about the benefit of VEGF blockade have kick-started a debate on whether antiangiogenic treatment may trigger more invasive and metastatic tumors. On the upside, ‘‘sustained normalization’’ of abnormal tumor vessels may offer benefit for fighting metastasis (Goel et al., 2011).

1.6 A snapshot of melanoma

Melanoma is a cutaneous tumor characterized by abnormal proliferation of melanocytes that invade the basement membrane. Recent epidemiologic evidence has documented both an increase in incidence of and in mortality from malignant melanoma. The importance of this relatively uncommon

malignant neoplasm (incidence less than 5/100,000 population) is attested to the fact that despite accounting for only 3% of all cutaneous malignant neoplasms, malignant melanoma causes 67% of the deaths attributable to skin cancer (Cummins et al., 2006). Malignant melanoma has a poor prognosis and limited therapeutic options, particularly in advanced tumors. The 5-year-survival rate of advanced tumors with distant metastases is still as low as 5-10% (Balch et al., 2009). Surgical resection of the primary tumour offers a significant chance of cure and remains the mainstay of treatment where possible. However, melanoma, which can progress to a stage of spreading with low invasive potential (radial growth phase) to the next stage (vertical growth phase), disseminates early, both intradermally and through lymphatic and haematogenous routes and therefore despite resection, once there is invasion into the dermis of the skin, the outlook changes dramatically.

Chemotherapy with the alkylating agent dacarbazine as monotherapy was established as treatment for metastatic melanoma thirty years ago and remains the standard of care outside of clinical trials. However the response rate of melanoma to dacarbazine is only in the region of 15 to 20% and it has not been shown to improve overall survival. Therefore, there is an urgent need to find more effective treatments for this condition (Zaki et al., 2012). An area of significant interest for modern cancer therapeutic strategies is targeting angiogenesis, as this is one of the cardinal patho-physiological features of invasive cancer, essential for tumour growth and metastasis (Hanahan and Weinberg, 2000). Indeed, melanoma is well-recognised to be a highly vascular tumour. However the impact on tumor-induced angiogenesis for disease progression and metastasis remains controversial (Helfrich and Schadendorf, 2011). Anyway, it is well known that the overproduction of $VEGF_{165}$ and its association with VEGF receptor (VEGFR) expression promotes melanoma

cell growth and survival through MAP kinase and phosphatidyl inositol-3-kinase (PI3K) signaling pathways (Graells et al., 2004). Moreover, immunohistochemical studies suggest that VEGF is expressed by 20–77% of human primary melanomas. VEGF also increased during follow-up (Zaki et al., 2012). Expression of VEGF, VEGF-R1, VEGF-R2 and VEGF-R3 was observed to be significantly higher in malignant melanocytes when compared with samples from their benign counterparts, supporting the hypothesis that in particular the upregulation of VEGF-R2 may select for an angiogenic phenotype. Clinically, the expression and activation of MMPs is related to the degree of invasiveness and metastasis of melanoma and also correlates with low survival rates in melanoma patients (Hofmann et al., 2000). In summary, it is clear that angiogenesis represents a relevant process to target in melanoma. There is therefore a strong biological rationale to incorporate the anti-angiogenic strategy into therapeutic plans. Whereas cytotoxic chemotherapy targets DNA repair and the cell cycle to induce cell killing through apoptosis, antiangiogenic therapy is more cytostatic. The main targets are: pro-angiogenic ligands; kinases that are intrinsic to extracellular endothelial cell receptors or growth factor pathways essential for survival and proliferation within endothelial cells; MMPs and integrins. Agents used in these anti-angiogenic strategies may be further sub-divided according to their chemical entity in monoclonal antibodies (mAbs), small molecule kinase inhibitors that abrogate receptor or cytoplasmic kinases and VEGF-trap, that is a composite decoy receptor based onVEGFRs, fused to an Fc segment of IgG1 (Holash et al., 2002). Early phase trials suggest clinical activity using a variety of anti-angiogenic drugs, but the data are as yet too immature to provide conclusive evidence of clinical benefit in melanoma patients. Given the existence of redundant pathways that may compensate for inhibition of a single angiogenic axis, it is highly unlikely that targeting a single pathway

will be sufficient to achieve optimal tumor control in melanoma. Therefore there are ongoing questions over whether targeting multiple ligands, receptors or kinases within several signaling pathways may be advantageous over specific inhibition of single targets.

1.7 AMP-activated protein kinase, sensor of cellular energy

AMP-activated protein kinase (AMPK) is a highly conserved sensor of cellular energy status that exists in the form of heterotrimeric complexes containing a catalytic α-subunit combined with regulatory β- and γ-subunits (Hardie et al., 2012). Metabolic stress caused by nutrient deprivation, prolonged exercise, ischemia or hypoxia mediates the activation of AMPK, initiating a cellular program to conserve energy by turning on ATP-generating catabolic pathways and switching off ATP-consuming anabolic pathways through direct phosphorylation of target proteins and modulation of gene expression (Hardie et al., 2006). Changes in the AMP- or ADP/ATP ratio, alterations in intracellular calcium concentrations as well as AMP mimetics cause AMPK activation. Recently, in addition to AMPK role in energy homeostasis, emerging evidence indicates that AMPK regulates endothelial cell function, modulating vascular tone by activation of endothelial nitric oxide synthase (eNOS) (Morrow et al., 2003). Moreover, AMPK exerts important anti-inflammatory effects by blocking the expression of adhesion molecules and chemokines by endothelial cells (Ewart et al., 2008). Significantly, many of the beneficial actions of AMPK on endothelial cell function are related to the activation of eNOS or the induction of the vasoprotective protein heme oxygenase HO-1 (Liu et al., 2011). Although the ability of AMPK to preserve endothelial cell viability is well appreciated, the role of AMPK in regulating endothelial cell proliferation is limited and not well

understood (Reihill et al., 2011). AMPK activation is related with inhibition of endothelial cells proliferation and migration (Peyton et al., 2012) or with decreased angiogenesis and inhibition of macrophage infiltration associated to the inhibition of retinoblastoma proliferation *in vivo* (Theodoropoulou et al., 2013).

Although AMPK has not yet been formally demonstrated to be a tumour suppressor, there are many indications that this is the case: AMPK activation inhibits cell growth and proliferation; AMPK exerts many effects of LKB1, a known tumour suppressor; AMPK up-regulates oxidative metabolism and would therefore be expected to mediate an 'anti-Warburg' effect; and similar to other known tumour suppressors, AMPK activation is down-regulated in many tumour cells, by loss of LKB1 and other mechanisms (Dandapani and Hardie, 2013). These considerations led to studies investigating whether the use of AMPK-activating drugs in humans might affect the incidence of cancer. Indeed, Type 2 diabetics taking the AMPK-activating drug metformin have significantly reduced the incidence of cancer compared with those on other medications (Decensi et al., 2010). The nucleotide ZMP, also referred as AICAR (5-amino-4-imidazolecarboxamide 1-β-Dribofuranoside) monophosphate, is an intermediate in purine nucleotide synthesis, but also acts as an AMP mimetic that mimics all of the effects of AMP on the AMPK system (Corton et al., 1995). Incubation of most cells with the equivalent riboside (AICAR) causes accumulation of ZMP, because its uptake and phosphorylation to ZMP is rapid compared with subsequent metabolism; it has therefore been widely used to activate AMPK in intact cells and *in vivo*. Recently, some reports have implicated AMPK in the regulation of autophagy. The activation of AMPK leads to the suppression of mammalian target of rapamycin (mTOR), thereby activating autophagy (see below) (Wang et al., 2011).

1.8 Double face of autophagy: promoter of cell survival or cell death?

The word autophagy is derived from the Greek roots “auto” (self) and “phagy” (eating) and broadly refers to the cellular catabolic processes in which cytoplasmic materials are transported to lysosomes for degradation. Christian de Duve, who was awarded the Nobel Prize for his work on lysosomes, first used the term autophagy in 1963 (Wang and Qin, 2013). There are several different types of autophagy: macroautophagy, microautophagy and chaperone-mediated autophagy (Fig. 5). Macroautophagy (hereafter referred to as autophagy) is the main route for the sequestration of cytoplasm into the lytic compartment.

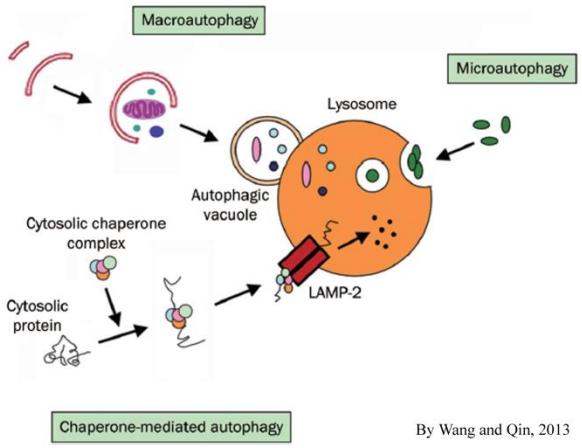

Figure 5. Three main forms of autophagy

Autophagy is a lysosomal pathway involved in the turnover of cellular macromolecules and organelles. The first step of autophagy is the envelopment of cytosol and/or organelles in the isolating membrane, which wraps around the cargo forming an autophagosome, a vesicle surrounded by a double membrane. Autophagosome then undergoes a progressive maturation by fusion with endolysosomal vesicles creating an

autolysosome, where the cargo is degraded. Autophagy is controlled by a set of evolutionarily conserved autophagy-related proteins (Atg proteins).

The initial nucleation and assembly of the primary autophagosomal membrane requires a kinase complex that consists of class III phosphatidylinositol 3-kinase (PI3K), p150 myristylated protein kinase and beclin 1 (also known as Atg6). The further elongation of the isolation membrane is mediated by two ubiquitin-like conjugation systems one of them resulting in the conversion of microtubule-associated protein 1 light chain 3 (LC3; also know as Atg8) from free form (LC3-I) to a lipid-conjugated membrane-bound form (LC3-II) (Fig. 6). The accumulation of LC3-II and its localization to vesicular structures are commonly used as markers of autophagy (Høyer-Hansen and Jäättelä, 2007). Autophagy in mammalian systems occurs under basal condition and can be stimulated by stress, including starvation, oxidative stress, or by treatment with the pharmacological agent rapamycin. In addition to its roles in maintaining normal cellular homeostasis by liberating nutrients from macromolecules and by assisting the clearance of misfolded proteins and damaged organelles, autophagy plays a role in the destruction of some bacteria within the cells.

Autophagy is also involved in removing damaged or excess organelles. For example, mitochondria that have lost their membrane potential and peroxisomes in response to changing environmental cues can be selectively removed by autophagy (Rodriguez-Enriquez et al., 2004). Endoplasmic reticulum (ER) stress caused by the accumulation of unfolded proteins threatens cell survival and triggers the evolutionarily conserved ER to nucleus signaling pathway called the unfolded protein response (UPR), which reduces global protein synthesis and induces the synthesis of chaperones and other proteins that increase the capacity of the ER to fold its client proteins. When the ER stress is extensive or sustained, and the

function of ER cannot be restored, it leads to the removal of the affected cells by apoptosis. Accumulating data now indicate that ER stress is also a potent trigger of autophagy (Høyer-Hansen and Jäättelä, 2007). Whereas the induction of autophagy by ER stress is conserved from yeast to mammals, the signaling pathways responsible for autophagy induction and its cellular consequences appear to vary according to the cell type and the stimulus. A better understanding of the signaling pathways controlling autophagy and the cellular fate in response to ER stress will hopefully open new possibilities for the treatment of the numerous diseases related to ER stress. In addition to activating the UPR by the pathways discussed above, ER-stress leads to a release of calcium from the ER into the cytosol, which, in turn, can activate various kinases and proteases potentially involved in autophagy signaling, as AMPK. It is not clear whether activation of AMPK is enough to trigger autophagy or whether other independent signals are required in parallel. The data presented above encourage the development of autophagy promoting therapies for diseases associated with protein aggregates either in the ER or the cytosol. If this proves to be the case, combination therapies with ER stressors and autophagy inhibitors may prove useful in cancer therapy. The direct link between ER stress and autophagy was reported recently. Thus, it is natural that many burning questions concerning the signaling pathways linking ER stress to autophagy, the mechanisms by which ER is selected as autophagic cargo, the crosstalk between ER stress-induced autophagy and cell death pathways, and the impact of autophagy in diseases associated with ER stress remain largely unanswered. The future research will hopefully clarify these points and pave the way for pharmacological exploitation of the signaling pathways involved (Høyer-Hansen and Jäättelä, 2007).

It has also been proposed that autophagy results in the total destruction of cells. Autophagic cell death represents one of several types of programmed

cell death. Autophagy is vital in a range of physiological and pathological situations, including cell growth, aging, cell death and clearing pathogenic bacteria (Rami, 2009). This mechanism provides an internal source of nutrients for energy generation and survival. When the supply of nutrients is limited, stimulating autophagy contributes to the lysosomal recycling of nutrients to maintain protein synthesis and glucose synthesis from amino acids and to form substrates for oxidation and ATP production in the mitochondria and the inhibition of the default apoptotic pathway. Moreover, starvation-induced autophagy is cytoprotective by blocking the induction of apoptosis upstream of mitochondrial events. Some metabolic changes (ATP levels, amino acids, and insulin) may regulate autophagy. AMPK is a crucial cellular energy sensor. Once activated by falling energy status, it promotes ATP production by increasing the activity or expression of proteins involved in catabolism while conserving ATP by switching off biosynthetic pathways (Hardie et al., 2012). The AMPK pathway appears to be involved in autophagy induced by nutrient deprivation, growth factor withdrawal and hypoxia. The activation of AMPK leads to the suppression of mammalian target of rapamycin (mTOR), thereby activating autophagy. Under nutrient-rich conditions, ER-associated Bcl-2 and Beclin 1 interact to sequester Beclin 1 from the autophagy complex (Wang and Qin, 2013). This association is broken by starvation and is triggered by Bcl-2 phosphorylation by JNK1. Recruitment of the Beclin 1-PI3-kinase complex to the autophagic membrane is also dependent on the ULK1 complex.

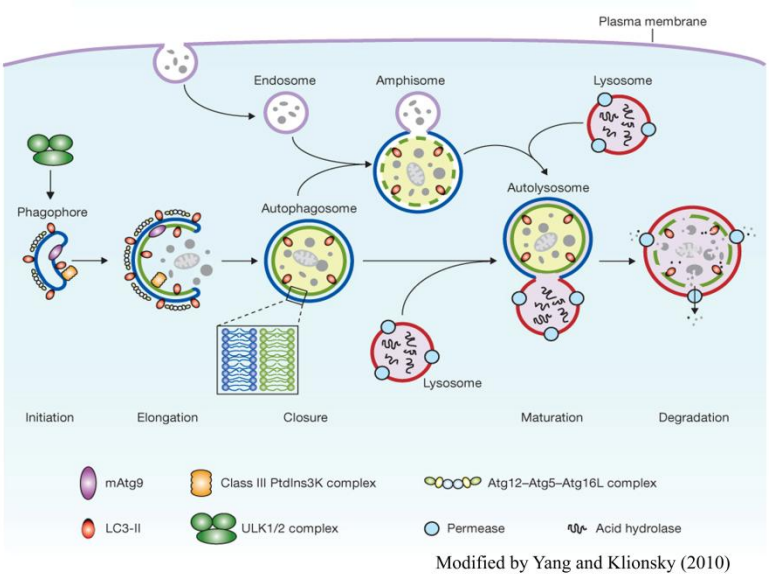

Figure 6. Schematic depiction of autophagy. Mammalian autophagy is initiated by the formation of the phagophore, followed by a series of steps, including the elongation and expansion of the phagophore, closure and completion of a double-membrane autophagosome (which surrounds a portion of the cytoplasm), autophagosome maturation through docking and fusion with an endosome (the product of fusion is known as an amphisome) and/or lysosome (the product of fusion is known as an autolysosome), breakdown and degradation of the autophagosome inner membrane and cargo through acid hydrolases inside the autolysosome, and recycling of the resulting macromolecules through permeases. The core molecular machinery is also depicted, such as the ULK1 and ULK2 complexes that are required for autophagy induction, class III PI3K complexes that are involved in autophagosome formation, mammalian Atg9 (mAtg9) that potentially contributes to the delivery of membrane to the forming autophagosome and two conjugation systems, the LC3-II and Atg12–Atg5–Atg16L complex, which are proposed to function during elongation and expansion of the phagophore membrane.

This biosynthetic pathway may be an attractive target for cancer treatment (Wang and Qin, 2013). Autophagy is a cell survival mechanism that involves the degradation and recycling of cytoplasmic components. In addition, autophagy mediates cell death under specific circumstances. Autophagic cell death (type II cell death) and apoptosis (type I cell death) have taken center stage as the principal mechanisms of programmed cell death in mammalian tissues. Although autophagy and apoptosis are

markedly different processes, autophagy and apoptosis can act as partners to induce cell death in a coordinated or cooperative fashion. Several signaling pathways that are induced by common cellular stressors regulate both autophagy and apoptosis. For example, Bcl-2 phosphorylation may not only be a mechanism for regulating apoptosis and a mechanism for regulating autophagy, but may also be a mechanism for regulating the switch between the two pathways. It is suggested that Bcl-2 also plays an essential role in limiting autophagy activation and preventing the initiation of programmed cell death (Zhang et al., 2009). The tumor suppressor p53 regulates both autophagy and apoptosis. Among other mechanisms, p53 can initiate apoptosis by inducing the expression of p53-upregulated modulator of apoptosis (PUMA), which leads to the release of cytochrome c from mitochondria and apoptotic cell death. In addition, p53 affects autophagy by modulating signaling through the mTOR nutrient-sensing kinase, which controls autophagy at the initiation stage. Autophagy proteins can play a role in cellular events that occur during apoptosis. For example, Atg5 may be a point of crosstalk between autophagic and apoptotic pathways (Wang and Qin, 2013). On the other hand, autophagy is emerging as a built-in mechanism that malignant cells can exploit for protection against a variety of intrinsic and extrinsic stress signals. However, excessive or derailed autophagy can also favor cell death. How these two seemingly opposing roles of autophagy can have an impact upon cancer chemoresistance remains unclear (Wang and Qin, 2013).

1.9 Immune regulation in cancer: focus on melanoma

Immune responses to cancer can be readily demonstrated, which indicates that immune-surveillance plays a role in control of tumor development. However, tumors growing under immune pressure might develop various

mechanisms to evade immune recognition; a process generally known as immune-evasion. Two key processes that counter immune-surveillance are immune-subversion, in which tumor cells or the tumor microenvironment suppresses the immune response, and immune-editing, which refers to the role of the immune response in selecting tumor variants that have become poorly immunogenic, thus allowing for their outgrowth. One mechanism that can have opposing outcomes on subset of innate effector cells, cytotoxic T lymphocytes (CTLs) and natural killer (NK), is the loss or downregulation of HLA class I molecules. Metastatic melanoma is the most lethal form of skin cancer despite its immunogenicity (Tsao et al., 2004). Indeed, melanoma antigens do elicit T cell responses, but T cell-based immunotherapies have shown limited success (Carrega et al., 2009). Although potent T cell responses are desirable, the downregulation of HLA class I on melanoma cells might play a significant role in the pathogenesis and clinical course of the disease, and it represents a considerable problem for T cell-based immunotherapy. Therefore, new strategies are required.

Belonging to innate immunity, NK cells are cytolytic lymphocytes that can directly kill transformed and microbe-infected cells. Moreover besides their ability to kill aberrant cells, NK cells have the capacity to produce a variety of cytokines and chemokines (TNF-α, IFN-γ, CCL3, CCL5, IL-8, IL-10 etc), through which they also participate in the shaping of adaptive immune response (Vivier et al., 2009). These NK cell effector functions are regulated by multiple activating and inhibitory NK cell receptors (Lanier, 2005). Engagement of activating receptors, such as natural cytotoxicity receptors (NCRs; NKp30, NKp44, and NKp46) and NKG2D, leads to the activation of a variety of downstream signaling molecules, which result in the activation of MAPKs, particularly ERK, which are crucial for cytolytic granule release and cytokine generation (Vivier et al., 2004).

Despite the prevailing view that immunological surveillance is triggered by danger signals, signals that arise from injured cells, toxins, pathogens and mechanical damage, a recent work has shown that locally resident immune cells in the skin can detect early signs of cellular stress, through the recognition of ligands on premalignant cells and thus overt tumor transformation (Strid et al., 2008). NK cells reside in the skin (Luci et al., 2009), thus melanocytes are susceptible to NK cell recognition from early stages of dysregulation. NK cells preferentially target tumor cells with low HLA class I expression. Although there is the potential for early NK cell recognition of transformed melanocytes, some studies have indicated that NK cells are poorly represented among tumor-infiltrating lymphocytes during melanoma progression, whereas others have demonstrated NK cells in all biopsies evaluated. Understanding how NK cells migrate into the tumor microenvironment is important to redirect NK cells to the tumor in the therapeutic setting. To appreciate the role of immunosurveillance during melanoma, the factors that influence NK cell recognition of nascent dysregulated melanocytes need to be identified. In turn, how these factors change at different stages of disease, both in primary lesions and metastases, must be deciphered.

This involves characterizing the spatio-temporal expression of ligands during melanomagenesis, which hitherto has been poorly described, and the consequences of this on NK cell function (Burke et al., 2010).

Surgery is still the elective treatment for most solid cancers. Radiotherapy, chemotherapy and biological agents (cytokines, vaccines, adjuvants and immune cells) are generally used as palliative therapy and most cellular immunotherapies remain experimental. A limitation of cellular immunotherapy is the disease stage that can be approached with biological therapy, and usually only after all other options have failed. This clinical constraint limits the efficiency of immunotherapy because it gives an

advantage to the tumor cell clones that have escaped the immune system. NK cells are crucial cytotoxic effectors that complement the action of CLTs. In particular, NK cells can influence other immune cells by producing cytokines that promote dendritic cell (DC) differentiation, antigen presentation and CTL activity, and can eliminate immature DCs, thus further improving the presentation of tumor antigens to T cells (Burke et al., 2010). One limitation to the use of NK cells in immunotherapy is the number of cells required. However large-scale production is now possible for human NK cells (Spanholtz et al., 2010).

Recently, growing body of evidence indicates that a fine manipulation of the isoprenoid metabolism may constitute an important adaptive host response to stress, triggering immune response against tumor cells or infectious agents (Nassbaumer et al., 2011). Human peripheral blood Vγ9Vδ2 T cell subsets are the principal actors in monitoring the accumulation of phosphorylated isoprenoid metabolites (such as isopentenyl pyrophosphate, IPP). The reduced activity of the IPP-consuming enzymes, farnesyl diphosphate synthase (FDPS) seems to be the key mechanism in stimulation of this cytotoxic T cell subset by tumor cells (Li et al., 2009). In light of this, several groups have shown that the specific FDPS inhibitor zoledronic acid, the most potent aminobisphoshonate (NBPs) currently available for clinical use, can be exploited to intentionally activate Vγ9Vδ2 T cell by inducing IPP accumulation in tumor cells or antigen professional cells (APC) (Dieli et al., 2007).

Interestingly enough, NK cells can also be activated by the manipulation of the mevalonate pathway either by using zoledronate or statins (Nassbaumer et al., 2011; Gruenbacher et al., 2010) that are specific inhibitors of the hydroxymethylglutaryl coenzyme A (HMG-CoA) reductase, the first committed step of the mevalonate pathway acting

upstream to FDPS (Gazzerro et al., 2012). However, it has been reported that NK cells are not directly activated by isoprenoid products, like γδ T cells, but only indirectly through the action of a population of DC-like cells (Nassbaumer et al., 2011; Gruenbacher et al., 2010). This might be responsible of a delay in the first fast line of defense usually provided by NK cells. However this event seems not occur after treatment with mevalonate pathway inhibitors, leading to think that the accumulation of other isoprenoid end products might directly and immediately affect NK cell functions.

2. AIMS OF THE STUDY

This study arises from some reflections on iPA, an endogenous end-product derived from the mevalonate pathway, that has been already reported to exert a suppressor effect against various tumors *in vitro* and *in vivo*, even if its precise mechanism of action is until unknow. It is possible carrying out an efficacious anticancer strategy through different ways: using cancer cytotoxic drugs, anti-angiogenic agents or immune response activators able to attack specifically neoplastic cells. An important goal could be the identification of a drug with all these pleiotropic anticancer effects.

In the light of these observations, the main aims of this work were:

- to evaluate the ability of iPA to inhibit tumor progression through the interference with the angiogenic process, since angiogenesis is a key step to nourish the neoplastic mass, using human umbilical vein endothelial cells (HUVECs) as a suitable *in vitro* model of angiogenesis;
- to study the antitumor activity of iPA against a model of cancer characterized by a highly angiogenic phenotype as melanoma, employing human melanoma cell line, A375 cells;
- to verify the ability of iPA, due to its isoprenoid moiety and in analogy with IPP, to expande and activate selectively natural killer (NK) cells, the cytotoxic subset of innate immunity, using NK cells purified from healthy donors peripheral blood;
- to provide key informations on the mechanism through which iPA exerts its biological effects in all the models studied.

As additional deliverables it was possible to obtain basic informations about structure-activity relationship of iPA testing also its congeners, both isoprenoid, purine and structural analogues.

Moreover, it was clarified the non-involvement of the classical adenosine pathway in the biological effects exerted by iPA that are indeed mediated by intracellular targets.

Data obtained in this work will allow to give novel insights into the biological activity of this promising endogenous isoprenoid showing pleiotropic effects as anticancer drug.

3. MATERIALS AND METHODS

Materials

iPA, IPP triammonium salt solution, adenine, isopentenyladenine, dipyridamole and erythro-9 (2-hydroxy-3-nonyl)-adenine (EHNA) powders as well as acridin orange powder were purchased from Sigma-Aldrich (St. Louis, MO, USA); 5-iodotubercidin (5-Itu), PSB 1115 and ZM 241385 from Tocris Bioscience (Bristol, UK); iPA analogues CM 223, CM 224, CM 226 and CM 226 were provided by Prof. Ciuffedra (University of Milan); whilst carboxyfluorescein diacetate succinimidyl ester (CFSE) and LysoTracker- Red (DND-99) from Molecular Probes-Invitrogen (Paisley, UK). Anti-caspase-3 and -9, anti-PARP [poly (ADP-ribose) polymerase], anti-pChk1 (Ser296), anti-pATR (Ser428), anti-phospho p53 (Ser15), anti-pHistone H2AX (Ser139), anti LC3-B, anti-pSTAT5 (Tyr 694) and anti-STAT5, anti-phospho p44/42 MAPK (Thr202/Tyr 204), anti-p44/42 MAPK, anti-phospho p38 MAPK (Thr180/Tyr182) and anti-p38 MAPK antibodies were all from Cell Signaling Technology (Danvers, MA, USA); anti p-AMPK and AMPK, anti-β-actin and anti-FDPS were from Abcam (Cambridge, UK). Anti-pan Ras and anti-tubulin were from Sigma-Aldrich (Dorset, UK). The MEK1/2-specific kinase inhibitor UO-126 was purchased from Cell Signaling technology (Beverly, MA).

Cell cultures

Human umbilical vein endothelial cells (HUVECs) were cultured on 1% gelatin-coated culture flasks with vent caps in M199 with heparin, 10% heat-inactivated fetal bovine serum (FBS), 2 mM L-glutamine and complete angiogenic factors (aFGF, bFGF, EGF, hydrocortisone and

heparin). The HUVECs were used at passages 2 to 6. Reagents were obtained from Sigma-Aldrich; aFGF, bFGF, and EGF were from Peprotech (London, UK).

Human malignant melanoma cells (A375) were cultured in DMEM High Glucose (Sigma-Aldrich, St. Louis, MO, USA) supplemented with 2 mM L-glutamine, 50 ng/ml streptomycin, 50 units/ml penicillin and 10% heat-inactivated FBS (Hyclone Laboratories, Logan, UT, USA).

All donors gave written informed consent in accordance with the Declaration of Helsinki to the use of their residual buffy coats for research purposes, with approval from the University Hospital of Salerno Review Board. Peripheral blood mononuclear cells (PBMC) from healthy donors were isolated over Ficoll-Hypaque gradients (lymphocyte separation medium; MP Biomedicals, Aurora, OH, USA). Human NK cells were negatively selected from PBMC by immunomagnetic procedure (NK-cell isolation kit; Miltenyi Biotec, Calderara di Reno, Italy). They were cultured for different time intervals in RPMI 1640 in the presence of IL-2 at 100 U/ml alone or in combination with different concentrations of iPA. Also the human chronic myelogenous leukemia cell line K562 (ATCC) was maintained in RPMI 1640 (Invitrogen, San Diego, CA, USA) supplemented with 2 mM L-glutamine, 50 ng/ml streptomycin, 50 units/ml penicillin and 10% heat-inactivated FBS. All cell cultures were mantained at 37°C in humidified 5 % CO2 atmosphere.

Drug treatments

iPA was dissolved in DMSO (20 mM) and used at indicated concentrations. For each experiment, fresh dilutions were made from the stock solution and added to cell cultures at the indicated concentrations in serum-containing medium. 5-Itu was used in pre-treatment at a final concentration of 30 nM for 30 min. iPA analogues, as well as IPP, adenine

and isopentenyladenine were dissolved in DMSO and used at indicated concentrations. Also inhibitors and antagonists used were dissolved in DMSO. Human NK cells were stimulated for different time intervals in RPMI 1640 in the presence of IL-2 at 100 U/ml alone or in combination with different concentrations of iPA.

Viability assay

To determine cells viability, we used the colorimetric MTT metabolic activity assay. Cells were cultured in a 96-well plate at 37°C, with or without growth factors, and exposed to various concentrations of iPA, IPP, adenine and isopentenyladenine, as well as iPA analogues for 24 h. To each well, 10 µl of MTT solution (5 mg/ml, in water) was added for 4 h. The resultant formazan crystals were dissolved in 100 µl of solubilization solution (10% Triton X-100 and 0.1 N HC1 in isopropanol), and the absorbance intensity was measured on a microplate reader (ThermoScientific, Basingstoke, UK) at 595 nm with a reference wavelength of 650 nm. All experiments were performed in triplicate, and the relative cell viability was expressed as a percentage comparison with the untreated control cells.

Proliferation assay by BrdU incorporation

Cell proliferation was evaluated by measuring BrdU incorporation into DNA (BrdU colorimetric assay kit; Roche Applied Science, South San Francisco, CA, USA). Endothelial or melanoma cells, pretreated or not with 5-Itu (30 nM, 30 min) or with adenosine receptors antagonists, were treated with increasing concentrations of iPA. Cells were seeded into 96-well plates for the indicated time at 37°C. Newly synthesized BrdU-DNA was determined on an ELISA plate reader (ThermoScientific) at 450 nm.

Liquid chromatography–coupled tandem mass spectrometry (LC-MS/MS) and sample preparation

iPA and iPAMP extraction was performed with ice-cold acetone. Briefly, 4 volumes of ice-cold (-20°C) acetone were added to 100 µl of cell lysate and incubated for 3 h at -20°C, to allow protein precipitation. Then, insoluble proteins were precipitated by centrifugation (10,000 g, 10 min, 4°C), and the supernatant was collected, dried *in vacuo*, and resuspended in 500 µl of H_2O:acetonitrile (1:1) for mass spectrometric analysis. LC-MS/MS analysis was performed with the Accela 600 pump and Accela AutoSampler system equipped with an LTQ-Orbitrap XL mass spectrometer (ThermoScientific). The mixture separation was performed with a Jupiter C4 column (50×2.00 mm; Phenomenex, Torrance, CA, USA) with a linear gradient from 2% of solution A (H_2O and 0.05% acetic acid) to 50% of solution B (acetonitrile and 0.05% acetic acid) for 25 min at a flow rate of 100 µl/min. The electrospray ionization (ESI) ion source was set in positive ion mode, and the capillary temperature was kept at 240°C, with the sheath and the auxiliary gas flow rates set at 8 and 2, respectively. The mass spectrometer was set to operate in selected-reaction monitoring (SRM) mode. The transitions of the protonated iPA and iPAMP to their product ions were recorded at *m/z* 336.1578→204.0476 and at *m/z* 416.1346→204.0675, respectively. The collision energy was set at 30. All experiments were performed in triplicate.

Cell cycle analysis

Endothelial or melanoma cells were plated in 100-mm dishes. To synchronize endothelial cells at the G_1/S interface, they were serum starved in medium with 0.5% serum for 18 h. Cells pretreated or not with 5-Itu (30 nM, 30 min) were treated with iPA. After 24 h, the cells were collected,

fixed in 70% ethanol, and kept at -20°C overnight. Propidium iodide (PI; 50 µg/ml) in PBS containing 100 U/ml DNase-free RNase was added to the cells for 15 min at room temperature. The cells were acquired by a FACSCalibur flow cytometer (BD Biosciences, San Jose, CA, USA). The analysis was performed with ModFit LT v3.2 (Verity Software House, Inc., Topsham, ME, USA); 10,000 events, corrected for debris and aggregate populations, were collected.

Apoptosis analysis

Quantitative assessment of apoptosis was analyzed by anti-human annexin V (BMS147FI; eBioscience, San Diego, CA, USA) and PI staining. Briefly, cells grown in 100-mm dishes were harvested with trypsin and washed in PBS. The cells were resuspended in annexin V binding buffer (10 mM HEPES/NaOH, pH 7.4, 140 mM NaCl, 2.5 mM $CaCl_2$) and stained with annexin V-FITC and then with PI at room temperature for 15 min in the dark. The cells were acquired by flow cytometer within 1 h after staining. At least 10,000 events were collected, and the data were analyzed by CellQuest Pro software (BD Biosciences).

Western blot analysis

Cells treated as described were washed with ice-cold phosphate-buffered saline and scraped into lysis buffer (50 mM Tris-HCl, 150 mM NaCl, 0.5% Triton X-100, 0.5% deoxycholic acid, 10 mg/ml leupeptin, 2 mM phenylmethylsulfonyl fluoride and 10 mg/ml aprotinin). After removal of cell debris by centrifugation (14,500 g for 20 min at 4°C), the proteins were estimated. From 10 to 30 µg of proteins were loaded on 6- 15% SDS–polyacrylamide gels under reducing conditions and then transferred to nitrocellulose membranes. The membranes were blocked with 5% nonfat

dry milk (Bio-Rad, Richmond, CA, USA) and incubated with the specific antibody. After washes, the filters were incubated for 1 h at room temperature with horseradish peroxidase–conjugated secondary antibody. The membranes were stained by using a chemiluminescence system (ECL; Amersham Biosciences, Amersham, UK) and then exposed to X-ray film (Amersham Biosciences). Immunoreactive bands were quantified with Quantity One 1-D analysis software (Bio-Rad). If necessary, the membranes were stripped and reprobed with another antibody.

Wound-healing assay

Confluent HUVEC monolayers were grown on 1% gelatin coated 24-well plates. Endothelial cells, pretreated or not with 5-Itu (30 nM, 30 min), were treated with increasing concentrations of iPA and wounded with a 200-µl tip. Images of wound closure were captured with a phase-contrast microscope (AF6000 LX; Leica Microsystems GmbH, Wetzlar, Germany) in time-lapse video microscopy every 10 min with the Leica LAS AF software (×10). The width of the wound from each image was measured at selected time points (0, 6, 12, and 24 h) with ImageJ 1.45 software (U.S. National Institutes of Health, Bethesda, MD, USA). The degree of wound regeneration was calculated as the percentage of the remaining cell-free area compared with the vehicle control.

Endothelial cell gel invasion assay

A Matrigel (BD Biosciences, San Jose, CA, USA) invasion assay was performed using cell culture inserts (3.0 µm) for 24-well plates (BD Falcon; BD Biosciences) coated with Matrigel (300 µg/ml) diluted in a coating buffer (0.01 M Tris and 0.7% NaCl, pH 8) for 2 h at 37°C. Endothelial cells were stained with the fluorescent probe CFSE (3µM) and

seeded (6×10^3 cells/well) on cell culture inserts in 250 µl of serum-free medium. The lower compartments were filled with M199 medium (10% FBS) containing complete angiogenic factors as a chemotactic stimulus. The cells were treated with increasing concentrations of iPA, with or without 5-Itu pretreatment (30 nM, 30 min). After incubation of the cells for 18 h at 37°C, serial micrographs (9 microscopic fields/well) of invading cells were obtained with an inverted fluorescence microscope (AF6000 LX; Leica) at ×10. The cells were quantified by ImageJ 1.45 software. Background levels of invading cells in the absence of chemotactic factors (chemokinesis) were subtracted from all the experimental points.

Capillary-like tube formation on gel

Prechilled 48-well plates were coated with Matrigel, which was allowed to polymerize for 30 min at 37°C. Endothelial cells, pretreated or not with 5-Itu (30 nM, 30 min), were seeded (1×10^4 cells/well) in 250 µl of complete medium. iPA at the indicated concentrations was added. After 6 h, capillary-like tube formation was examined under an inverted phase microscope (×4) and photographed. The number of network intersections was quantified by ImageJ 1.45 software.

Gel plug angiogenesis assay

Liquid gel (Cultrex BME Growth Factor Reduced; Trevigen, Gaithersburg, MD, USA) was prepared at 4°C and combined with iPA (5 µM), IPP (5 µM), or 5-Itu (30 nM) in the presence or absence of FGF2 (27 nM) and injected subcutaneously (0.5 ml/mouse) into the flank of 6–8-wk-old C57BL/6 mice (Charles River, Calco, Italy). Cultrex with PBS alone was used as a negative control. At 1 wk after injection, the mice were euthanized, and the plugs were harvested, weighed, and processed for RT-

qPCR analysis. When specified, the harvested plugs were divided into halves: one half underwent RT-qPCR analysis, and the other half was embedded in Tissue Tec optimal cutting temperature (OCT) compound (Sigma-Aldrich), snap-frozen by immersion in liquid nitrogen-cooled isopentane, and analyzed by immunofluorescence microscopy. Immunofluorescence was performed on 5-µm frozen sections by staining with anti-CD31 antibody (red) and DAPI (blue). The sections were examined under an Axioplan 2 epifluorescence microscope (Carl Zeiss Microscopy, Thornwood, NY, USA) at ×200.

Endothelial-melanoma cells co-culture

A co-culture was performed using cell culture inserts (0.9 µm) for 12-well plates (BD Falcon; BD Biosciences). Endothelial cells were seeded (6×10^3 cells/cm^2) on 12-well plates, while melanoma cells (2×10^5 cells/cm^2) were seeded on cell culture inserts and treated with increasing concentrations of iPA (1-10 µM). After incubation of the cells for 24 h at 37°C, inserts were placed in 12-well plates containing the endothelial cells for 24 h of co-culture. Endothelial cells were then fixed and stained with crystal violet (0.5% w/v in methanol 20%) and solubilized with a solution of acetic acid (33% in water). The absorbance intensity was measured on a microplate reader (ThermoScientific, Basingstoke, UK) at 570 nm.

Tumor clonogenic assay

Melanoma cells were seeded in 6-well plate (200 cells/well) and treated at time 0 h with increasing concentrations of iPA alone (1-10 µM) with or without the pre-treatement with 5-Itu (30 nM, 30 min) and monitored for ten days. Colonies are fixed and stained with crystal violet (0.5% w/v in methanol 20%) and photographed.

Flow cytometric analysis of autophagy

Briefly, melanoma cells grown in 100-mm dishes were harvested with trypsin and washed in PBS. The quantification of acidic vesicular organelles (AVO), as a marker of autophagy, was detected by staining melanoma cells (1×10^4) with lysosomotropic agent acridine orange (2 μg/ml) for 15 min at 37°C. LysoTracker-Red DND-99 (excitation/emission, 577/590 nm), a red-fluorescent dye for labeling and tracking acidic organelles in live cells, was added to melanoma cells at a final concentration of 50 nM for 30 min at 37°C. The cells stained were measured by flow cytometry (Flow Cytometer, BD Biosciences, San Jose, CA, USA). For autofluorescence, cells were analyzed without any staining. The data were analyzed by FlowJo software (TREE STAR, Inc., San Carlos, CA).

Proliferation assay by CFSE incorporation

Proliferation was assessed by flow-cytometric analysis of CFSE (Molecular Probes, Eugene, Oregon) dilution as described. To this end freshly isolated human NK cells were labeled by incubation at 5×10^6/ml in PBS with 3μM CFSE at 37° for 10 min under gentle agitation, washed and resuspended in RPMI 1640 complete culture medium and cultured at the concentration of 4×10^5 cells/well in a round bottom, 96-well plate. Stimulation was effected by addition of IL-2 at 100 U/ml alone or in combination with different concentrations of iPA for different time intervals (3-8-10 days). A portion of the population was arrested at the parent generation using mitomycin C (Sigma-Aldrich). All data were acquired by CellQuest Pro software while the percentage of total proliferated NK cells, the maximum number of cells division, and the numerical values for proportions of proliferated cells at each cell division

were obtained by using ModFit LT software (Verity Software House, USA).

mAbs and cytofluorimetric analysis

NK phenotype was assessed by flow cytometry. Fluorochrome-conjugated monoclonal antibodies (mAbs) against CD56, CD3, CD69, CD107a, NKp30, NKp44, NKp46, NKG2D, as well as the corresponding isotype immunoglobulin of control were purchased from BD Biosciences (San Diego, CA, USA). Data were collected using a FACSCalibur flow cytometer (Becton Dickinson, USA) and analyzed by CellQuest Pro program (Becton Dickinson, San Jose, CA). Data are expressed as logarithmic values of fluorescence intensity.

Flow cytometric assay of NK-cell cytotoxicity

Purified NK cells of healthy donors were stimulated with IL-2 in the presence or absence of iPA and then used as effectors against K562 human cell line using CFSE NK cytotoxicity assay. Briefly, the K562 target cells were labeled with CFSE. Target cells were mixed with effector cells at different E:T ratios and incubated at 37° C for 4 hours in 96-well round-bottom plates in a final volume of 200 µl of RPMI 1640 complete medium per well. In parallel, target cells were incubated alone to measure spontaneous cell death. At the end of the incubation time, the total contents of the U bottom plate were transferred to Falcon tubes, put in ice and incubated with PI 30 µg/ml for 5 min, followed by flow cytometric analysis within 1 h. During data acquisition, "a live gate" was set on CFSE-stained target cells population using an FL1-histogram, and 5000 target events were collected. For data analysis, target cells (R1) were further analyzed in a F1/F3 dot plot where dead target cells (CFSE+PI+) were visualized on upper right quadrant. The percentage of target cell

death (cytotoxicity) was calculated as follows:

$$\text{Cytotoxicity}(\%) = \frac{\text{Dead target cells in the sample}(\%) - \text{Spontaneously dead target cells}(\%)}{100 - \text{Spontaneously dead target cells}(\%)} \times 100$$

CD107a mobilization assay

Activated NK cells were cultured in complete medium with or without K562 cells at 1:1 E:T ratio in the presence of PE-conjugated CD107a/IgG1 antibody (BD Pharmingen) in U bottom 96 well plates. After 1 h, Brefeldin A (5μg/ml, Sigma-Aldrich St. Louis, MO, USA) was added to cultures for an additional 3 h of incubation. At this time cells were collected, washed with PBS with 2% FBS, stained with anti-CD56 PE-Cy5 (BD Biosciences), anti-CD3 FITC (BD Biosciences) and analyzed by flow cytometry.

Cytokines secretion measurements

Purified NK cells were stimulated with IL-2 in the presence or absence of iPA. After 18h activated NK cells ($2x10^5$) were washed twice and mixed with 4×10^5 K562 cells in 200μl of complete medium. Cells were incubated for the indicated time. Thereafter, supernatants were collected and stored at -20°C pending measurement while cell pellets were analyzed for the surface expression of CD69 NK activating marker. The concentration of IFN-γ was measured by ELISA assay according to manufacturer's specification (R&D Systems and Biosource International) while the concentrations of TNF-α, RANTES, MIP-1α were quantified by a multiplex immunoassay (Fluorokine MAP cytokine multiplex kits, R&D Systems and Biosource International) according to manufacturer's instructions.

Farnesyl diphosphate synthase assay

Cells were washed twice with 1 ml ice-cold PBS and scraped in 0.2 ml ice-cold lysis buffer (Imidazol 40 mM and DTT 50 mM). The cell lysate was centrifuged at 10000 rpm for 5 min and the supernatant was used for FDPS assay. FDPS was assayed in 150 µl containing 25 mM HEPES, pH=7.4, 2 mM MgCl2, 1 mM dithiothreitol, 5 mM KF, 1% n-octyl-β-glycopyranoside, 3.3 µM [4-14C] IPP (18 Ci/mmol), 3 µM unlabeled IPP and 20 µM geranyl diphosphate. Reactions were started adding 40 µl of lysate containing 100 µg of total protein and incubated for 45 min at 37°C. Reactions were stopped by the addition of 150 µl 2.5 N HCl in 80% ethanol containing 100 µg/ml farnesol as a carrier. The samples were hydrolyzed for 30 min at 37°C to convert the FDP to farnesol and neutralized by the addition of 150 µl of 10% NaOH. The reaction product (farnesol) was extracted into 1 ml of n-hexane and an aliquot (200 µl) of the organic phase was used for radioactivity counting. One unit of enzyme activity is defined as the amount of enzyme required to synthesize 1 pmol of FDP/min. Parallel samples were assayed to evaluate the total and the non-specific radioactivity. In all experiments, enzyme assays were carried out in duplicate. The coefficient percentages (CV%) of intra- and inter-assay variation were 3% and 4%, respectively.

RAS-GTP selective precipitation

Ras-GTP was identified by precipitation with Gst-tagged Raf1-RBD (Ras Activation Assay Kit; Cytoskeleton Inc., Denver, CO, USA) followed by immunoblotting. Cellular lysates were prepared according to the manufacturer's instructions. The following antibodies were used: mouse monoclonal anti-human pan-Ras (Sigma-Aldrich Inc St Luis, MO, USA or Cytoskeleton Inc.), rabbit monoclonal anti-human phospho-STAT5 (p-

STAT5; Tyr 694), rabbit polyclonal anti-human STAT5, rabbit monoclonal anti-human phospho-p44/42 MAPK (p-ERK, Thr202/Tyr 204), rabbit monoclonal anti-human p44/42 MAPK, mouse monoclonal anti-human phospho-p38 MAPK (Thr180/Tyr182) and rabbit monoclonal anti-human p38 MAPK (Cell Signaling Technology, Danvers, MA), rabbit polyclonal anti-human β-actin and rabbit polyoclonal anti-human FDPS (Abcam, Cambridge, UK).

Statistical analysis

Statistical computations were performed with Prism 6.0 software (GraphPad, San Diego, CA, USA). Data obtained from multiple experiments were calculated as means ± SD and analyzed for statistical significance by using the 2-tailed Student t-test, 1- or 2-way ANOVA for independent groups, with the Tukey or Bonferroni correction for multiple comparisons. Values of $P < 0.05$ were considered statistically significant.

4. RESULTS

4.1 iPA inhibits endothelial cell proliferation

To investigate the effects of iPA (Fig. 7*A*) on the angiogenesis process, we used, as a common model of angiogenesis *in vitro*, HUVEC cells stimulated with proangiogenic growth factors or in a quiescent state, for comparison. First, we evaluated cell viability by the MTT assay. The treatment of endothelial cells for 24 h with increasing concentrations of iPA (0.3–20 µM) inhibited viability in a dose-dependent manner (IC50 0.98 µM; Fig. 7*B*). Up to 5 µM, iPA showed an inhibitory effect on the viability of endothelial cells that was specific for cells stimulated by pro-angiogenic factors *vs* quiescent cells. Only the highest concentrations of iPA tested (>10 µM) exerted a slight cytotoxic effect inhibiting also the viability of quiescent endothelial cells. Then, to evaluate whether iPA inhibits the proliferation rate of endothelial cells, we performed a more sensitive BrdU proliferation assay in a kinetic analysis at 24 and 48 h. iPA induced a concentration-and time-dependent block of proliferation (IC50 0.67 µM; Fig. 7*C*); after a treatment of 48 h, a near-total ablation of proliferation was clear at concentrations as low as 1.25 µM (Fig. 7*D*). From these data, we selected the 1- to 10-µM range and the 24-h maximum time point of iPA treatment for all further experiments.

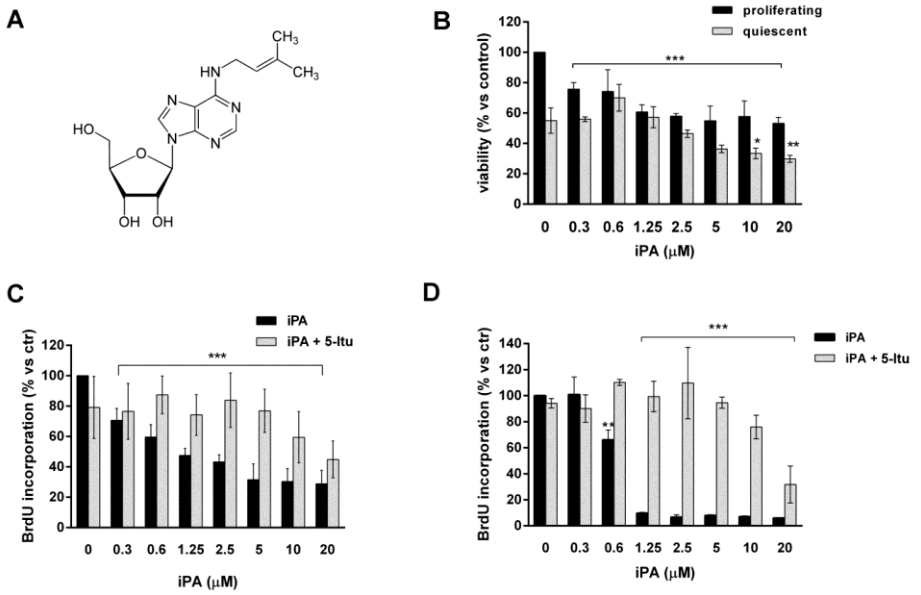

Figure 7. iPA inhibited endothelial cell proliferation. *A*) Structure of iPA. *B*) Histogram shows the inhibition of the viability of endothelial cells treated with increasing concentrations of iPA (0.3–20 μM) and stimulated (solid bars) or unstimulated (shaded bars) with proangiogenic growth factors for 24 h, evaluated by MTT assay. *C, D*) Inhibition of proliferation of endothelial cells, pretreated or not with the ADK inhibitor 5-Itu (30 nM, 30 min), was confirmed by a BrdU proliferation assay for 24 h (*C*) and 48 h (*D*). Results are expressed as means ± SD of 3 independent experiments performed in triplicate. **P* < 0.05, ***P* < 0.01, ****P* < 0.001 *vs* control (cells untreated or treated without 5-Itu: ANOVA).

4.2 The peculiar structure of iPA is responsible for the antiproliferative effects on endothelial cells

Since iPA is a modified adenosine characterized by an isopentenyl chain linked to the nitrogen at position 6 of the purine base, we evaluated, by comparison, the effects of structural analogues of iPA to understand whether the observed effects of iPA were ascribable to the purine base or to the isopentenyl chain, in order to identify the portion of the molecule responsible for the anti-proliferative effect observed in endothelial cells. We therefore evaluated, by MTT viability assay, the effects of isopentenylpyrophosphate (IPP), adenine and N6-isopentenyladenine (Fig.

8 *A-C*). Whereas adenosine is already known to stimulate angiogenesis (Auchampach, 2007), neither IPP, adenine nor isopentenyladenine affected endothelial cell viability (Fig. 8). These data suggest that the antiproliferative effects of iPA cannot be ascribed to the isoprenoid chain alone or to the purine group, but are due to the peculiar structure of iPA composed of the specific combination of the adenosine moiety and the isopentenyl chain. Thus, depriving the overall structure of iPA of its individual components, namely ribose, adenine and isopentenyl chain, the molecule loses its activity.

As described above, iPA has no activity *in vivo* when administered intraperitoneally because of pharmacokinetic instability (Colombo et al., 2009). In order to find iPA analogues with a major stability *in vivo*, a series of iPA analogues differently substituited in N6 position were synthesized by the group of Prof. Ciuffedra (Ottria et al., 2010). Among these, we tested adenosine analogues characterized by a phenyl ring in N6 position (CM 223), or isopentyl (CM 224), or allylic (CM 226) or butyl (CM 227) chain. The Figure 9 shows the effects of these structural synthetic analogues on the viability of the endothelial cells. Whereas CM 224 did not exerted any effect on endothelial cell viability (Fig. 9*B*), CM 223 resulted to be cytotoxic on proliferating and quiescent endothelial cells (Fig. 9*A*). The compounds CM 226 and 227, harbouring respectively allylic and butyl chain, were less potent compared to iPA, inhibiting endothelial cells viability in a reduced range of the concentrations (Fig. 9*C-D*).

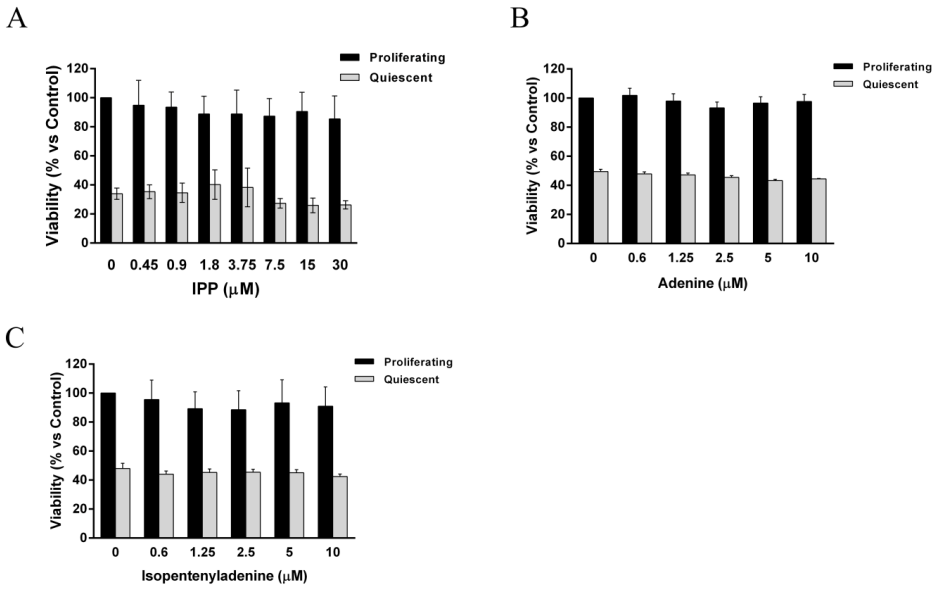

Figure 8. Peculiar structure of iPA was responsible for the antiproliferative effects on endothelial cells. Histograms show the effects on the viability of endothelial cells treated with increasing concentrations of the (*A*) IPP (7.5–30 μM), (*B*) nitrogenous base adenine (0.6–10 μM) and (*C*) N6-isopenteyladenine stimulated (solid bars) or unstimulated (shaded bars) with proangiogenic growth factors for 24 h, evaluated by MTT assay. Results are expressed as means ± SD of 2 independent experiments performed in triplicate, ANOVA.

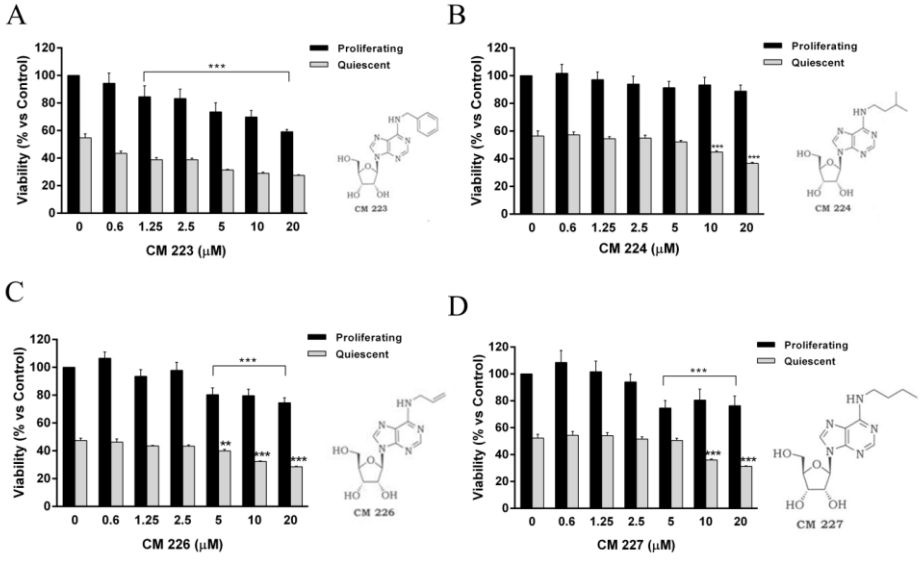

Figure 9. N6-substituted iPA derivatives were less active compared to iPA. Histograms show the effects of adenosine analogues characterized by a phenyl ring in N6

position (CM 223, *A*), or isopentyl (CM 224, *B*), allylic (CM 226, *C*) or butyl (CM 227, *D*) chain on the viability of the endothelial cells stimulated (solid bars) or unstimulated (shaded bars) with proangiogenic growth factors for 24 h, evaluated by MTT assay. Results are expressed as means±SD of 2 independent experiments performed in triplicate. $^{**}P < 0.01$, $^{***}P < 0.001$ *vs.* control (cells untreated), ANOVA.

In the light of the results obtained by our research group and by others (Ottria et al., 2010), we are able to have a basic possible structure-activity relationship of iPA (Fig. 11), indispensable to better understand which portion of the structure has to be preserved in order to synthesize new and more potent analogues of iPA able to have a long plasma half-life, useful to the *in vivo* administration.

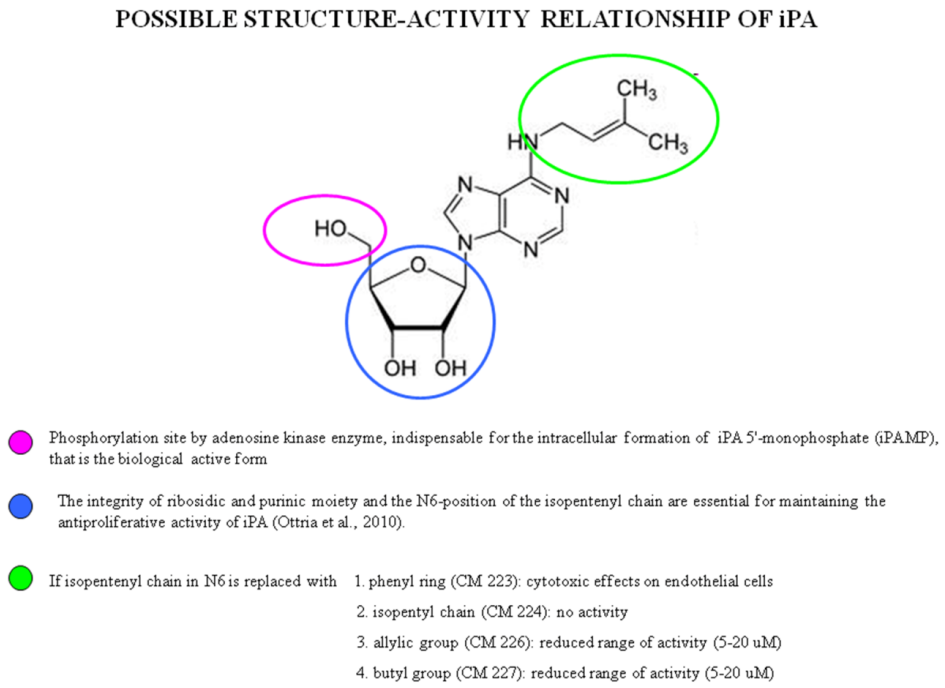

Figure 10. Possibile structure-activity relationship of iPA

4.3 The classical adenosine pathways are not involved in biological effects exerted by iPA

Since iPA is a derivative of adenosine and so it could potentially bind to adenosine receptors to exert its biological effects on endothelial cells, we

treated cells with different antagonists of adenosine receptors and inhibitors of adenosine uptake.

Based on mRNA levels and stimulation of adenylate cyclase, HUVEC cells have been reported to preferentially express A2A adenosine receptors, while microvascular cells express A2B. Neither cells expressed A1 or A3 receptors (Feoktistov et al., 2002). Both the A2A and A2B receptors are however thigtly implicated with angiogenesis (Auchampach, 2007). To verify whether iPA could be recognized as adenosine by cells interacting thus with adenosine receptors, that are G-protein coupled receptors, in the extracellular environment, we pre-treated endothelial cells with specific and selective A2A and A2B antagonists, respectively ZM241385 (1 µM, 30 min) (Fig. 11*A*) and PSB1115 (1 µM, 30 min) (Fig. 11*B*). The pre-treatment with these antagonists did not affect in any way the inhibitory effects of iPA on endothelial cells proliferation, therefore excluding their involvement in the action of iPA at least in this model.

To evaluate if iPA could be substrate of the adenosine deaminase, an enzyme involved in purine metabolism, we also pre-treated endothelial cells with erythro-9-(2-hydroxy-3-nonyl) adenine (EHNA, 10 µM, 30 min), an inhibitor of this enzyme, and then we added iPA at increasing concentrations (Fig. 11*C*). Moreover, since the passage of nucleosides across plasma membranes or between intracellular compartments occurs primarily *via* specialized nucleoside transporter proteins (King et al., 2006), to assess whether iPA needs to be transported into the cell via these transporters, in particular those sensitive to dipyridamole, we used in pre-treatment dipyridamole (10 µM, 30 min), a pharmacological inhibitor of nucleoside transporters (Fig. 11*C*). The graph clearly shows that iPA is not a substrate of adenosine deaminase since the antiproliferative action of iPA did not decrease following the inhibition of this enzyme. Moreover, not even the inhibition of nucleoside transporters was able to revert inhibitory

effects of iPA, suggesting that iPA is not recognized as nucleoside and is not transported into the cell through dipyridamole-sensitive adenosine carriers (Fig. 11*C*).

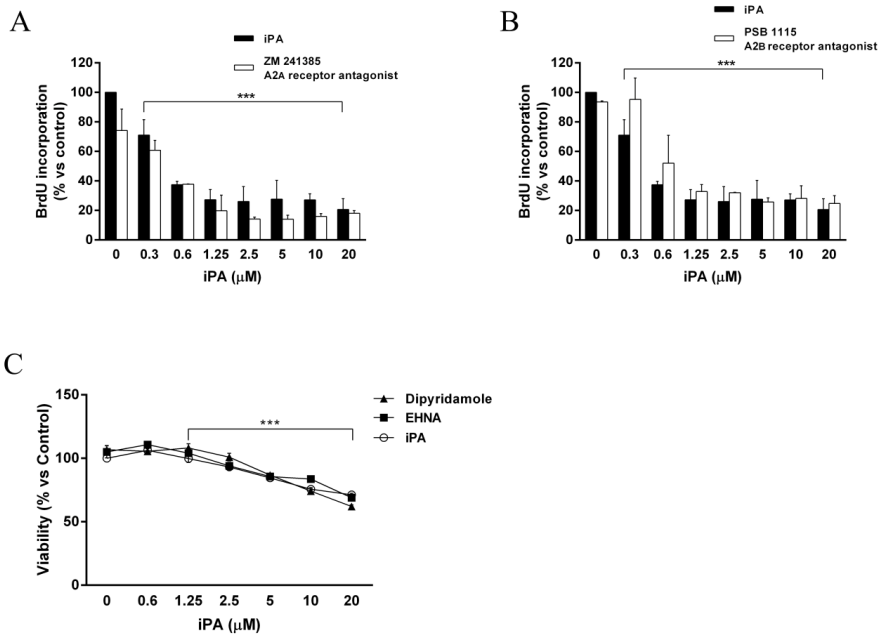

Figure 11. **iPA did not act as an adenosine mimetic.** iPA is not recognised as adenosine mimetic, since neither the A2A receptor (ZM 241385, 1 μM, 30 min *A*) nor the A2B receptor (PSB 1115, 1 μM, 30 min *B*) antagonists were able to revert the antiproliferative effect of iPA in endothelial cells, as showed by BrdU proliferation assay. iPA is not catabolised by adenosine deaminase and does not entry into the cells by dipyridamole-sensitive nucleoside transporters, since EHNA (inhibitor of adenosine deminase, 10 μM, 30 min) and dipyridamole (inhibitor of nucleoside transporters, 10 μM, 30 min) did not affect the effect of iPA on the endothelial cells viability (*C*). Results are expressed as means±SD of 2 independent experiments performed in triplicate. ***$P < 0.001$ *vs.* control (cells untreated or treated with iPA), ANOVA.

4.4 iPA must be phosphorylated into iPAMP to exert its biological effects through AMPK activation

To understand the molecular mechanism by which iPA exerts its antiproliferative effects, we pretreated endothelial cells with 5-Itu, an ADK inhibitor (*k*i=30 nM). We wanted also to evaluate whether iPA is a

substrate of this enzyme. 5-Itu-pretreated endothelial cells (30 nM, 30 min) were exposed to increasing concentrations of iPA for 24 and 48 h (Fig. 7*C*, *D*). Of note, we found that 5-Itu pretreatment completely reversed the inhibitory effect of iPA on endothelial cells proliferation at each concentration tested, suggesting that iPA must be phosphorylated into iPAMP by ADK inside the cell to exert its inhibitory effects on endothelial cells. To demonstrate the effective formation of iPAMP, we analyzed the intracellular levels of iPA and iPAMP by LC-MS/MS. Cells were treated with iPA at different time points (0, 1, and 3 h), as reported above. Treated and untreated samples were lysed and subjected to a protein precipitation procedure, to isolate cell metabolites before LC-MS/MS analysis, performed in SRM mode. Two chromatographic peaks were obtained for iPA and iPAMP at 15.2 and 0.9 min retention time, respectively, and then integrated to give the areas reported in Fig. 12. iPA was efficiently internalized (Fig. 12*A*) and converted into iPAMP (Fig. 12*B*) in a time-dependent manner. Moreover, to demonstrate that iPA is converted within the cells into iPAMP by ADK, we treated the cells with 5-Itu before iPA administration and then performed an MS analysis, as previously shown.

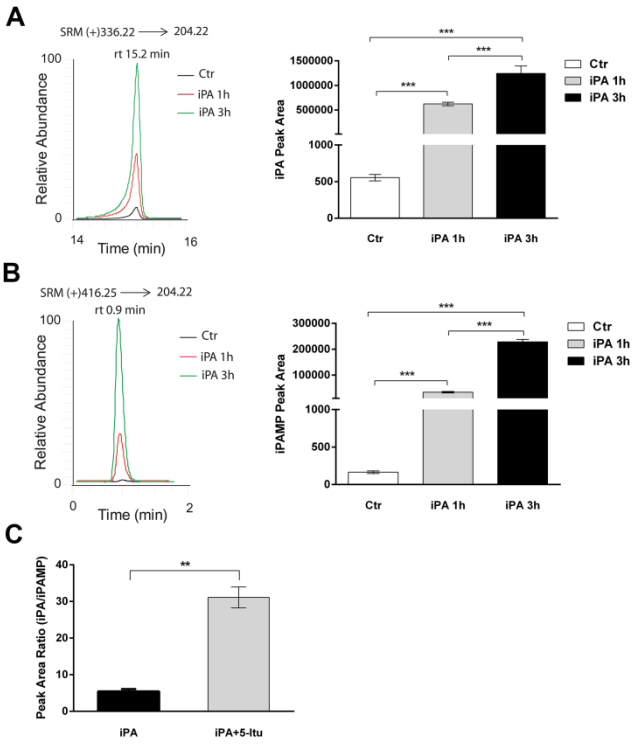

Figure 12. iPA was effectively converted in its monophosphorylated form, iPAMP, inside the cells. *A*, *B*) Overlapping chromatographic peaks (left panel) and the corresponding peak areas (right panel) of iPA (*A*) and iPAMP (*B*), obtained after different incubation times by LC-MS/MS in SRM mode. *C*) iPA/ iPAMP species ratio in cells treated with iPA alone and subjected to 5-Itu pretreatment. Results are expressed as means ± SD of results of 3 independent experiments performed in triplicate. $^{**}P < 0.01$, $^{***}P < 0.001$; ANOVA.

Our results clearly showed a strong incremental change in iPA/iPAMP ratio as a consequence of ADK inhibition. Indeed, as reported in Fig. 12*C*, the iPA/iPAMP ratio moved from 5:1 to 30:1 when the cells were pretreated with 5-Itu to inhibit ADK activity. We also observed that iPA internalization was slightly decreased by 5-Itu pretreatment (data not shown). These data, taken together, demonstrate that 5-monophosphorylation of iPA to form iPAMP, catalyzed by ADK, is indispensable for the activity of iPA and that iPAMP is therefore responsible for all the biological effects observed.

As proof of the correlation between iPAMP and AMP the treatment of endothelial cells with increasing concentrations of iPA (1–10 μM) resulted in persistent, dose- and time-dependent increases in AMPK activity, as reflected by the phosphorylation induction of AMPK-α catalytic subunit (Fig. 13). Induction of AMPK activity was detected as early as 6 h after iPA administration and remained elevated during 24 h of iPA exposure. Furthermore, the increase in AMPK activity was completely reversed by 5-Itu pretreatment. AMPK is therefore a biochemical target of iPA in endothelial cells.

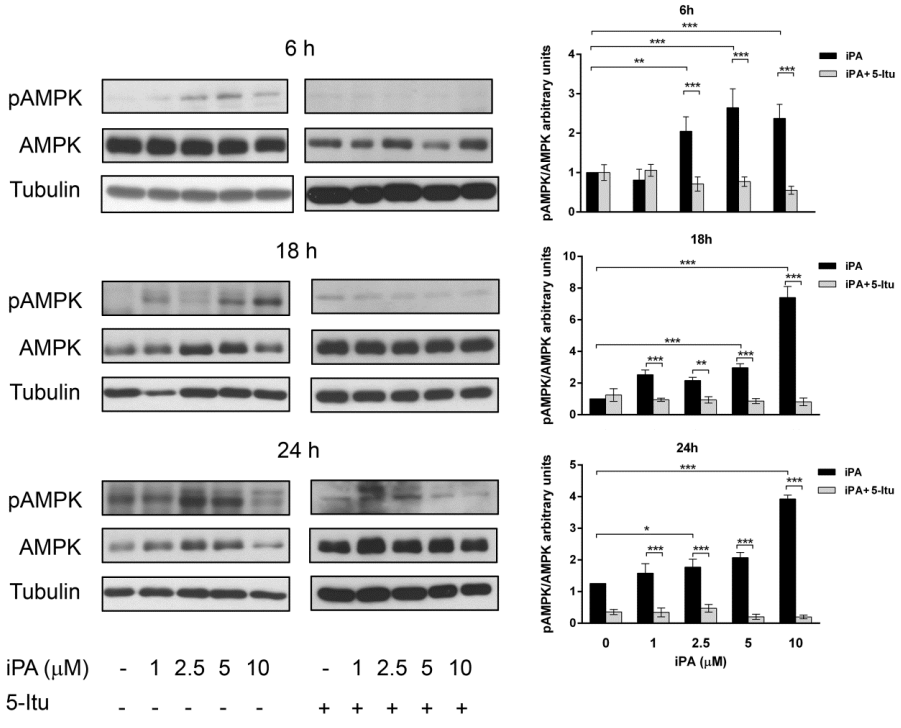

Figure 13. iPA activated AMPK, inducing its phosphorylation. Dose- and time-dependent increase in AMPK activity was analyzed by Western blot. Endothelial cells, grown in serum containing medium, were treated with iPA at the indicated concentrations, with or without 5-Itu pretreatment (30 nM, 30 min) for 6, 18, and 24 h. Tubulin served as the loading control. Blots were stripped and reprobed with the different antibodies. Data are representative of 3 different experiments with similar results. Histograms (right panels) report the results of the quantitative analysis (arbitrary units, pAMPK/ AMPK/tubulin) as means ± SD of 3 independent experiments. **P* <0.05, ***P* < 0.01, ****P* < 0.001 *vs.* control or treatment without 5-Itu; ANOVA.

4.5 iPA induces S-phase stasis and apoptosis, activating the intrinsic caspase cascade and DNA damage machinery

To investigate the nature of the antiproliferative action of iPA, we evaluated its effect on the progression of the endothelial cell cycle by flow cytometry, analyzing the distribution of cells in the different phases of cell cycle at increasing times in iPA-treated cells, pretreated or not with 5-Itu (30 nM, 30 min), in comparison with untreated cultures. Results in Fig. 14*A* (bottom panels) showed that treatment of endothelial cells with 5 and 10 μM of iPA for 24 h resulted in an increase in cells in the S phase, compared with that in the control-treated cells. The S-phase stasis induced by iPA was completely reversed by 5-Itu pretreatment, demonstrating also that the S-phase block was mediated by the iPAMP derivative. Beyond the S-phase stasis, we observed that the treatment of iPA at 5 and 10 μM was associated with the appearance of a cell population with a reduced DNA content (hypodiploid), usually referred to as sub-G_0, characteristic of apoptosis. To confirm the induction of apoptosis, we performed an annexin V binding assay in endothelial cells treated with increasing concentrations of iPA, pretreated or not with 5-Itu (30 nM, 30 min). As shown in Fig. 14*B*, both annexin V-positive (early apoptotic cells, bottom right quadrant) and annexin-PI double-positive cells (late apoptotic cells, top right quadrant) were significantly increased in cells treated with 5 and 10 μM iPA (5 μM, 20.2±5.1 and 11.3±2.5%; 10 μM, 23.5±11.4 and 25.8±9.7%, respectively), compared to untreated cells (3.8±0.8 and 4.6±1.1%, respectively) (Fig. 14*B*). The results confirmed apoptosis induction by iPA. Also in this case, phosphorylation into iPAMP was essential in the induction of apoptosis, since the pretreatment with 5-Itu restored the control conditions. To corroborate the proapoptotic effect of iPA, we examined the expression of caspases and key proteins that play essential

roles in apoptosis induction. Treatment with iPA strongly induced the expression of cleaved caspase-9 and -3, as well as cleaved PARP, in a time- and concentration-dependent manner (Fig. 14*C*). We therefore demonstrated that iPA activated the intrinsic caspase cascade, leading to caspase-9 cleavage followed by caspase-3 activation that resulted in PARP-1 cleavage and execution of the apoptotic cell program. To investigate whether iPA induces cell cycle arrest and apoptosis after the activation of typical DNA damage checkpoints, such as the ATR-Chk1 pathway and p53, we analyzed the phosphorylation and hence activation of ATR at Ser428, Chk1 at Ser296, p53 at Ser15, and histone H2AX at Ser139. We found that iPA elicited the phosphorylation of all these proteins in a concentration-dependent manner, suggesting involvement of the DNA damage pathways in the proapoptotic effects elicited (Fig. 14*D*).

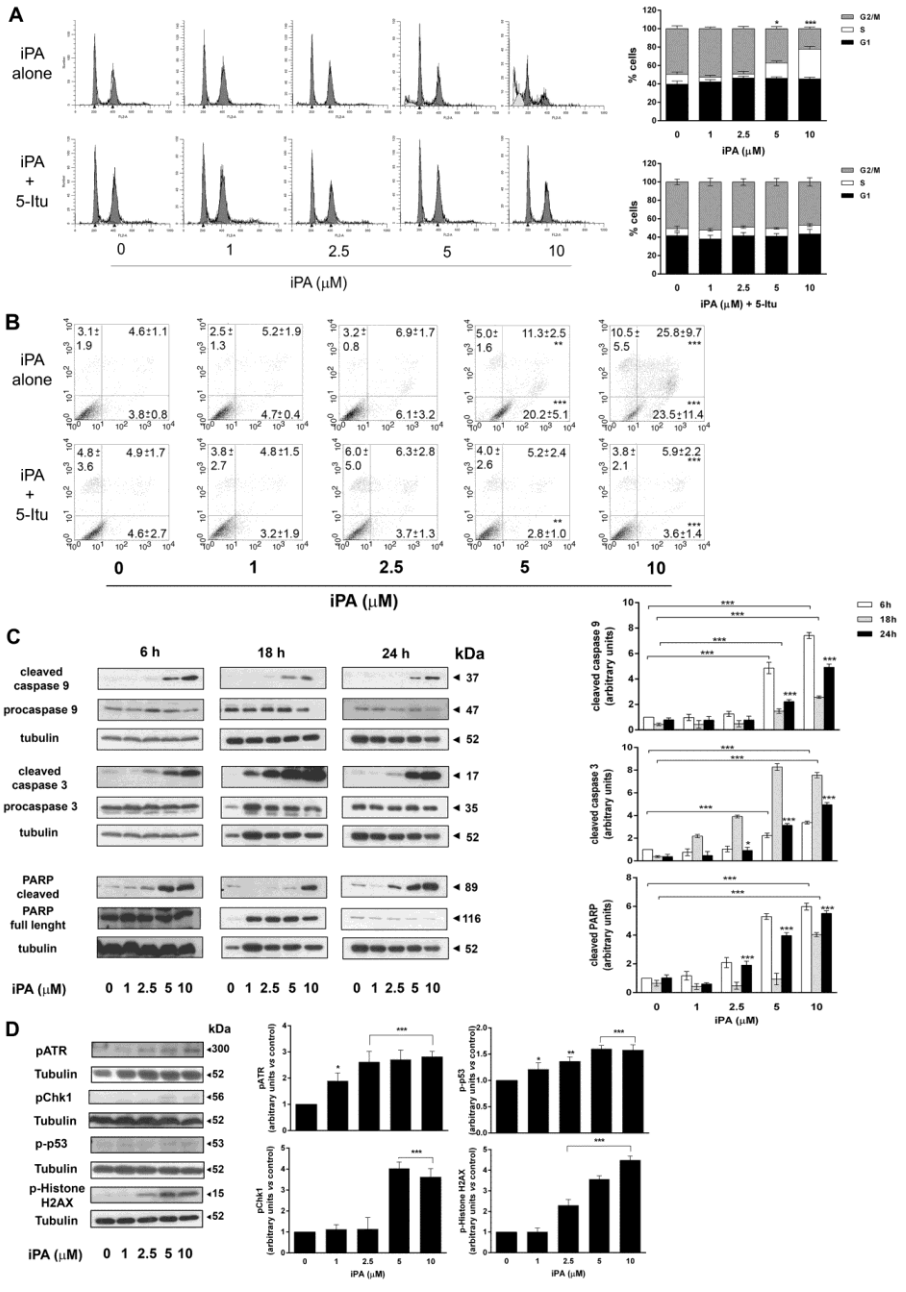

Figure 14. iPA induced S-phase stasis of endothelial cells and apoptosis via caspases and DNA damage. *A*) Distribution of endothelial cells in the different phases of the cell cycle in iPA-treated (1–10 μM) cells, pretreated or not with 5-Itu (30 nM, 30 min), and in parallel untreated cultures. Histograms show results of the quantitative analysis of cells in each phase of the cell cycle, expressed as a percentage. Results are representative of 3 independent experiments performed in duplicate and are expressed as means ± SD. **P* <0.05, ****P* < 0.001 *vs.* control; ANOVA. *B*) Annexin V binding assay in endothelial cells treated with iPA (1–10 μM), pretreated or not with 5-Itu (30 nM, 30 min). Panels

show quantitative analysis of annexin V-positive cells (apoptotic cells, bottom right quadrant), PI-positive cells (necrotic cells, top left quadrant), and annexin-PI positive cells (late apoptotic cells, top right quadrant). Results are representative of 3 independent experiments performed in duplicate and are expressed as means ± SD. $**P < 0.01$, $***P < 0.001$ *vs.* control or treatment without 5-Itu; ANOVA. *C*) Concentration- and time-dependent increase of the intrinsic apoptosis pathway by expression of cleaved caspase-3 and -9, as well as of cleaved PARP, determined by Western blot analysis. Endothelial cells, grown in serum-containing medium, were treated with iPA (1–10 μM) for 6, 18, and 24 h. Tubulin served as the loading control. Same tubulin is shown for filters that were stripped and reprobed with different antibodies. Data are representative of 3 independent experiments. Histograms (right panels) report the quantitative analysis (arbitrary units) expressed as means ±SD of 3 independent experiments with similar results. $*P < 0.05$, $***P < 0.001$ *vs.* control; ANOVA. *D*) Analysis of the DNA damage pathway. Endothelial cells, grown in serum-containing medium, were treated with iPA (1–10 μM) for 1 and 18 h. Phosphorylation of ATR at Ser428, Chk1 at Ser296, p53 at Ser15, and histone H2AX at Ser139 were determined by Western blot analysis at 1 h (p-ATR and p-Chk1) and 18 h (p-p53 and p-HistoneH2AX). Tubulin served as the loading control. Histograms (right panels) report the quantitative analysis (arbitrary units) expressed as means ± SD of 3 independent experiments with similar results. $***P < 0.001$ *vs.* control; ANOVA.

4.6 iPA inhibits endothelial cell migration, invasion, and capillary network formation

Angiogenesis involves the formation of new microvessels, their growth and stabilization, and a series of phases besides proliferation that include migration of endothelial cells toward an angiogenic stimulus, invasion into the extracellular matrix, and proliferation and organization into 3-dimensional tube-like structures. To assess whether iPA influences not only the proliferation but also the migratory and invasive properties of endothelial cells, we performed the wound-healing and Matrigel invasion assays, respectively. A monolayer of endothelial cells was scratched with a pipette tip, and the subsequent closure of the wounded area was monitored every 10 min by time-lapse video microscopy, to evaluate the capacity for cell migration. Control endothelial cells forming the boundaries of the wound migrated, filling the wound within 24 h. Treatment with iPA at all concentrations inhibited endothelial cell migration and therefore did not allow the healing of the wound at 24 h (Fig. 15*A*, *B*). The invasion of the

endothelial cells through the extracellular matrix was also inhibited by iPA in a concentration-dependent manner, as demonstrated by the count of CFSE-positive endothelial cells that invaded the Matrigel coating (Fig. 15*C*). It was clear once again that these effects were attributable to iPAMP, because the pretreatment of endothelial cells with 5-Itu reversed almost completely the anti-migratory and anti-invasive effects of iPA at all concentrations, allowing wound closure within 24 h and the invasion of the Matrigel coating (Fig. 15*A*–*C*). Afterward, iPA was tested for its effect on the morphologic differentiation of endothelial cells into tube-like structures, another endothelial cell property that is fundamental to angiogenesis. A 2-dimensional tube formation assay was performed by plating endothelial cells into a Matrigel coat, which replicates *in vitro* the conditions that best mimic the microenvironment that allows the differentiation of the capillaries. The angiogenic response was assessed by quantification of the capillary network that was formed in a 2-dimensional matrix of Matrigel in the presence of complete proangiogenic medium after 5 h.

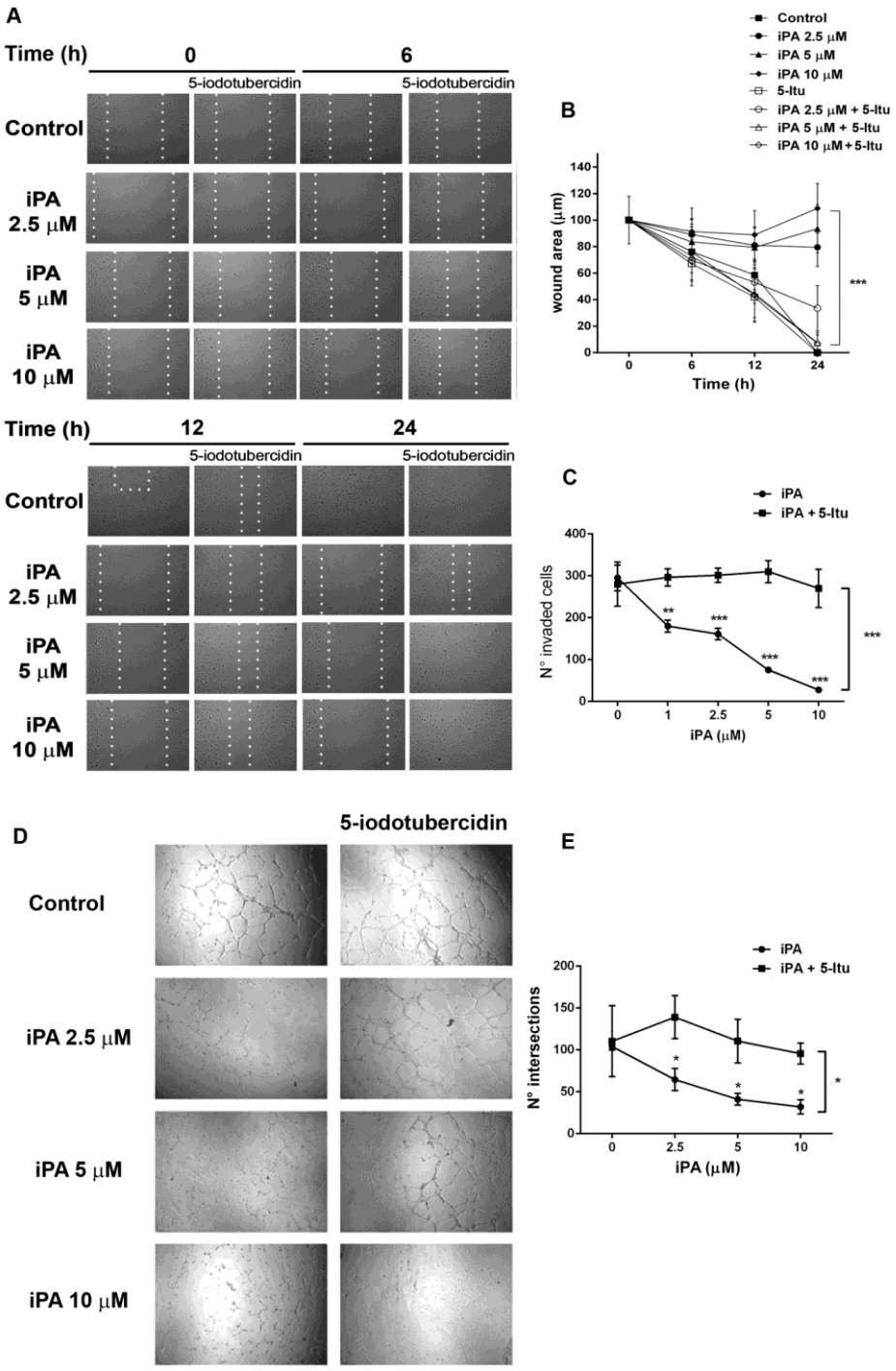

Figure 15. iPA inhibited endothelial cell migration, invasion and capillary network formation. *A*) Confluent endothelial cell monolayers were treated with iPA (2.5–10 μM), with or without pretreatment with 5-Itu (30 nM, 30 min), and wounded with a 200 μl tip, as described in *Materials and Methods*. Image of wound closure are representative,

captured within 24 h by a time-lapse video microscopy system (×10; AF6000 LX; Leica). White dotted lines mark the wound area. *B*) Width of each wound, calculated from images at different time points (0, 6, 12, and 24 h) measured by ImageJ 1.45 software. Degree of wound regeneration was calculated as the percentage of the remaining cell-free area compared to the vehicle control or respective treatment without 5-Itu, expressed as means ± SD of 2 independent experiments in triplicate., ***$P < 0.001$ *vs.* control or treatment without 5-Itu; ANOVA. *C*) Matrigel invasion assay in transwells was performed as described in *Materials and Methods*. Endothelial cells were treated with iPA (1–10 µM), with or without 5-Itu pretreatment (30 nM, 30 min). Graph reports the number of invading cells during 18 h, expressed as means ± SD of 3 experiments in triplicate. **$P < 0.01$, ***$P < 0.001$ *vs.* control [invading cells in the absence of chemotactic factors (cells moved by chemokinesis), or respective treatment without 5-Itu]; ANOVA. *D*) For the capillary-like tube formation assay, endothelial cells were treated with iPA (2.5–10 µM), with or without 5-Itu pretreatment (30 nM, 30 min), and seeded on a thick layer of Matrigel. Images are representative of 3 experiments in triplicate. *E*) Number of intersections analyzed by ImageJ 1.45 software, expressed as means ± SD of 3 independent experiments in triplicate. *$P < 0.05$ *vs.* control or respective treatment without 5-Itu; ANOVA.

The images show that iPA inhibited the formation of the capillary network in a dose-dependent manner. In 5-Itu-pretreated endothelial cells, there was a complete reversal of the anti-angiogenic effects of iPA at 2.5 and 5 µM, because the capillary network was comparable to that of the control. With 10 µM iPA, there was no capillary network, showing that 5-Itu pretreatment did not reverse the effect of specific inhibition of the capillary network formation exercised by iPA, but only the effect on cell viability. Indeed, endothelial cells were present in the Matrigel matrix, but they did not align and organize themselves to form capillary-like vessels (Fig. 15*D, E*).

4.7 iPA inhibits angiogenesis *in vivo*

The antiangiogenic effect displayed by iPA *in vitro* prompted us to confirm its activity *in vivo* by the Matrigel plug assay. FGF2 administered in the Matrigel plugs induced a consistent angiogenic process, as demonstrated by expression of the CD31 endothelial marker, measured both by quantitative RT-PCR (Fig. 16*A*) and immunofluorescence (Fig. 16*B*).

Accordingly, treatment with iPA significantly reduced the neovascularization process induced by FGF2, whereas any inhibitory effect was observed when the isoprenoid IPP was added to the plugs as the negative control.

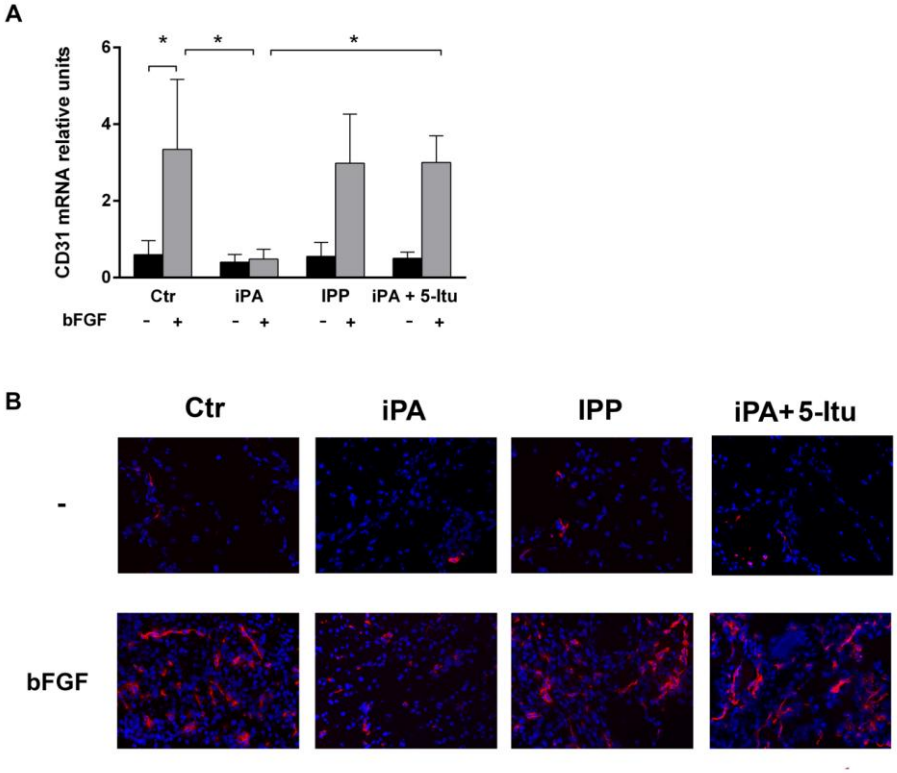

Figure 16. iPA inhibited angiogenesis *in vivo*. *A*) Matrigel plugs containing 27 nM of FGF2/plug (shaded bars) were added with vehicle, 5 µM/plug of iPA, 5 µM/plug of IPP, or 30 nM 5-Itu 5 µM/plug of iPA and implanted subcutaneously in mice. After 1 week, the plugs were assessed for CD31 mRNA expression levels by RT-qPCR, and data were normalized to hGAPDH. Data are expressed as means ± se of 6–8 plugs/group. **P* < 0.05; ANOVA. *B*) For immunofluorescence, 5 µm sections were stained with anti-CD31 antibody; $CD31^+$ blood vessels developed in Matrigel plugs containing different treatments are visualized in red. Micrographs are representative (×200).

In keeping with our *in vitro* observations, the addition of 5-Itu to iPA abolished the inhibitory effect displayed by iPA alone. Of note, no significant pro- or antiangiogenic effect was observed when treatments were added in the absence of FGF (Fig. 16*A*, solid bars).

4.8 iPA inhibits angiogenic phenotype of melanoma cells

To better understand the effects of iPA on tumor angiogenesis process, which provides necessary oxygen and nutrients for the tumor, we used A375 human melanoma cells, well known for their highly angiogenic phenotype.

First of all, we evaluated endothelial cells viability when co-coltured with melanoma cells pre-treated for 24 h with increasing concentrations of iPA (1-10 μM). The results in Figure 13 show that iPA treatment (from 2.5 to 10 μM) was able to affect the angiogenic phenotype of melanoma A375 cells, significantly inhibiting the viability of endothelial cells.

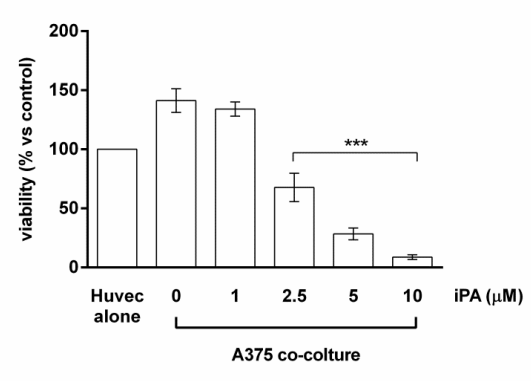

Figure 17. iPA treated-melanoma cells inhibited endothelial cells viability. The histogram shows the inhibition of endothelial cells viability after 24 h of co-culture with melanoma cells previously treated for 24 h with increasing concentrations of iPA (from 1 to 10 μM), evaluated by quantitative detection of absorbance intensity (570 nm) of crystal violet solubilized in acetic acid. Results are representative of two independent experiments performed in duplicate. Mean±SD is shown (ANOVA, ***P<0.001 *vs* endothelial cells untreated).

4.9 iPA inhibits melanoma cells proliferation and colony formation

Then, we assessed the direct effect of iPA on A375 melanoma cells biological functions. The treatment of A375 for 24, 48 and 72 hours with increasing concentrations of iPA (from 1.25 μM to 40 μM) inhibited the proliferation after 24 h of treatment only at highest concentrations used (20

and 40 μM), whilst after 48 and 72 hours iPA was able to block the proliferation already at 5 μM. In order to investigate the mechanism through which iPA exerted its inhibitory effects also in melanoma cells and to confirm that phosphorylation in position 5'- by ADK was indispensable for its action, we pre-treated melanoma cells with ADK specific inhibitor, 5-Itu (30 nM, 30 min). According with the mechanism of action of iPA in endothelial cells model, the pre-treatment with 5-Itu (Fig. 18*A*-*C*, gray bars) reverted the effects of iPA on melanoma cells proliferation at all the concentrations and time points, confirming that phosphorylation of iPA in C5 by ADK is crucial also to its anti-tumor activity and that the active metabolite is precisely N6-isopentenyladenosine 5'-monophosphate (iPAMP).

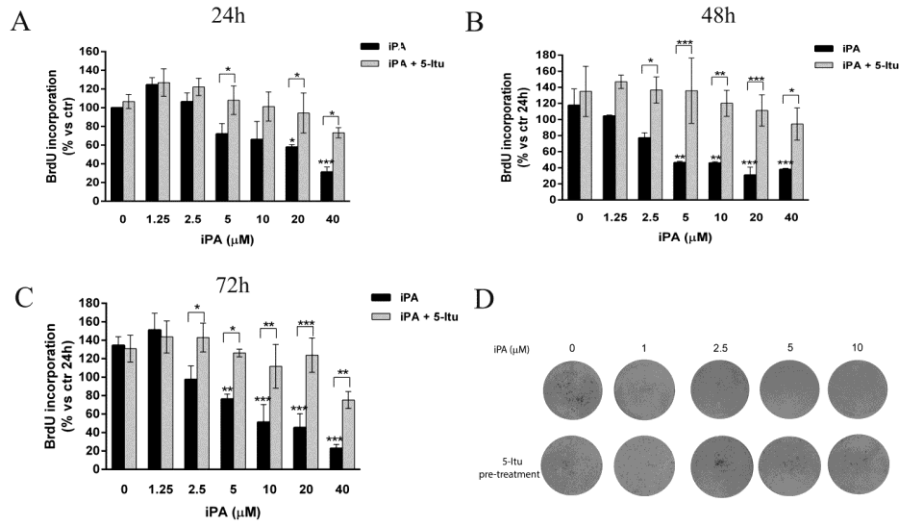

Figure 18. iPA inhibited melanoma cells proliferation and colony formation. *A*-*C*) Histograms show the inhibition of proliferation of melanoma cells, pre-treated (shaded bars) or not (solid bars) with the ADK inhibitor 5-Itu (30 nM, 30 min), performed by BrdU proliferation assay for 24 h (*A*) 48 h (*B*) and 72 h (*C*). Results (*A*-*C*) are expressed as mean±SD of one experiment performed in triplicate. *D*) The image shows representative pictures of melanoma cells after ten days of treatment with increasing concentrations of iPA (1-10 μM) pre-treated or not with 5-Itu (30 nM, 30 min). Colonies have been fixed, stained with crystal violet and photographed. Experiment was performed in duplicate. (ANOVA, *P<0.05, **P<0.01, ***P<0.001 *vs* control, represented by cells untreated or treated without 5-Itu).

Moreover, to test iPA sensitivity on melanoma cells proliferation after a

prolonged *in vitro* exposure, we also performed human tumor clonogenic assay. Cells were treated at time 0 h with increasing concentrations of iPA alone (1-10 μM) with or without the pre-treatement with 5-Itu (30 nM, 30 min) and were monitored for ten days. Results in Figure 18*D* show the ability of iPA to inhibit colony formation in a concentration-related manner, reducing the number and dimension of colonies. Moreover, at higher concentrations (2.5-10 μM) iPA did not allow the formation of any colony, whereas when cells were treated with iPA 1 μM only the dimensions of colonies were reduced. Once again, the pre-treatment with 5-Itu completely reverted the inhibitory effect of iPA on colony formation (Fig. 18*D*).

4.10 iPA induces a G1-phase stasis and apoptosis in melanoma cells

To analyze the nature of the anti-proliferative action of iPA, we evaluated its effect on melanoma cells distribution during cell cycle by flow cytometric analysis. Thus, melanoma cells were treated with increasing concentrations of iPA alone (from 1 to 10 μM) or following 5-Itu pre-treatment (30 nM, 30 min) for 24, 48 and 72 hours. Subpopulations of G1- and S/G2M-phase were then analyzed. As shown by quantitative analysis, iPA blocked proliferation of melanoma cells in G1 phase of cell cycle already after 24 h of treatment at the highest concentration tested and this effect was potentiated after 48 hours of treatment (Fig. 19*A*). After 72 h of treatment the G1 phase stasis was no more relevant.

In order to evaluate whether the block of cell cycle correlated with the induction of apoptosis, we analyzed the percentage of apoptotic cells, by staining with Annexin V and propidium iodide (PI) in response to various iPA concentrations in human melanoma cells, with or without 5-Itu pre-treatment (Fig. 19*B*). Data obtained show that already after 24 hours of

treatment iPA exerted a slight induction of apoptosis, while this pro-apoptotic effect became substantially clear after 48 and even more after 72 hours of treatment with increasing concentrantions of iPA (1-10 μM). Indeed, the percentage of apoptotic cells after 24 h was about 15%, after 48 h about 30% and finally after 72 h of treatment with iPA 10 μM was about 70%. As expected, 5-Itu reverted the effect on the cell cycle arrest and the pro-apoptotic action of iPA, highlighting that the active form of iPA is iPAMP, as well as in endothelial cells.

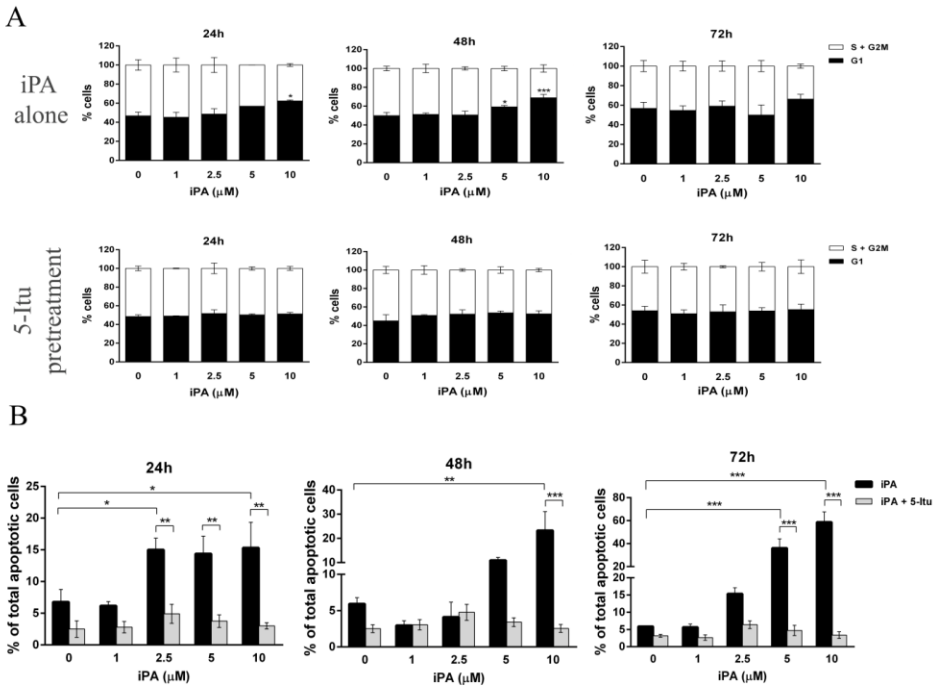

Figure 19. iPA induced a G1-phase stasis and apoptosis in melanoma cells. *A*) The histograms report the quantitative analysis of melanoma cells in the different phases of cell cycle following treatment with iPA (from 1 to 10 μM) with or without pre-treatment with 5-Itu (30 nM, 30 min) in time course (24, 48 and 72 h), expressed as percentage. *B*) The histrograms report the quantitative analysis of melanoma cells Annexin V positive and Annexin V/PI double positive with or without 5-Itu pre-treatment (30 nM, 30 min) in time course (24, 48 and 72 h). Results are representative of two independent experiments. Mean±SD is reported. (ANOVA, *P<0.05, **P<0.01, ***P<0.001 *vs* cells untreated or cells treated with 5-Itu).

4.11 iPA induces AMPK-dependent activation of autophagy in melanoma cells

To corroborate the parallelism between endothelial system and cancer model, the activity of the energy sensor AMPK was analyzed. After 24 hours of treatment, iPA was able to induce the phosphorylation of AMPK-α catalytic subunit also in melanoma cells (Fig. 20). Since in a great number of cancer models the AMPK pathway appears to be involved in autophagy, we also investigated this possible correlation. To this end, specific assays to analyze acid autophagy flux by flow cytometry were performed.

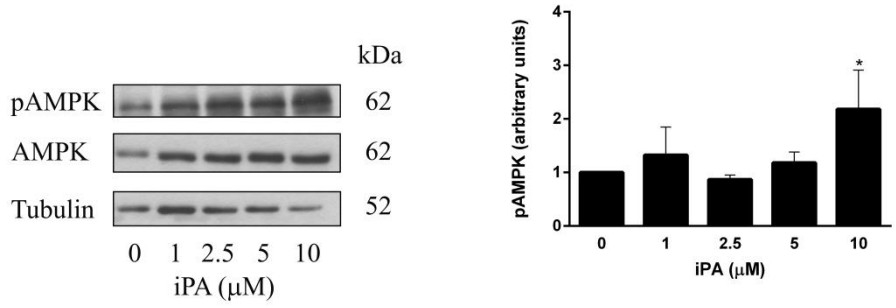

Figure 20. **iPA activated AMPK inducing its phosphorylation**. Increase in AMPK activity was analyzed by western blot. Melanoma cells, grown in serum containing medium, were treated with iPA at the indicated concentrations for 24 h. Tubulin served as the loading control. Data are representative of two different experiments with similar results. Histogram (*right panel*) reports the results of the quantitative analysis (arbitrary units, pAMPK/ AMPK/ tubulin) as mean ± SD of two independent experiments. (ANOVA, **P*<0.05 *vs.* control).

The acidotropic dye LysoTracker Red DND-99, a probe which exhibits fluorescence that is largely independent of pH, was diluted in PBS. Red lysosomal fluorescence of 10,000 cells per sample was determined by flow cytometry using the FL3 channel. The histograms clearly show the time- and concentration- dependent autophagic flux (Fig. 21*A*). Already after 24 hours of treatment with iPA there was an evident trend of increasing in the

acidic flux due to autophagolysosome formation, peculiar of autophagic dynamic process. The MFI value increased in a dose- and time-dependent manner. Interestingly, after 72 h of treatment was visible also a characteristic peak of dead cells (see above), indicating that the autophagic process in this case is not a protective mechanism but on the contrary a preliminary step to cell death induction.

In order to detect the acidic compartment, we also used the lysosomotropic agent acridine orange, a weak base that moves freely across biological membranes when uncharged. Its protonated form accumulates in acidic compartments, where it forms aggregates that fluoresce bright red.

Through this latter assay iPA appeared an autophagy activator already after 24 h of treatment until 72 h. This pro-autophagic effect was completely reverted by 5-Itu pre-treatment (Fig. 21*B*).

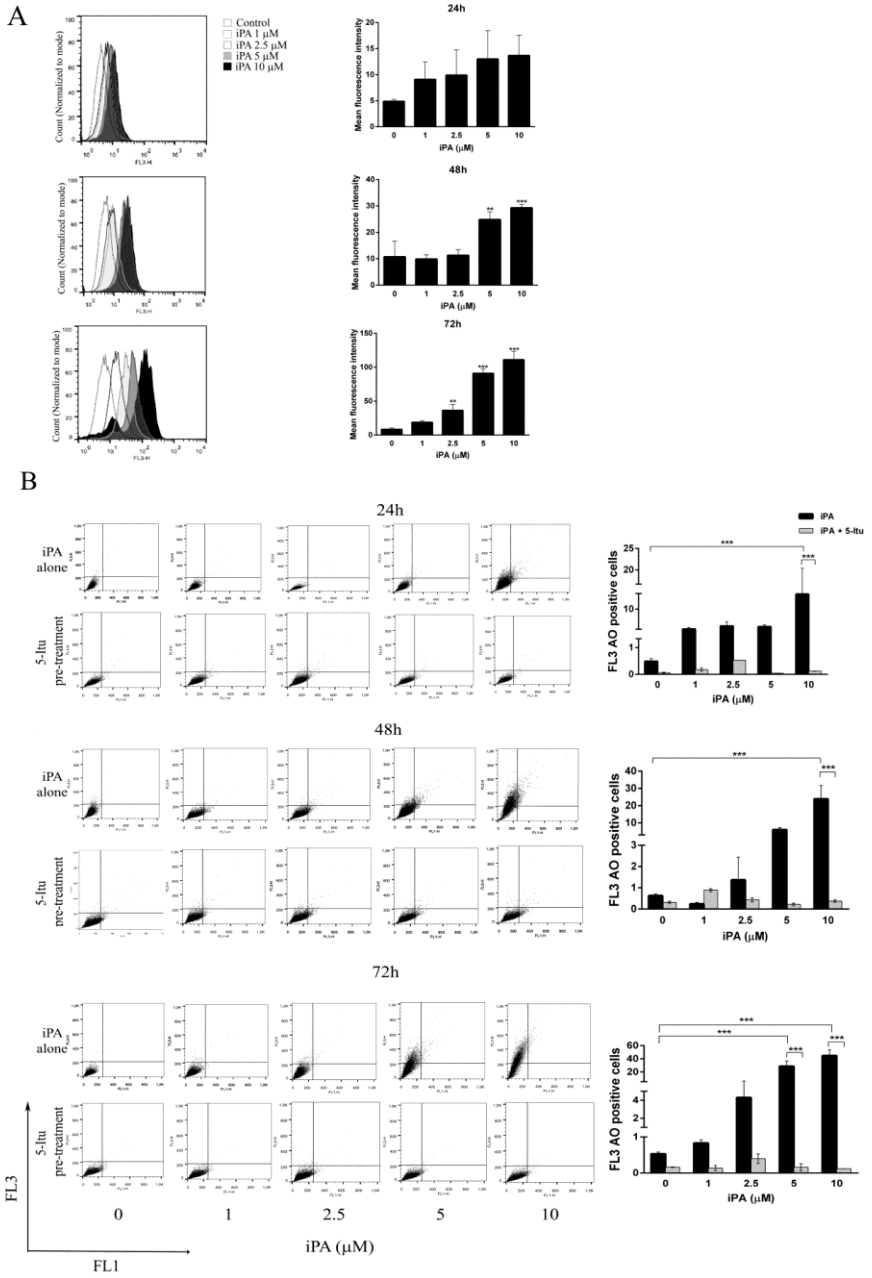

Figure 21. iPA induced autophagy in melanoma cells. (*A)* Melanoma cells were treated with increasing concentrations of iPA (from 1 to 10 µM) for 24, 48 and 72 h. Cells in suspension (1×10^4) were labeled with lysotracker-red (70 nM) and then activity of lysosomal acid phosphate of melanoma cells was analyzed by flow cytometry (excitation/emission, 577/590 nm). In the *left panel* the most representative images of flow cytometer analysis are shown, whilst in the *right panel* the histrograms show the quantitative analysis of two independent experiments in the three different time points. *(B)* Melanoma cells were treated with increasing concentrations of iPA (from 1 to 10 µM)

with or without 5-Itu pre-treatment (30 nM, 30 min) for 24, 48 and 72 h. Cells (1×10^4) were labeled with acridine orange (10 μg/mL) for 15 min at 37°C and quantified using flow cytometry. FL1-H indicates green color intensity (cytoplasm and nucleus), whereas FL3-H shows red color intensity (acidic vesicular organelles, AVO, peculiar of autophagy process). In the *left panel* the most representative images of flow cytometer analysis are shown, whilst in the *right panel* the histrograms show the quantitative analysis of three independent experiments in the different time points. Data were analyzed by FlowJo software version 8.2 (Tree Star, Inc., Ashland, OR, USA). The histograms (*right panels*) report the quantitative analysis (arbitrary units) expressed as mean±SD of two (*A*) or three (*B*) independent experiments with similar results (ANOVA, **P<0.01, ***P<0.001 *vs* control).

4.12 iPA activates autophagy and apoptosis pathways to induce cell death in a coordinated and cooperative manner

Since autophagy can act as an apoptosis-alternative pathway to induce cell death or act together with apoptosis as a combined mechanism for cell death, the correlation between these mechanisms was analyzed. Levels of peculiar proteins involved in both the processes were evaluated by western blot. During autophagy, LC3-I is converted to LC3-II through the Atg4-dependent insertion of a phosphoethanolamine moiety and recruited into the membrane of the forming phagophore, a double membrane required for the recycling of protein aggregates and organelles. To analyze the relationships between apoptosis and autophagy in melanoma cell death, we treated cells with increasing concentrations of iPA (from 1 to 10 μM) for 24h and 48 h. The expression of the peculiar autophagic protein, LC3-II, resulted increased starting from 24 h and remained augmented until 48 h of treatment with iPA (Fig. 22). The activation of the intrinsic apoptosis pathway was monitored by the analysis of the caspase cascade. Caspase-9 activation, started from 24h (Fig. 22*A*), followed by caspase-3 activation and resulted in DNA repair enzyme poly (ADP-ribose) polymerase (PARP) cleavage (Fig. 22*B*), that finally leads to apoptotic cell death. Indeed, as shown in Figure 22*B*, a clear activation of caspase-3 was detected, followed by PARP cleavage that was significantly increased after

48 h of treatment with 5 and 10 μM iPA (Fig. 22*B*).

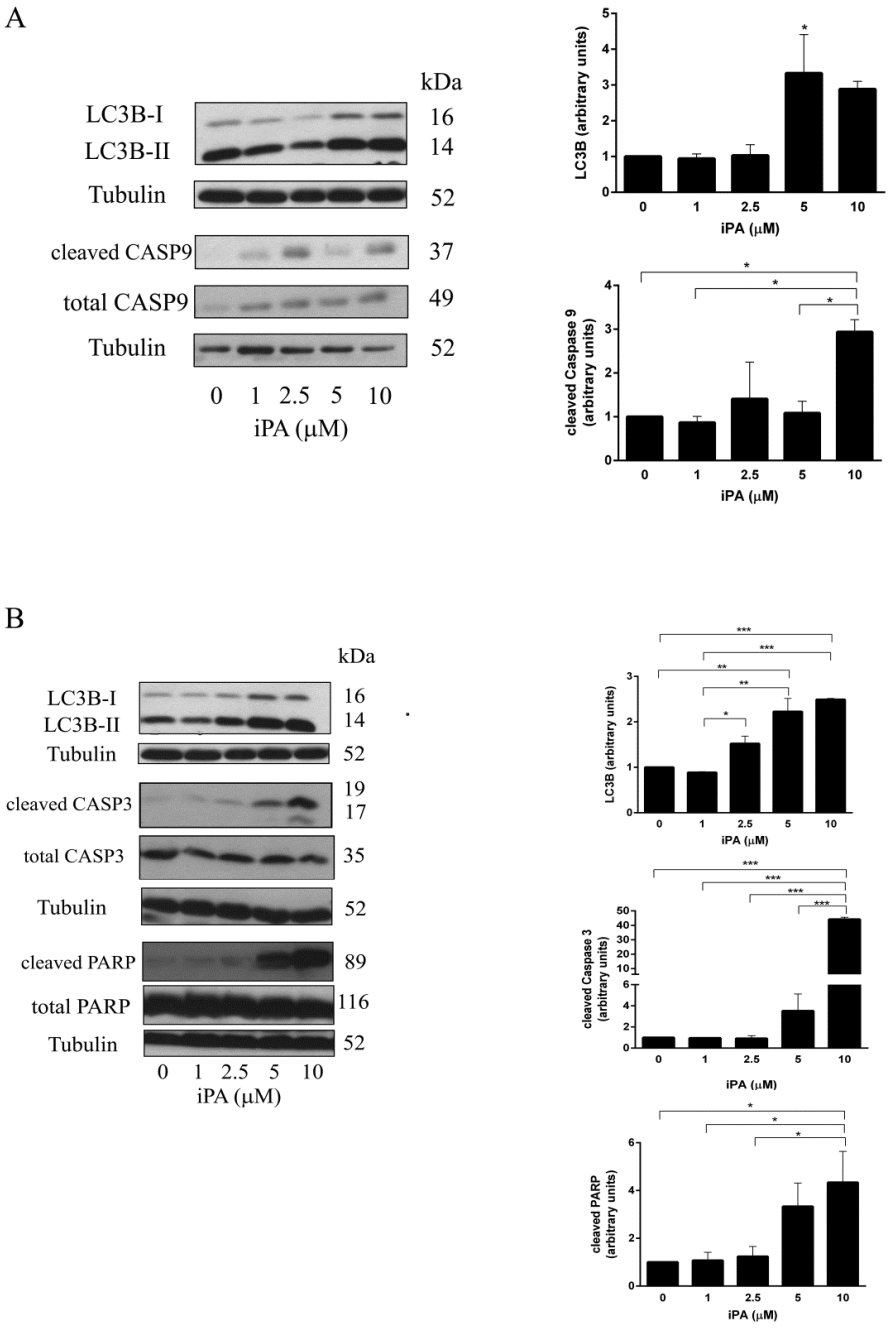

Figure 22. iPA activates autophagy and apoptosis pathways to induce cell death in a coordinated and cooperative manner. Melanoma cells were treated with iPA at the indicated concentrations for 24 h (*A*) and 48 h (*B*). Increase of the autophagic marker LC3B (*A* and *B*) that leads to the activation of the intrinsic apoptosis pathway by expression of cleaved caspase 9 *(A*) and subsequently the increase of expression of

cleaved caspase 3 (*B*) and finally cleaved PARP (*B*), were analyzed by western blot. Tubulin serves as loading control. The data shown are representative of two experiments. The histograms (*right panels*) report the quantitative analysis (arbitrary units) expressed as mean±SD of two independent experiments with similar results (ANOVA, *P<0.05, **P<0.01, ***P<0.001 *vs* control).

4.13 iPA selectively expands NK cells in human primary PBMCs culture

Since immune-surveillance plays a role in control of tumor development and a study published almost 50 years ago suggested that iPA could affect mitosis of the phytohemagglutinin-stimulated human lymphocytes (Gallo et al., 1969), we asked which specific lymphocyte cell population was affected by the iPA 'mitogenic' capacity. We then analyzed the expansion of CFSE labeled unfractionated PBMCs stimulated with IL-2 alone (100 U/mL) or in combination with iPA at selected concentrations, ranging from 0.1 to 1μM. The choice of these specific concentrations was due to previously observations in which the addition of iPA at a concentration above 10^{-6} molar resulted in the inhibition of mitosis of phytohemagglutinin-stimulated lymphocytes, while lower concentrations (between 10^{-7} and 10^{-6} molar) had a stimulatory effect (Gallo et al., 1969). As highlighted in flow cytometric analysis of CFSE dye-dilution (Fig. 23*A*), after a 10-day culture in the presence of IL-2 and iPA, a slight but statistically significant expansion of NK cells (82.27±2.3%; $p<0.05$, iPA 0.1 μM and 79.1 ±3.4%; $p<0.05$, iPA 1 μM) was observed in comparison to IL-2 alone (73.7±3.8%) with no effects on other lymphocyte subpopulations like T and NKT cells or B cells (data not shown). Of note, a similar synergistic effect could not be observed in PBMCs treated with the well-known isoprenoid intermediate IPP or with the purine nucleoside adenosine (data not shown).

4.14 iPA directly stimulates human purified NK cells

These first evidence prompted us to investigate if iPA directly affects NK cell functions or if other cells and/or soluble mediators are required for achieving this effect. NK cells reside in the skin (Luci et al., 2009), thus melanocytes and neoplastic cells are susceptible to NK cell recognition from early stages of dysregulation. Understanding how NK cells migrate into the tumor microenvironment is important to redirect NK cells to the tumor in the therapeutic setting. For this purpose, we evaluated the effects on human purified NK cells of 48h-treatment with iPA alone in the absence of cytokine support. Interestingly, iPA 0.1 μM and, to a lesser extent, iPA 1 μM activated human resting NK cells, as measured by a significant increase in the percentage of CD69 positive NK cells (Fig. 23*B*) (25 ±3.9%; $p<0.01$, iPA 0.1 μM vs 16.3±2.9 of NK alone and 23.6±2.9%; $p<0.01$, iPA 1 μM vs 16.3±2.9 of resting NK alone).

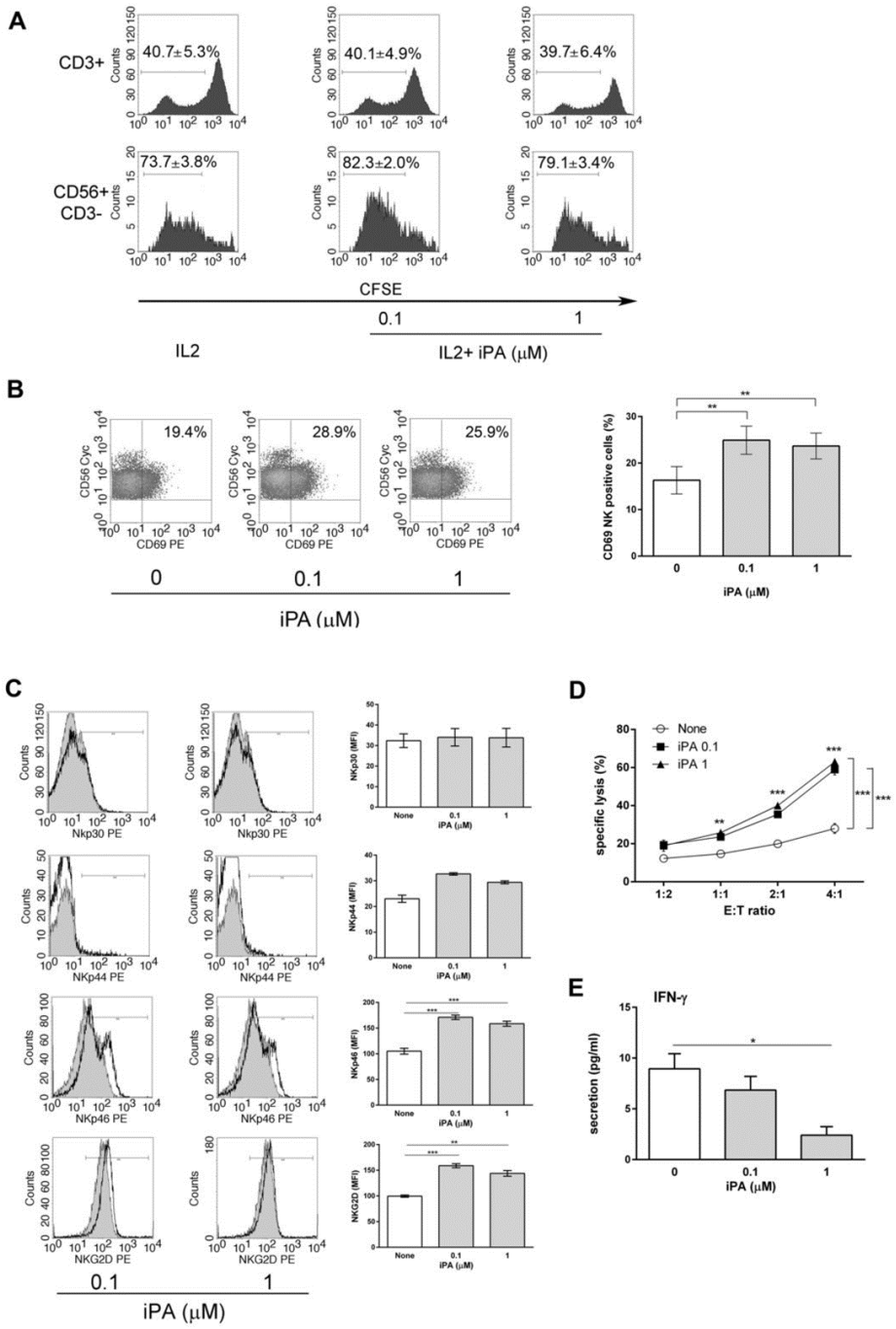

Figure 23. iPA selectively expanded and directly activated NK cells in human primary PBMCs cultures . (*A*) Cultured CFSE-labeled human PBMCs stimulated with IL-2 (100U/mL) alone or in combination with iPA at the indicated concentrations were analyzed for expansion (CFSE dye dilution) by flow cytometry. Data in *A* are gated to show CFSE staining on viable CD3+ T cells or alternatively on viable CD56+CD3- NK cells. Mean percent ± SD of dividing cells of five different donors is reported in

histograms. (*B*) Human purified CD56+CD3- NK cells cultured in complete medium with or without iPA for 48 h were stained using anti-CD3, anti-CD69 and anti-CD56 mAbs and analyzed by flow cytometry. A representative dot plot (*left*) is presented. Bars graph (*right*) report the percentage ± SD of CD69+ of CD56+CD3- gated NK cells from five independent experiments using different donors. Statistical analysis is indicated (ANOVA, $^{**}P<0.01$ compared with resting NK cells cultured in medium alone). (*C*) Representative example (*left*) for cytofluorimetric histogram profiles of purified NK cells maintained in culture for 48 h with iPA (empty profiles) or without iPA (gray profiles). Bars graph (*right*) reports mean and SD of the MFI for each marker in CD56+CD3- gated NK. Results are representative of four independent experiments using different donors. (ANOVA, $^{*}P<0.05$, $^{**}P<0.01$ and $^{***}P<0.001$ compared with resting NK cells cultured in medium alone). (*D*) Human purified CD56+CD3- NK cells cultured in complete medium alone (none; circles) or treated with the selected iPA concentrations (iPA 0.1 μM, squares and iPA 1 μM, triangles) for 48 h were then tested for cytotoxic activity against K562 cells. E:T ratios are indicated. Duration of the assay was 4 h. Results were expressed as the mean ± SD of 4 independent experiments. All pairwise comparisons are statistically significant between treatment groups (ANOVA, $^{**}P<0.01$ and $^{***}P< 0.001$). (*E*) ELISA IFN-γ assay of purified NK cells cultured with complete medium alone or in combination with increasing concentrations of iPA for 48 h, before being incubated with K562 for additional 6 h at 37°C. At the end of the co-incubation period, supernatants were harvested and the concentrations of IFN-γ were determined. Values represent mean ± SD of 3 different donors. Selected statistical analyses are indicated. (ANOVA, $^{*}P<0.05$, compared with resting NK cells cultured in medium alone).

Moreover, in the same experimental condition, cytofluorimetric analysis revealed that in the presence of iPA, NK cells displayed a sharp and significant up-regulation of NKp46 and NKG2D activating receptors while surface expression of NKp30 and NKp44 was not affected (Fig. 23*C*). Accordingly, this phenotype correlates with a significant greater cytotoxicity exerted by iPA-treated NK cells against the classic K562 tumor target ($p<0.001$, iPA 0.1 μM *vs* resting NK alone and $p<0.001$, iPA 1 μM *vs* resting NK alone) measured by using the fluorescent carboxy-Fluorescein Diacetate c'FDA NK cytotoxic assay, as described in *Materials and Methods* (Fig. 23*D*). Of note, iPA did not induce IFN-γ secretion in treated NK cells upon K562 target cell encounter (Fig. 23*E*), suggesting its presumptive role in specifically amplifying NK cell contact-dependent cytotoxicity.

4.15 iPA synergizes with IL-2 for the proliferation and activation status of human purified NK cells

Because usually NK cells do not survive for a long period of time without cytokine support (Taguchi et al., 2004) and, most importantly, to reproduce an experimental setting more similar to *in vivo* microenvironment where both proinflammatory cytokines and target cells may coexist, we analyzed the iPA immunostimulatory properties on IL-2 stimulated NK cells and where indicated, in presence or absence of the classical NK target K562 erythroleukemia cell line.

First we tested the effects of iPA on NK cells proliferative response to IL-2, isolating CD56+CD3-NK cells from healthy donors by immunomagnetic separation. The NK cell proliferation index was then measured at different time intervals (at days 3, 8 and 10 of culture) by CFSE dye-dilution. In line with the results obtained with unpurified PBMC cultures, the treatment with iPA (0.1 μM and 1 μM) caused a significant increase in IL-2 driven purified NK cell expansion at day 10 of culture (P<0.001) (Figg. 24*A*, *B*). Then, to fully measure NK activity in response to iPA, we performed a parallel assessment of the cell surface up-regulation of CD69, a molecule associated with NK cell early activation, after co-incubation with K562 (Dons'koi et al., 2011). To this end, human purified NK cells were co-treated for 48 hours with the selected concentrations of iPA plus IL-2. The expression of CD69 was then evaluated after co-incubation with K562 at 1:2 effector:target (E:T) ratio for additional 6 hours. As shown in figure 24*C*, IL-2 primed NK cells cultured with media alone express low levels of CD69 (8%). In contrast, after incubating with K562, 59% of IL-2 treated NK cells express CD69 on their surface and the co-treatment with iPA 0.1 and 1 μM further increases the expression of CD69 on NK cells to 65% and 69%, respectively. These results clearly indicate that iPA synergizes with IL-2 for the proliferation

and activation status of human purified NK cells.

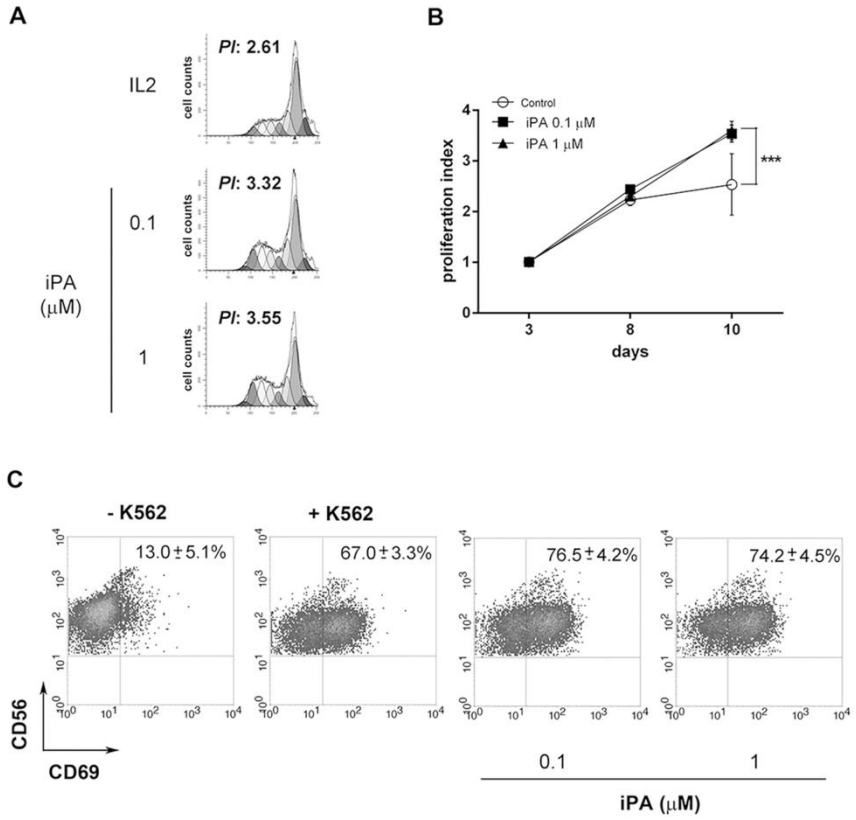

Figure 24. iPA positively affected the proliferation of IL-2 stimulated NK cells and CD69 surface expression. (*A*) Human purified CD56+CD3- NK cells were labeled with CFSE and cultured with medium containing IL-2 (100U/mL) with or without iPA at the indicated concentrations. After 3,8 and 10 days cells were collected and analyzed by flow cytometry. Panel *A* shows representative data of the CFSE fluorescence intensity and proliferation kinetics model of NK cells maintained in culture for 10 days. The indicated numerical values for proportions of proliferated cells among NK cell population were calculated by using ModFit LT software. (*B*) Composite data from three different donors showing means ± SD for rates of dividing NK cells in the same experimental conditions as in *A*. All pairwise comparisons are statistically significant between treatment groups (ANOVA, ***P*< 0.01 and ****P*< 0.001). (*C*) NK cells were cultured for 48 h in medium supplemented with IL-2 (100U/mL) with or without different concentrations of iPA, then washed and incubated with K562 at 1:2 ratio for 6 h. Therefore cells were collected and analyzed by flow cytometry for the cell surface expression of CD69 on gated CD3-CD56+ NK cells. The basal activation of IL-2 primed NK cells without K562 is also reported. The 1 donor-representative dot plots with mean percent ± SD from five separate experiments are presented.

4.16 Stimulatory effect of iPA on NK cell-mediated antitumor cytotoxicity and on the surface expression of NKp30

K562-induced CD69 expression displays NK lymphocyte functional condition that is associated with their cytotoxic function (Dons'koi et al., 2011). To determine whether iPA stimulation of IL-2 primed NK cells enhances their cytolytic activity, we tested treated and untreated NK cells against the NK susceptible target cell line K562. To this end, NK cells were stimulated with IL-2 in the presence or absence of increasing doses of iPA (from 0.1 to 1 μM). After 48 hours of culture, NK cells were washed and used as effectors against K562 target cells at different E:T ratios. The detection of $CFSE^+PI^+$ labeled dead target cells revealed that IL-2 primed NK cells displayed intermediate levels of cytotoxicity with respect to the higher efficiency of killing by IL-2 primed NK cells co-treated with iPA 0.1 μM and with iPA 1 μM ($p<0.01$, iPA 0.1 μM *vs* IL-2 alone and $p<0.01$, iPA 1 μM *vs* IL-2 alone) (Fig. 25*A*). To confirm the lytic potential of NK cells *in vitro*, we used another parameter of NK cell activation, which is the expression of the lysosomal-associated membrane protein-1 (LAMP-1, also known as CD107a) (Alter et al., 2004). After short term co-cultures at 1:1 E:T ratio, cells that stain positive for CD107a have degranulated and can be readily enumerated by flow cytometry. Consistent with previous data, the highly susceptible K562 tumor cell lines induced a strong CD107a expression in IL-2 primed NK cells (consistently greater than 30%) but, remarkably, in NK cells co-treated with 0.1 μM and 1 μM doses of iPA, CD107a expression, in terms of percentage of positive cells, was higher (48.2 ± 6.2 %; $p<0.05$, iPA 0.1 μM *vs* 28.4±5.6 of IL-2 alone and 49.6±6.1%; $p<0.05$, iPA 1 μM *vs* 28.4±5.6 of IL-2 alone) (Fig. 25*B*). Several structurally different activating receptors are involved in NK cell mediated cytotoxicity (Moretta et al., 2001; Alter et al., 2004). After 48 hours of culture, cytofluorimetric analysis revealed that in presence of iPA

0.1 μM and 1 μM, NK cells that had been stimulated with IL-2, displayed a significantly sharp upregulation of NKp30 ($p<0.001$, iPA 0,1 μM *vs* IL-2 alone and $p<0.001$, iPA 1 μM *vs* IL-2 alone) and to a minor extent of NKG2D, even though this is observed only in response to the concentration of iPA of 0.1 μM ($p<0.05$, iPA 0.1 μM *vs* IL-2 alone). On the other hand, surface expression of NKp44 and NKp46 was not significantly affected (Fig. 25*C*).

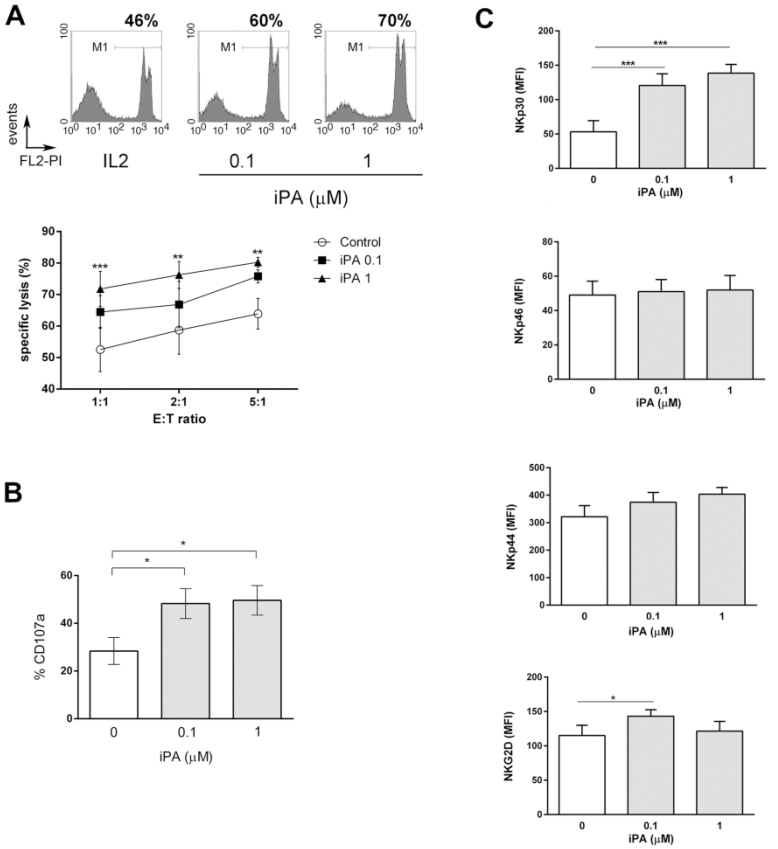

Figure 25. iPA potentiated cytotoxic effector fuctions of IL-2 primed NK cells. Cytotoxic activity of IL-2 primed NK cells or IL-2/iPA co-treated NK cells *vs* K562 was assessed by flow cytometry. Percent of specific lysis was calculated. (*A*) A representative histogram profile (*upper panel*) of K562 incubated with IL- 2 treated NK or alternatively with NK cells treated with increasing doses of iPA at 1:1 E:T ratio. Each sample was then tested in triplicate at three E:T ratios. Results (*lower panel*) are expressed as mean ± SD of 4 independent experiments. All pairwise comparisons are statistically significant between treatment groups (ANOVA, $^{**}P<0.01$ and $^{***}P< 0.001$). (*B*) NK cells were

treated with IL-2 alone or in combinations with increasing doses of iPA for 48 h, before being tested for their ability to degranulate in response to K562. Bars graph report the percentage of CD107a+ of CD56+CD3- gated NK. Results shown are representative of three independent experiments (ANOVA, **P*<0.05 compared with NK cells cultured in presence of IL-2 alone). (*C*) Surface expression of NKp30, NKp44, NKp46 or NKG2D was monitored by FACS using purified NK cells cultured for 48 h with IL-2 (100U/mL) in the presence or absence of increasing concentrations of iPA. Bars graph reports mean and SD of the MFI for each marker in CD56+CD3- gated NK cells. Results are representative of 4 independent experiments using different donors. (ANOVA, **P*<0.05, ***P*<0.01 and ****P*<0.001 compared with NK cells cultured in presence of IL-2 alone).

4.17 Cytokines and chemokines secretion profile of iPA treated-NK cells upon interaction with K562 cells

When an NK cell encounters its cognate ligand on a target cell, it mediates cytotoxicity and besides its ability to secrete the effector cytokine, IFN-γ (Lanier et al., 2005), it has the capacity to produce a variety of other cytokines, like tumor necrosis factor-α (TNF-α) and chemokines (CCL3/MIP-1α and CCL5/RANTES) (Vivier et al., 2008; Fauriat et al., 2010). We then evaluated the ability of iPA-treated NK cells to release these soluble factors, with particular focus on early time interval (6 hours) upon K562 target cell recognition (Fauriat et al., 2010). Therefore, NK cells from healthy donors were maintained in culture medium supplemented with IL-2 (100 U/mL) in the presence or absence of increasing doses of iPA. After 48 hours, NK cells were washed and incubated alone or with K562 for 6 hours. Supernatants were harvested and the concentration of different released factors was determined by a multiplex immunoassay (Fig. 26). As expected, stimulation of NK cells by K562 induced IFN-γ and TNF-α secretion as well as an ample secretion of CCL3 and CCL5 by IL-2 primed NK cells. Notably, the treatment with iPA 0.1 μM resulted in a significant increase in the secretion of all soluble factors measured ($P<0.05$ for IFN-γ, $P<0.001$ for TNF-α, CCL3 and CCL5), instead iPA 1 μM positively affected only the secretion of the effector cytokines IFN-γ and TNF-α ($P<0.05$), with no effects on the

chemokines, CCL5 and CCL3, whose secretion is particularly dependent on NKG2D engagement that iPA 1 μM is not able to upregulate, like iPA 0.1 μM does (Fauriat et al., 2010) .Thus, the costimulatory effects of IL-2 primed NK cells by the selected doses of iPA are not confined only to cytotoxic effector mechanisms, but also involve the release of cytokines and chemokines by which NK cells can instruct and shape adaptive immune response (Vivier et al., 2008).

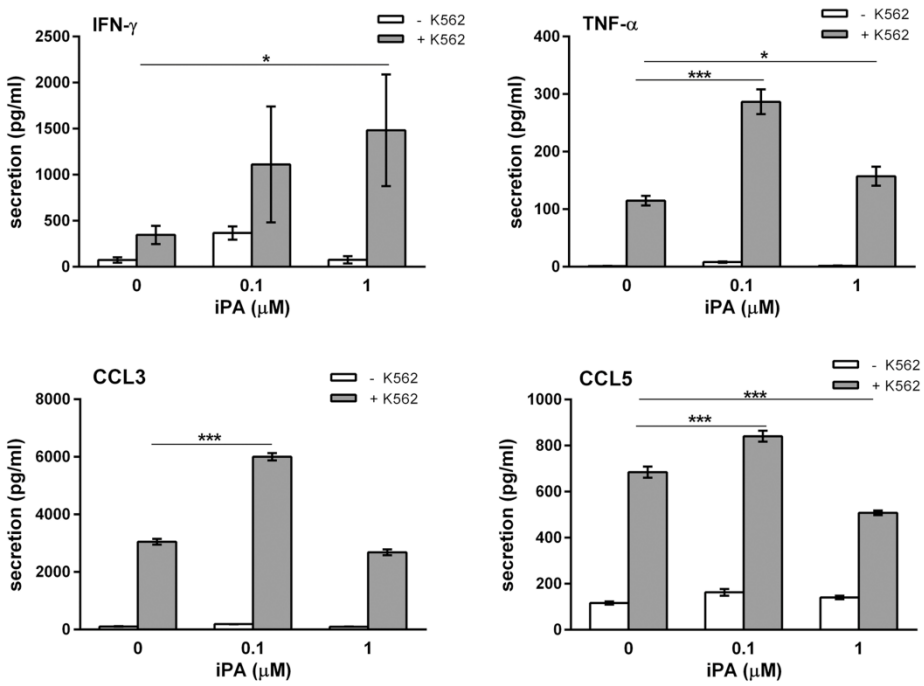

Figure 26. Cytokines and chemokines secretion profiles of IL-2 plus iPA-treated NK cells upon target cell recognition. Purified NK cells were treated with IL-2 alone or in combination with the indicated concentrations of iPA for 48 h, before being incubated alone or with K562 for 6 h at 37°C. Supernatants were harvested and the concentrations of cytokines and chemokines were determined by a multiplex immunoassay that concurrently detect multiple analytes in a single sample by Luminex Platform. Values represent mean ± SD of 3 different donors. Selected statistical analyses are indicated. (ANOVA, **P*<0.05, ***P*<0.01 and ****P*<0.001 compared with NK cells cultured in presence of IL-2 alone).

4.18 MAPK signal transduction is uniquely modulated by iPA plus IL-2 stimulation

To gain insight into the molecular bases of the synergistic actions of IL-2 and iPA on human primary NK cells, we next investigated whether and in which way the IL-2 signal transduction pathways were affected by increasing doses of iPA, with particular attention to JAK-STAT and MAPK signaling pathways, primarily used by IL-2 to drive cytokine expression and lytic granule exocytosis and cytotoxicity (Liu et al., 2012; Li et al., 2008; Yu et al., 2000; Chiossone et al., 2007). As shown in Figure 27*A*, ERK was phosphorylated in response to IL-2 stimulation. However, iPA 0.1 μM and iPA 1 μM led to significant greater levels of phosphorylated ERK compared with the effect observed in response to IL-2 alone ($p<0.01$, iPA 0.1 μM *vs* IL-2 alone and $p<0.05$, iPA 1 μM *vs* IL-2 alone). On the other hand, p38 phosphorylation was not affected by iPA treatment. Moreover, in contrast to the findings in the ERK/MAPK pathway, no differences were observed in the activation of STAT signal transduction pathways. Specifically, there was no evidence for enhanced tyrosine phosphorylation of STAT5 in response to co-stimulation with the indicated doses of iPA, compared with the effect observed in response to IL-2 alone. Similarly, the combination of iPA low doses plus IL-2 did not alter signaling intermediates in the PI3K pathway, compared to stimulation with IL-2 alone (data not shown). It is of note that kinetic studies (Fig. 27*B*) revealed that the enhancement of ERK activation by iPA co-treatment started 30 minutes after the exposure of cells to iPA when the stimulatory effect of IL-2 alone was not yet evident. This co-stimulatory effect, that was still observed after 3 hours, only occurred at the highest iPA concentration ($p<0.01$, iPA 1 μM *vs* IL-2 alone at 1 hour and $p<0.05$, iPA 1 μM *vs* IL-2 alone at 3 hours) while iPA 0.1 μM caused a slight increase in the levels of phosphorylated ERK species that did not reach statistical

significance before 18 hours of treatment (Fig. 27*A*). These data support the notion of a long-lasting effect of iPA and are compatible with its sustained action over the time, on different aspects of NK cell biology.

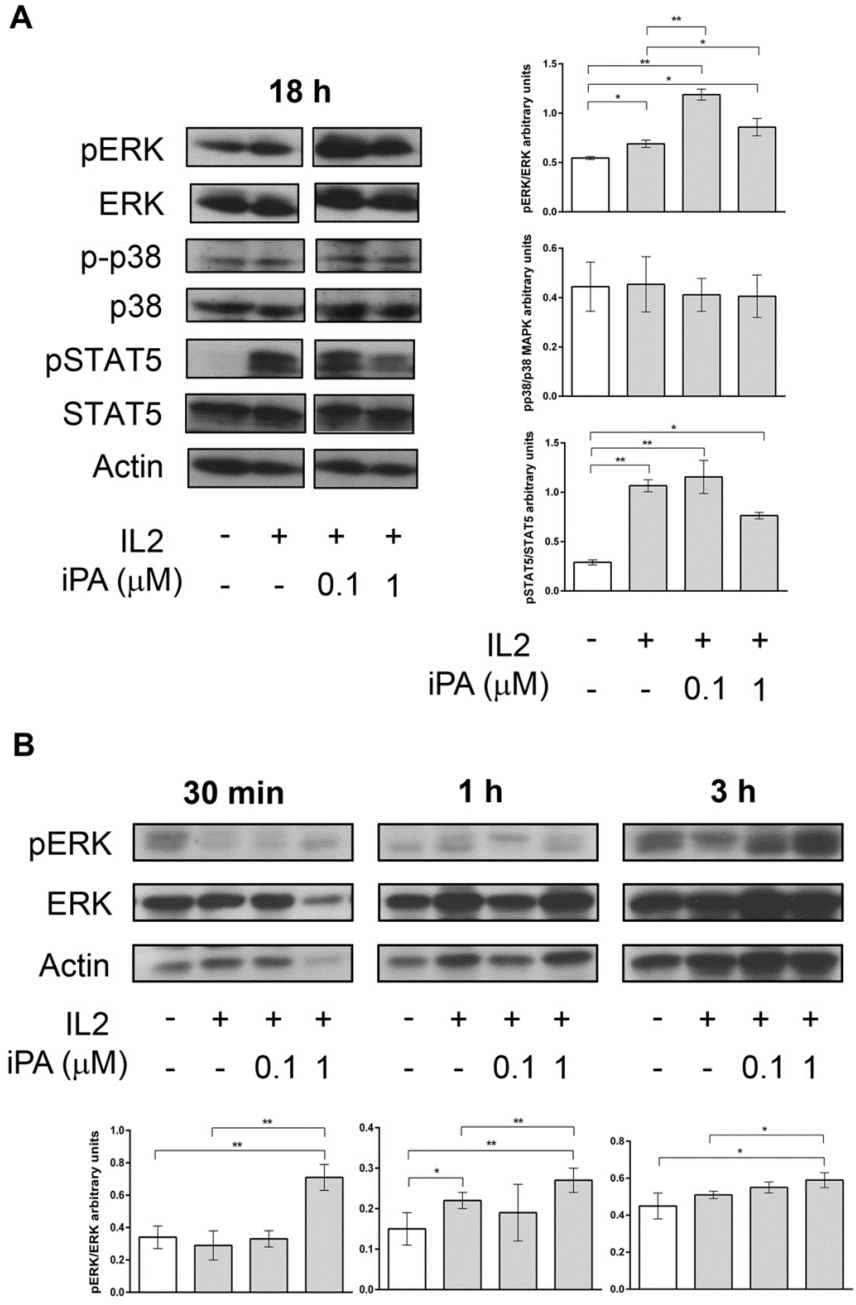

Figure 27. Molecular analysis of the iPA-mediated effects on NK cells functions:

evidence for an exclusive modulation of MAPK. (*A*) Purified NK cells were treated with IL-2 alone or in combination with the indicated concentrations of iPA for 18 h (*overnight*). Representative blots (*left)* and quantitative/densitometric analysis (arbitrary units) (*right*) of results from 4 different experiments are shown. All the relative protein levels were calculated by normalizing the levels of these proteins with the levels of β-actin which serves as internal loading control. The relative levels of specific phosphorylation of ERK (*p/ERK*), p38 (p/p38) and STAT5 (*p/STAT5*) were then calculated by normalizing the levels of phosphorylated forms with the levels of their cognate proteins. All 4 experiments were performed in duplicate with similar results (ANOVA, *P<0.05 and **P <0.01). (*B*) Representative western blot (*upper panel)* and quantitative/densitometric analysis (arbitrary units) (*lower panel*) of results from 3 different experiments conducted on purified NK cells stimulated with IL-2 alone or in combination with the indicated concentrations of iPA at different time points are shown. All 3 experiments were performed with similar results (ANOVA, *P<0.05 and **P <0.01).

4.19 iPA–mediated effects on IL2- stimulated NK cells are MAPK dependent

Because iPA appeared to increase ERK activation, we further characterized the functional correlates of this finding. Figure 25 shows combined data from experiments conducted in fresh primary human NK cells pretreated for 30 min with 10 μM UO-126, a small molecule MEK1/2- specific inhibitor and then put in culture with IL-2 with or without iPA for the indicated time points. We confirmed that NK-cell activation in response to IL-2 alone, both in terms of upregulation of CD69 (Fig. 28*A*) and NKp30 activating receptor (Fig. 28*B*), as well as secretion of IFN-γ (Fig. 28*C*) and cytotoxic potential against K562 (Fig. 28*D*), were dependent on MAPK signaling, since the presence of the MAPK inhibitor impaired the NK responses (Yu et al., 2000). Interestingly, the MEK inhibitor also had a profound effect in inhibiting the NK cell activation in response to the synergic action of iPA 0.1 and 1 μM plus IL-2 (P<0.001), but to higher extent than it can do in NK cells cultured with IL-2 alone.

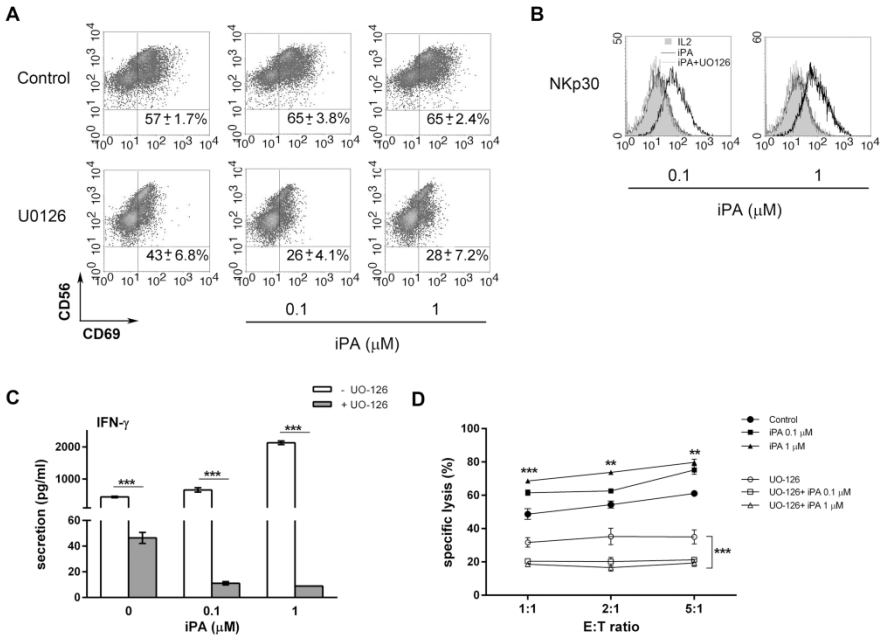

Figure 28. The effects on NK cells by iPA plus IL-2 were inhibited by UO-126. Before the treatment with IL2 ± iPA at different concentrations, purified NK cells were pretreated with UO- 126 (10 μM) for 30 min. They were then tested for the different assays in the same experimental conditions described above. Data are expressed as means ± SD of experiments performed on 3 different donors. Selected statistical analyses are indicated. (ANOVA, ***P* <0.01 and ****P*<0.001 compared with NK cells cultured with IL-2 alone in presence or absence of the inhibitor).

4.20 Analysis of the mechanism underlying the stimulatory effect of iPA: a role for the farnesyl diphosphate synthase

Finally, we started to investigate the molecular mechanism explaining, at least in part, the observed enhancement in NK cell functions by iPA. Activation of ERK follows a highly conserved set of molecular events and Ras protein is an essential factor in the regulation of MAPK (Mor and Philips, 2006). So, we decided to verify the effects of iPA costimulation on Ras activity. IL-2 stimulation induced Ras activation but the co-treatment with iPA (only at 1 μM) led to greater levels of bound Ras-GTP, the active form of Ras, confirming the synergy between IL-2 and iPA low doses (Fig. 29*A*). Ras needs post-translational modification (generally, farnesyl and

palmitoyl lipidation) for membrane binding and activation (Ahearn et al, 2011; Gazzerro et al., 2012). Our previous *in vitro* and *in vivo* findings highlighted a role for iPA in modulating the expression and activity of the farnesyl diphosphate synthase (FDPS) an enzyme of the isoprenoid pathway, crucial in generating lipids moieties used for the activity of the small GTP-ase proteins (Laezza et al., 2006). In light of this, we started to investigate the expression and the activity of the FDPS in primary human NK cells treated with IL-2 in presence or absence of iPA for 24 hours. Of note, in Fig. 29*B* we documented for the first time the expression of FDPS in human primary NK cells and we observed that FDPS expression was increased in IL-2 activated NK cells co-treated with iPA 0.1 and 1 μM. In parallel, also the FDPS activity was found to be increased after co-incubation with iPA, especially in response to the co-treatment with iPA 0.1 μM (P<0.01) (Fig. 29*C*).

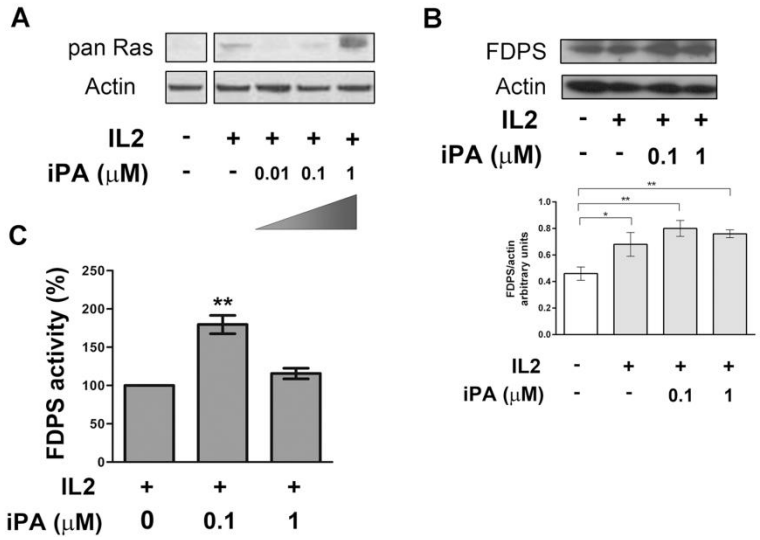

Figure 29. Ras and FDPS were activated after induction of iPA-mediated response in NK cells. (*A*) Quantification of Ras activation. Purified NK cells were incubated overnight alone or with indicated stimuli. Cells were then lysed and subjected to pulldown assay with Raf-RBD-GST. The amount of precipitated Ras-GTP was determined by immunoblotting using pan-Ras antibody. Actin serves as loading control. The data shown is representative of 3 different experiments. (*B*) Representative blot for FDPS protein expression (*upper panel*) and quantitative analysis (arbitrary units) (*lower panel*) of results from 3 independent experiments conducted on purified NK cells incubated

overnight alone or with indicated stimuli are shown. Densitometric mean values of FDPS were normalized by β-actin expression under each treatment condition. (*C*) Quantification of FDPS enzymatic activity. Bars graph reports mean±SD of the FDPS activity. The experiments were performed in the same conditionsdescribed above, with NK cells purified from 4 different donors and similar results were obtained (ANOVA, **P<0.01 *vs* control).

These experimental evidence suggest that the activation of IL-2 primed NK cells exerted by low concentrations of iPA appears to be due to the activation of the FDPS enzyme. Even if we cannot exclude the involvement of other signaling pathways, our first preliminary results reinforce the role of isoprenoids in the regulation of physiological cellular processes in the immune compartment.

5. DISCUSSION

In the present work, we investigated whether iPA, an end product of the mevalonate pathway with an isopentenyl chain linked to the nitrogen at position 6 of the purine base, could be considered as a potential lead compound for a new class of antitumoral agents. Indeed, while anticancer activity of iPA *in vitro* is well documented, iPA (i.p., 10 mg/kg) has been reported to exert a modest activity *in vivo*, probably because of its short plasma half-life, as happens with other nucleosides (Colombo et al., 2009). Anyway, it has been previously demonstrated the ability of iPA, even at very low doses (s.c., 0.5 mg/kg), to inhibit cancer growth also *in vivo* in a nude mouse xenograft model (Laezza et al., 2006). Probably, the reasons of this apparent discrepancy could be attribuited to the way of drug administration. In the light of this, new analogues of iPA with more pharmacological stability *in vivo* result to be necessary.

Specifically, we evaluated if iPA could directly interfere with the angiogenic process, fundamental to tumor growth and progression, and with melanoma growth, a tumor well known for its angiogenic phenotype. Finally, we investigated if iPA could have also an immunomodulatory role, in order to provide a cooperative and multifactorial mode of action to arrest cancer growth.

5.1 N6-isopentenyladenosine inhibits angiogenesis *in vitro* and *in vivo* through AMPK activation

The antitumoral effects of iPA have already been reported (Bifulco et al., 2008), whereas to date there was no evidence of its effects on the angiogenic process. In the current study, we found that iPA inhibited all the steps of angiogenesis. Indeed, treatment with iPA affected endothelial cell viability with minimal effects on quiescent cells, observable only at

higher concentrations. iPA strongly blocked endothelial cell proliferation in a concentration- and time-dependent manner (Fig. 7*B-D*). It is important to note that the antiproliferative effects of iPA can be ascribed to its peculiar structure, composed of the specific combination of the adenosine moiety and the isopentenyl chain. Indeed neither the sintetic analogues (Fig. 9), nor nitrogenous base adenine, nor adenine harboring the same modification in N6, nor yet the isopentenyl pyrophosphate resembling the isoprenoid chain alone affected endothelial cell proliferation (Fig. 8). As regard to adenosine it is well known its ability to stimulate angiogenesis in response to ischemic/hypoxic stress that stimulates vascular endothelial growth factor (VEGF) production (Auchampach, 2007). Given the structural similarities of iPA with adenosine, we investigated if it could act through specific adenosine receptors, A2A and A2B, expressed on endothelial cells and thightly involved with angiogenesis process. Obtained data exclude any interaction with adenosine receptors in endothelial cells since specific A2A and A2B antagonists used in pre-treatment had no effect on inhibitory action of iPA (Fig. 11). Given the absence of specific membrane receptors, the way by which iPA could enter into the cells remained an open question. So, we wondered whether iPA could enter into cells through nucleoside transporters. The passage of nucleosides across plasma membranes or between intracellular compartments occurs primarily *via* specialized nucleoside transporter proteins (NTs) (King et al., 2006). Once inside, they are activated by intracellular metabolic steps to triphosphate derivatives. In general, active derivatives of nucleoside analogues can then exert cytotoxic activity by being incorporated into and altering the DNA and RNA macromolecules or by interfering with various enzymes involved in the synthesis of nucleic acids, such as DNA polymerases and ribonucleotide reductase. These actions result in the inhibition of DNA synthesis and apoptotic cell death, as we have shown

with the treatment with iPA (Galmarini et al., 2002).

Two major families of transporters, the equilibrative NTs (ENTs) and concentrative NTs (CNTs), have been identified by molecular cloning and functional expression of cDNAs encoding NT proteins from a variety of species, including mammals, protozoan parasites and bacteria (Kong et al., 2004). Four human ENT and three hCNT subtypes have been identified by molecular cloning and functional expression. hENTs have been reported to mediate facilitated diffusion of nucleosides across membranes bidirectionally according concentration gradients, whilst uman CNTs transport nucleosides work against concentration gradients (Kong et al., 2004). Dipyridamole is a well-known inhibitor of ENTs (Wang et al., 2013). In the light of all these considerations, pre-treating endothelial cells with dipyridamole before iPA treatment we found that its effects were not abolished (Fig. 11).

By LC-MS/MS analysis, our study provides clear evidence that iPA is effectively internalized into endothelial cells in a time-dependent manner and is converted to its 5'-monophosphorylated form iPAMP by the ADK enzyme (Fig. 12); thus, it can be considered an AMP mimetic. Only one study, published 40 years ago, suggested, from data obtained in a cell-free system, that iPA could be a substrate of ADK (Divekar et al., 1974). We have demonstrated for the first time that blocking ADK activity with its potent inhibitor 5-Itu (*k*i=30 nM) prevented all the effects of iPA on endothelial and melanoma cells, clearly indicating that phosphorylation of iPA into iPAMP is essential for its biological activity, as previously suggested in other cell systems (Divekar et al., 1974) and similar to the process described in plants (Mok and Mok, 2001). Indeed, in *Dictyostelium discoideum*, the synthesis of iPA is catalyzed by the enzyme isopentenyl transferase (IPT), which transfers the isoprenoid moiety from DMAPP to AMP, thus producing iPAMP in equilibrium with its nonphosphorylated

form iPA (Golovko et al., 2000). Moreover, we showed that ADK inhibition by 5-Itu effectively prevented the formation of iPAMP, increasing the iPA/iPAMP ratio inside the cells. 5-Itu, at the very low concentration used in our experimental setting (30 nM, 30 min), has been widely documented to be selective for ADK inhibition, whereas at higher concentrations (10–50 μM), it has been shown also to inhibit nucleoside transport (Sinclair et al., 2001). We indeed observed a slight decrease in iPA internalization after 5-Itu pretreatment (Fig. 12), but this effect was probably due to an alteration of the concentration gradient between the outside and inside of the cell, with an accumulation of nonphosphorylated iPA inside the cell that delays iPA entry for an inversion of the gradient, as happens with nucleosides (Sinclair et al., 2001). As expected, we found that iPAMP, behaving as an AMP mimetic, activated the key metabolic enzyme AMPK, thus inhibiting the angiogenic process. Also AMPK activation was completely reversed by pretreatment with 5-Itu (Fig. 13). Of note, all treatments for each experiment were performed with endothelial cells grown in serum containing medium; hence, an increase in AMPK activity cannot be attributed to metabolic stress. AMPK is active under conditions that deplete cellular ATP and elevate AMP, such as long-term nutrient starvation, hypoxia, ischemia, heat shock, and exercise (Lee et al., 2012). In addition to allosteric activation, AMPK activity can be regulated by AMP mimetics, such as the cell-permeable activator 5-aminoimidazole-4-carboxamide riboside (AICAR). As we observed in our study for iPA, AICAR has been reported to be rapidly taken up by cells and phosphorylated by ADK to 5-amino-4-imidazolecarboxamide ribonucleotide (ZMP), behaving as an AMP analogue that mimics the effect of the substrate AMP on AMPK activation (Corton et al., 1995), by competing with AMP for binding to the regulatory-subunit (Zou and Wu, 2008). Indeed, the ZMP proapoptotic effect in liver cells was completely

blocked by 5-Itu, as we observed in endothelial cells treated with iPA. Although the ability of AMPK to preserve endothelial cell viability is well known, the role of AMPK in regulating endothelial cell proliferation is not as well understood and depends largely on the nature and length of the angiogenic stimulus (Reihill et al., 2011). In particular, chronic activation of AMPK, such as that observed in our model where AMPK activation was sustained up to 24 h, may favor endothelial cell growth arrest. On the contrary, acute, transient activation of AMPK in response to angiogenic factors, such as VEGF or erythropoietin, may be involved in the induction of proliferation (Stahmann et al., 2010). It is known that AMPK exerts a protective effect on endothelial cells under conditions such as metabolic, oxidative, or inflammatory stress, mainly through the activation of eNOS (Nagata et al., 2003). On the other hand, the ability of AMPK to inhibit angiogenesis, an ATP-consuming process, represents the classic facet of the energy-preserving role of this kinase. AMPK activation is considered a promising strategy for the treatment of metabolic diseases such as type II diabetes and obesity and cardiovascular and neurologic diseases. It is also emerging as an interesting potential treatment in cancer, as a downstream target of the tumor suppressor LKB1 and because of its regulatory effects on mTOR, which is aberrantly activated in many tumors (Laplante et al., 2012). Recent studies have demonstrated that AMPK activation (*e.g.*, by AICAR or expression of constitutively active mutants) inhibits cancer cell proliferation and/or induces apoptosis in several cancer models and in myocardial cells and keratinocytes (Theodoropolou et al., 2010; Vakana et al., 2011). In our study, iPA treatment at the highest concentrations (5 and 10 μM) exerted proapoptotic effects (Fig. 14). The activation of the intrinsic apoptosis pathway was confirmed by the caspase cascade, which leads to caspase-9 activation followed by caspase-3 activation and results in PARP-1 cleavage, finally leading to apoptotic cell death. We found that

iPA induced the activation of typical DNA damage checkpoints, such as the ATR-Chk1 pathway and p53. We hypothesize that the putative triphosphate derivative of iPA, similarly to false bases such as 5-fluorouracil (5-FU), is misincorporated into RNA, causing alterations of its processing and functioning, or into DNA, resulting in DNA damage and checkpoint activation. This effect may also be related to AMPK activation, in that it has been reported that the activation of AMPK is associated with the phosphorylation of p53 (Ser15 and Ser20), which is coupled to its acetylation (Lee et al., 2012). Indeed, we found that iPA induces the phosphorylation of p53 on Ser15 (Fig. 14). Moreover, recent works describe a novel function for AMPK as a sensor of genomic stress and a participant of the DNA damage response (DDR) pathway (Sanli et al., 2013).

High interest is emerging in developing AMPK agonists for clinical use as antitumor agents. Moreover, blocking of endothelial cell proliferation and migration by AMPK activation is of potential pharmacological significance, because these processes contribute to several pathologic disorders in addition to cancer, such as atherosclerosis, diabetic retinopathy, and several autoimmune diseases (Folkman, 2006). Among the AMPK activators actually studied, there are also the selective small molecule A-769662, which directly binds and activates the kinase in a mode similar to AMP (Goransson et al., 2007) and metformin, the most widely prescribed oral hypoglycemic agent, which activates AMPK in endothelial cells by a complex mechanism that probably involves the inhibition of mitochondrial respiration, with a consequent elevation of the AMP/ATP ratio (Zhou et al., 2001). It is noteworthy that retrospective studies conducted in diabetic patients found that metformin is associated with a decreased risk in developing cancer and a better response to chemotherapy (Landman et al., 2010). Available AMPK activators, such as

metformin and AICAR, show relatively low efficacies. Indeed, metformin activates AMPK at millimolar levels, whereas AICAR acts at low millimolar concentrations (0.5–2 mM) (Meisse et al., 2002). The advantage of iPA with respect to these AMPK activators is a higher efficacy, with low micromolar concentrations effective in activating AMPK and exerting biological effects, such as the angiogenesis inhibition described herein or the tumor growth blockade (Bifulco et al., 2008). In our work, iPA clearly displayed antiangiogenic properties through AMPK-dependent mechanisms; however, we have to take into account that it may also elicit other effects, as demonstrated elsewhere. Indeed, iPA inhibits breast and colon cancer cell proliferation, affecting, respectively, the Akt/NFkB cell survival pathway and inducing JNK phosphorylation and hence activation (Laezza et al., 2009; Laezza et al., 2010). Both these signaling pathways are involved in apoptotic events downstream AMPK activation in several cancer models (Zheng et al., 2012; Yung et al., 2013). Furthermore, among the proposed mechanisms that explain the antiproliferative effects of iPA, inhibition of the mevalonate pathway enzyme FDPS, and hence of prenylation of key oncogenic proteins such as Ras and Rho, is noteworthy (Laezza et al., 2006). Of further interest, AMPK activation is involved in the regulation of lipid metabolism, being linked to the inactivation of acetyl-CoA carboxylase and of 3-hydroxy-3-methyl-glutaryl-CoA reductase, a limiting enzyme of the mevalonate pathway. The importance of interfering with the mevalonate pathway to arrest cancer growth is highlighted by the antitumor properties shown by several classes of drugs targeting this pathway, such as statins, bisphosphonates, and farnesyltransferase inhibitors (Laezza et al., 2008).

Our results demonstrating that iPA elicits a direct antimigratory action on endothelial cells (Fig. 15) are in agreement with those in recent articles reporting the inhibition of the migration of HUVECs, monocytes, and

neurons by AMPK activation (see enclosed Picardi et al., 2013). Also, in the case of migration, transient AMPK activation by VEGF is associated with endothelial cell migration stimulation through eNOS (Reihill et al., 2011; Nagata et al., 2003). Therefore, as is true of proliferation, the reasons for the disparate effects of AMPK on cell migration are strictly dependent on the activating stimulus, the metabolic status, and the degree of AMPK activation. Of note, iPA may exert an antimigratory effect, also affecting cAMP-mediated microfilament organization, as has been observed in thyroid cancer cells (Laezza et al., 1997), or through matrix metalloproteinase inhibition, as reported for AMPK activators (Laplante et al., 2012). AICAR has been shown to inhibit angiogenesis *in vitro* (Peyton et al., 2012) and *in vivo*, reducing retinoblastoma neovascularization, even if this effect is the consequence of tumor mass reduction rather than a direct effect on the vasculature (Theodoropoulou et al., 2013). In our study, we demonstrated that iPA directly affects angiogenesis, not only *in vitro*, but also maintains its properties in the *in vivo* setting, in the absence of tumor masses (Fig. 16). Moreover, unlike AICAR, which inhibited endothelial cell proliferation and migration *in vitro*, while paradoxically stimulating morphologic differentiation into capillary-like tube structures (a fundamental characteristic of the formation of new vessels), iPA inhibited all the successive phases of sprouting angiogenesis.

5.2 N6-isopentenyladenosine, activating AMPK, induces autophagy and apoptosis in a cooperative manner in melanoma

Since angiogenesis is a key step in tumor growth and metastasis providing necessary oxygen and nutrients for the tumor (Mazeron et al., 2009), the inhibition of any step of these processes that lead to the disruption of angiogenesis can be useful as a potential antitumor therapy. In the light of this paradigm, the effects of iPA on tumor angiogenesis process were

investigated, using A375 human melanoma cells, well known for their highly angiogenic phenotype, as well as co-cultures of endothelial and melanoma cells.

Although after 24 hours of treatment iPA did not significantly affect the viability of melanoma cells (data not shown), surprisingly melanoma cells treated with iPA (1-10 μM) for 24 hours and co-cultured with endothelial cells for the next 24 hours inhibited the viability of endothelial cells already at 2.5 μM (Fig. 17). When a more sensitive proliferation assay was performed, the time- and concentration-dependent anti-proliferative effect of iPA was clear (Fig. 18), with a concomitant block in G1 phase of melanoma cells cycle (Fig. 19).

In a recent study the authors hypothesized that the antiproliferative effects of iPA on prostate cancer cells could be mediated by adenosine receptor A3. In that study iPA is shown as agonist of A3 receptors, binding selectively to this isoform of adenosine receptors (Blad et al., 2011). A3 receptors are expressed also on A375 melanoma cells. Stimulation of these receptors activates PI3K inducing thus Akt activation, with concomitant decrease of ERK1/2 levels (Merighi et al., 2005). The authors conclude that the antiproliferative effects of iPA in the range of 10-100 nM on prostate cancer cells could be mediated by A3 receptors. Of note, in this range of concentrations iPA did not exert any antiproliferative effects in melanoma cells. The same authors speculated that iPA in the higher range of concentration (micromolar range) exerts its antiproliferative effects independently of A3 receptors (Blad et al., 2011). In our work antiproliferative effects of iPA observed in melanoma cells are in the micromolar range (1-20 μM) and for these reasons we exclude any involvement of the adenosine pathway, as already shown for endothelial cells system. In our opinion, iPA does not act as agonist or antagonist of a G-protein coupled receptor as A3 in extracellular environment, but it

indeed enters into the cells where is monophosphorylated in 5'-monophosphate isopentenyladenosine (iPAMP), its active form. Indeed, as observed in endothelial cells, the phosphorylation of iPA in C5 by ADK is crucial also to the anti-tumor activity of iPA, since the pre-treatment with 5-Itu reverted all its biological effects. Indeed, the active metabolite is precisely iPAMP, an AMP mimetic. According with what highlighted in endothelial cells, iPAMP was able to induce the phosphorylation and hence activation of AMPK also in melanoma cells (Fig. 20). The AMPK pathway appears to be involved in cell death and more specifically in autophagy induced by nutrient deprivation, growth factor withdrawal and hypoxia. Among proposed mechanisms, the activation of AMPK leads to the suppression of mammalian target of rapamycin (mTOR), thereby activating autophagy (Wang and Qin, 2013). Autophagic cell death (also referred as type II cell death) and apoptosis, known as type I cell death, have considered as the principal mechanisms of programmed cell death in mammals. Although autophagy and apoptosis are markedly different processes, they can act together to induce cell death in a coordinated and cooperative manner. Autophagy is emerging also as an escape mechanism associated to chemoresistance that cancer cells can exploit for protection against a variety of intrinsic and extrinsic stress signals, including chemotherapeutic agents (Farkas et al., 2011). However, excessive or derailed autophagy can also favor cell death. How these two seemingly opposing roles of autophagy can have an impact upon cancer chemoresistance is unclear (Wang and Qin, 2013). Some recent reports have implicated AMPK with regulation of autophagy. In colon cells, for example, autophagy, but not apoptosis, is considered as a major cause for C6 ceramide-induced cytotoxic effects and activation of AMPK/Ulk1 is required for the process (Huo et al., 2013). Activation of AMPK induces autophagic cell death in a great number of tumors also *in vivo* (Meley et

al., 2006; Xu et al., 2007; Vara et al., 2011; Salazar et al., 2011; Din et al., 2012; Liu et al., 2012). Also in endothelial cells AMPK-induced autophagy is observed (Wang et al., 2011; Zhang et al., 2013). On the other hand, a work reported that AICAR treatment and glucose deprivation of human mammary cancer derived cells (MCF-7s) is able to inhibit autophagy (Liang et al., 2007). Interestingly, more recent studies indicate that apoptosis and autophagy via a mitochondrial-mediated ROS–p38–p53 pathway have been observed in melanoma cells (Liu et al., 2008). The activation of AMPK is also involved in cell apoptosis induced by different stimuli including chemotherapy drugs (Kim et al., 2010; Lee et al., 2010) and in vincristine treated murine melanoma cells, probably by the activation of p53 and the inhibition of mTORC1 that is a complex composed by a serine/threonine kinase called mTOR, regulatory associated partner of mTOR (raptor) and mLST8 (lethal with sec thirteen), together to ROS production and LKB1 activation (Chen et al., 2011).

As reported above, there is a tight interconnection between unfolded protein response (UPR) and autophagy. Indeed, accumulating data indicate that ER stress is also a potent trigger of autophagy and there are evidences of an involvement of AMPK (Høyer-Hansen and Jäättelä, 2007). Interestingly, a recent work highlighted that iPA was able to induce cellular stress *in vitro* upregulating the genes belonging to gene ontology (GO) category, among others, just "unfolded protein response" (Colombo et al., 2009). Employing microarray analysis, the authors reported that iPA (100 μM for 6 hours) was able to upregulate this specific GO category in human lung and breast cancer cells. In our experimental setting, autophagy pathway is evidently activated treating melanoma cells in a range of concentrations very low (up to 10 μM) with respect to the cited work. These data, anyway, could be supported by previously evidences, showing a correlation between these upregulated genes and the trigger of

autophagy. In the same study, microarray analysis revealed also an involvement of the genes belonging to "cell cycle arrest" GO category. Moreover, cell cycle arrest in G0/G1 phase has been recently reported in bladder carcinoma cells treated with iPA (Castiglioni et al., 2013). These data are concordant with the cell cycle arrest in G1 phase that we have reported also in melanoma cells after iPA treatment (Fig. 19).

It is now well accepted that basal or low level of autophagy is responsible to protect cells from apoptosis depending on the physiopathological setting (Levine and Yuan, 2005; Gozuacik and Kimchi, 2004; Codogno and Meijer, 2005; Sato et al., 2007; Vara et al., 2011). On the other part, excessive or sustained autophagy causes cell death when cell faces significant stress conditions (Rosenfeldt and Ryan, 2011). Notably, autophagy does not always promote cell survival, but can also mediate non-apoptotic cell death for example in experimental conditions where apoptosis pathways are blocked, or in response to treatments that specifically trigger caspase-independent autophagic cell death. Thus, apoptosis or/and autophagy are interesting mechanisms to induce cancer cell death. To determine whether autophagy mediated by iPA could affect cell viability, we analyzed the percentage of apoptotic cells (Annexin V positive and Annexin V/PI double positive) after 24, 48 and 72 hours with increasing concentrations of iPA. The substantial induction of apoptosis was clear after 48 and aven more after 72 hours of treatment with iPA (Fig. 19*B*). Taken together, these results indicate that iPA induces a concomitant induction of autophagy (Fig. 21) and apoptosis processes in melanoma cells, both of which are involved in cell death. To identify the event sequence of autophagy and apoptosis, we have performed the analysis of biochemical pathways in time course. The results clearly showed that the increase of expression and the conversion of LC3 preceded the cleavage of PARP (Fig. 22), suggesting that the autophagy is set up before apoptosis,

in according with that flow cytometry analysis highlighted (Fig. 21).

These findings are consistent with results of a work showing that the AMPK activators AICAR and metformin reduced the proliferation of SKMel2 and SKMel28 melanoma cells. Metformin action is mainly mediated by AMPK activation (Woodard et al., 2010). However, very little is known about the role that the interchange between these two cellular processes have in the control of tumor growth in response to anticancer agents. Nevertheless, further research will be still necessary to clarify the precise mechanisms linking both death processes.

Undoubtedly, in cancer there are multiple functional relationship reported between apoptosis and autophagy, and these processes separately or/and jointly seal the fate of the cell (Maiuri et al., 2007). The discovery of new therapeutic compounds is a very important challenge to treat advanced melanomas that are became resistant to existing therapies.

5.3 N6-isopentenyladenosine directly affects cytotoxic and regulatory functions of human NK cells

Among the others, immune-surveillance plays a role in the control of tumor development. Belonging to innate immunity, NK cells are cytolytic lymphocytes that can directly kill transformed and microbe-infected cells. Despite the prevailing view that immunological surveillance is triggered by danger signals, injured cells arising signals, toxins, pathogens and mechanical damage, a recent work has shown that locally resident immune cells in the skin can detect early signs of cellular stress, through the recognition of ligands on premalignant cells, thus overting tumor transformation (Strid et al., 2008). NK cells reside in the skin (Luci et al., 2009), thus melanocytes are susceptible to NK cell recognition from early stages of dysregulation. Although there is the potential for early NK cell recognition of transformed melanocytes, some studies have indicated that NK cells are poorly represented among tumor-infiltrating lymphocytes

during melanoma progression, whereas others have demonstrated NK cells in all biopsies evaluated. Understanding how NK cells migrate into the tumor microenvironment is important to redirect NK cells to the tumor in the therapeutic setting. To appreciate the role of immunosurveillance during melanoma, the factors that influence NK cell recognition of nascent dysregulated melanocytes need to be identified. In turn, how these factors change at different stages of disease, both in primary lesions and metastases, must be deciphered. This involves characterizing the spatio-temporal expression of ligands during melanomagenesis, which hitherto has been poorly described, and the consequences of this event on NK cell function (Burke et al., 2010). In the light of these observations, in the last part of this work, we presented previously unrecognized functions of iPA in promoting a direct activation of human resting NK cells and a synergy of action with IL-2 in potentiating the effector arm of their responses. Of note, a similar synergistic effect has not been observed in NK cells treated with the isoprenoid intermediate IPP or with the purine nucleoside adenosine (data not shown). This observation correlates with previously published findings that IPP and IL-2 do not stimulate NK cells directly, rather IPP plus IL-2- induced soluble factors (e.g., cytokines) from γδ T cells that can stimulate indirectly NK cell mediated cytotoxicity (Alexander et al., 2008). At the same way adenosine, whose levels have been found elevated within growing tumors, seems to inhibit effector functions of tumor-infiltrating immune cells (Lokshin et al., 2006), mainly through the stimulation of the immunosuppressive A2A and A2B adenosine receptors subtypes. Even though in an *in vivo* mouse model the oral administration of an A3 adenosine receptor-selective agonist led to enhanced NK cell activity (Harish et al., 2003), the direct effect of adenosine on IL-12 producing dendritic cells rather than on NK cells has been reported to account for the observed effects. On the contrary, the

stimulation of peripheral blood lymphocytes (PBMCs) with iPA and low doses of IL-2 was not able to selectively expand γδ T cells (data not shown) like IPP does, confirming the specificity of action of this molecule on NK cells. These findings support the notion that the effects of iPA, in all the cell models that we have studied, are retained in its peculiar structure made of the specific combination of the adenosine molecule and the isoprenoid moiety. And maybe also thanks to the lipophilic nature of its isoprenoid chain, iPA can enter inside NK cells, as observed in endothelial cells, where it exerts its immunostimulatory activity. According to the far away work of Gallo et al., we have seen that also on NK cells sub-micromolar doses of iPA have a stimulatory effect on cell proliferation and activation status, measured by increased levels of CD69 (Fig. 24). Remarkably, NK cells did not undergo proliferation by iPA alone (data not shown). Moreover, going beyond the preliminary observations of Gallo, we investigated to what extent the reported synergistic effect of IL-2 and iPA applies only to NK cell proliferation or also holds true for other effector functions of NK cells. Consistent with proliferation results, also induction of granules' release and the NK cytotoxic potential against tumor target cells, were positively affected by iPA (Fig. 25). In fact, moreover besides their ability to kill aberrant cells, NK cells have the capacity to produce a variety of cytokines and chemokines (TNF-α, IFN-γ, CCL3, CCL5, IL-8, IL-10 etc), through which they also participate in the shaping of adaptive immune response (Vivier et al., 2009). These NK cell effector functions are regulated by multiple activating and inhibitory NK cell receptors (Lanier, 2005). Engagement of activating receptors, such as natural cytotoxicity receptors (NCRs; NKp30, NKp44, and NKp46) and NKG2D, leads to the activation of a variety of downstream signaling molecules, which result in the activation of MAPKs, particularly ERK, which are crucial for cytolytic granule release and cytokine generation

(Vivier et al., 2004).

Then we provided evidence, at least in part, of the selective involvement of NKp30 and to a minor extent of NKG2D, in mediating in particular iPA-IL-2 synergic effects on cytotoxicity (Fig. 25). Of note, the engagement of NKp30 and NKG2D by K562 cells that express cognate ligands for these natural cytotoxicity receptors (Brandt et al., 2009; Joyce et al., 2011) have been shown to induce not only cytotoxic effector mechanisms, but also the secretion of cytokines and chemokines (Fauriat et al., 2010). These findings, along with the recent report highlighting that the engagement of NKp30 on Vδ1 T cells triggers the production of high levels of CCL3/MIP-1α, CCL4/ MIP-1β, and CCL5/Rantes (Hudspeth at al., 2012) is in agreement with our results showing the ability of iPA low doses, after co-incubation with K562 cells, to stimulate not only the secretion of IFN-γ and TNF-α cytolytic cytokines, but also of chemokines like CCL3 and CCL5. The classic cytolytic cytokines may account for the observed enhanced cytotoxicity of IL-2 primed NK cells, whereas the chemokines may be useful to the complete host control of infections and tumor growth through the mobilization of immunocompetent cells to sites of infections and tumoral lesions (Lavergne et al., 2004; Thapa et al., 2008). If there is a concentration-dependent effect in the secretion of IFN-γ, the same has not been seen for chemokines, probably because their secretion requires only stronger activating stimuli (e.g. 0.1 μM dose), or simply because of the very high inter-individual variability of cytokine milieu of donors where may coexist different factors that can regulate the delicate balance in NK cell responsiveness to the two iPA doses. Moreover, the current vision of CD56dim NK cells as the rapid more prominent producers of cytokines and chemokines upon both target cell recognition (Fauriat et al., 2010) and exogenous cytokine activation (De Maria et al., 2011) led us to also verify which NK subset iPA might selectively target. Accordingly,

multiparametric intracellular staining revealed that IL-2 primed CD56dim NK cells were preferentially expanded and activated to secrete IFN-γ by iPA costimulation upon K562 short-term co-colture (data not shown). A molecular target candidate to mediate the action of iPA seems to be the ERK1/2 MAPK, whose phosphorylation status in human primary NK cells increased in response to the different concentrations of this isoprenoid compound. Our data show, in fact, that iPA positively modulates only ERK1/2 signal transduction, without affecting the STAT5-dependent pathways that could be fully operational in iPA-treated NK (Fig. 27). This was corroborated by the observation that the treatment of IL-2 primed NK cells with different concentrations of iPA does not change even the levels of p38 phosphorylation, which is crucial for the generation of cytokines upstream STAT5 signaling (Pujari et al., 2010). We further corroborated the role of ERK1/2 activation for cytolytic activity and cyto-chemokines generation using the UO-126 MEK inhibitor, that completely ablated the NK positive response to the co-treatment with IL-2 and iPA (Fig. 28). Activation of ERK follows a highly conserved set of molecular events and Ras protein is an essential factor in MAPK regulation (Mor and Philips, 2006). Accordingly to literature, we have found that the co-treatment with the stimulatory dose of iPA effectively led to greater levels of the active form of Ras, compared to the effect of IL-2 alone (Fig. 29). Of note, we started to know that the stimulatory action of iPA converges on ERK1/2 MAPK through the modulation of expression and activity of farnesyl diphosphate synthase (FDPS), the same enzyme implicated in the stimulation of the cytotoxic γδ T cells. Indeed, previous experimental observations by our group suggested that iPA could interfere with the cell growth of xenograft tumors induced by k-Ras transformed thyroid cells (KiMol), by inhibiting FDPS activity and hence downstream protein prenylation (Laezza et al., 2006), which suggests that this isoprenoid end

product might be used for antineoplastic therapy, an application emulating that of statins and/or FDPS inhibitors like bisphosphonates, as well as farnesyl transferase inhibitors (Thurnher et al., 2012). iPA has been reported to regulate FDPS also in fibroblasts from humans with progeroid syndromes, where the inhibition of the farnesylation of prelamin A is associated with a decrease in the frequency and nuclear shape abnormalities, making iPA a potential strategy for treating children with Hutchinson-Gilford progeria syndrome (Bifulco et al., 2013). In the present work, lowest doses (up to 1 μM) of iPA resulted in a surprising and effective boosting of NK activity. At these doses, iPA was able to enhance both the protein level expression and the enzymatic activity of FDPS. However how iPA exerts its effects remains to be further clarified. We believe that our findings can give us a satisfactory explanation of the stimulatory activity of iPA on human NK cells. Indeed, the FDPS activation can cause an accumulation of farnesylpyrophosphate (FPP) and of its downstream product geranylgeranylpyrophosphate (GGPP), both essential for the biological functions of the prenylated proteins (Thurnher et al., 2012). Prenylation occurs on many members of Ras and Rho family of small guanosine triphosphatases (GTPase) containing the CaaX sequencing, but also on many members of the Rab family of Ras-related G-proteins. Interestingly the activation of Rac, a member of Rho GTPase family, is seen as a booster for the effector cell-binding efficiency, recruitment ability, and consequently, cytotoxic activity in NK cells, through the regulation of the actin/microtubule interplay (Malorni et al., 2003). In this context, people affected by the Wiskott-Aldrich disease, a human pathology characterized by a defect in a protein controlled by the Rho family member Cdc42 (Wiscott-Aldrich syndrome protein [WASP]), exhibit an impaired NK cell function (Orange et al., 2002). At the same way, the absence of Rap1b, a small-molecular weight GTP-binding protein

that belongs to the Ras-like superfamily of GTPases, impaired NKG2D, Ly49D, and NCR1-mediated cytokines and chemokines production by NK cells of knockout mice (Awasthi et al., 2010). Moreover, isoprenylation has been proved to be important for the induction of elevated LFA-1 affinity and avidity in NK cells (Raemer et al., 2009), that was particularly important for IFN-γ secretion. Finally, it has been reported that a reduced Ras activity by the knockdown of Ras guanyl nucleotide-releasing protein (RasGRP), impaired NK cell effector functions affecting the Ras-MAPK pathway (Lee et al., 2009), generally sustained by all these isoprenylated proteins. Thus, in our opinion, iPA by increasing FDPS activity can expand and co-stimulate human NK cells regulating the rate of prenylation of key proteins in NK cell activation processes, like Ras, Rac, Rap1b, that signal through ERK1/2. Remarkably, this is not the first evidence that intermediates of the mevalonate pathway are able to expand the immune cytotoxic compartment; just we think about the enhanced expansion of Th1 effector cells seen to be promoted by accumulation of farnesyl-PP (Dunn et al., 2006), or simply to the expansion of γδ T cells following IPP plus IL-2 stimulation (Maniaret et al., 2010). Overall our data reflect the important action of iPA on the entire complexity of NK cell functions even though some questions need to be deepened in future. First of all if in a physio/pathological context *in vivo* iPA could be endogenously modulated in NK cells or if the NK activation could be rather largely dependent from an extracellular source of iPA, as suggested by the detection of iPA in human urine from normal subjects and cancer patients (Vold et al., 1982). Moreover, the upregulation of FDPS by iPA may not represent the unique mechanism responsible of iPA effects in NK cells and other potential molecular targets remain to be identified. This could help to explain some apparently paradoxical results, as for example, the observation that iPA treatment of IL-2 stimulated NK cells increases their proliferative potential

and IFN-γ production over that of IL-2 stimulation alone (Fig. 26), while it is not able to induce the same when used alone on resting NK cells (Fig. 21). The addition of IL-2 results in a morphologic and biological transformation to a fully activated NK cell capable of DNA synthesis, eventual mitosis, cyto-chemokines production and cytotoxicity. These events are preceded, of course, by an increase in RNA and protein synthesis. Gene expression profile analysis of iPA-treated cells revealed that the majority of modulated genes were those involved in transcription and its regulation (Colombo et al., 2009). Depending on the cytokines milieu or resting condition, iPA might then influence a specific gene expression program in NK cells (Ramirez et al., 2012). This could explain also the selective effect of iPA on the up-regulation of NKp46 (Fig. 23), whose high expression specificity on NK cell lineage, unlike other NCRs, needs a specific and fine transcriptional control (Lai and Mager, 2012), which iPA could affect. Collectively, the emphasis on this small isoprenoid product is that it could represent a novel endogenous signal able to complement the well characterized IPP-induced γδ T cells expansion, in order to achieve a combined and finely tuned innate artillery against infections and cancer.

Our findings highlighted a new mechanism of iPA anti-tumor action. In addition to this scenario, we can speculate that the pharmacological induction of IPP and iPA levels could lead to a collaborative reaction by activating respectively human γδ T cells and NK cells, that will be interesting to explore in more detail in different physiopathological contexts.

6. CONCLUSIONS

N6-isopentenyladenosine (iPA) is a modified adenosine characterized by an isopentenyl chain linked to the nitrogen at position 6 of the purine base. The isoprenoid chain derives from a product of the mevalonate pathway and, more specifically, from dimethylallyl pyrophosphate (DMAPP), which is in equilibrium with its isomer, isopentenyl pyrophosphate (IPP).

iPA belongs to the family of cytokinins that regulate plant cell growth and differentiation, but it is also present in mammalian cells in a free form in the cytoplasm or bound to tRNA. iPA biosynthesis in mammals has not been fully disclosed, whereas some of its biological effects are known. Antiproliferative and pro-apoptotic effects of iPA have been reported against various tumors *in vitro* and *in vivo* (Bifulco et al., 2008).

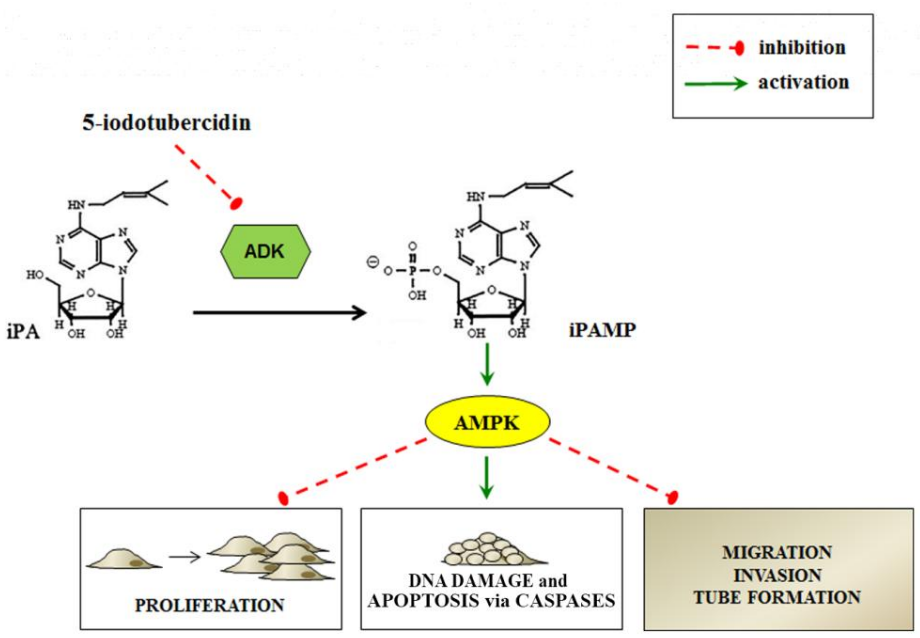

Figure 30. Proposed mechanism of action of iPA in endothelial cells

In this study new pleiotropic effects of iPA have been reported for the first time. Specifically, iPA, in the range of 1-10 µM, can be considered as a novel AMPK activator, in its 5'-monophosphorylated form (iPAMP) acting thus as an AMP mimetic. Indeed, AMPK activation is related to the inhibition of all the key steps of the angiogenesis process, including proliferation, migration, invasion and tube formation in endothelial cells, finally leading to the activation of apoptosis (Fig. 30).

Therefore, iPA could represent a useful tool for the inhibition of neovascularization in cancer and in other diseases where excessive neoangiogenesis is the underlying pathology, as atherosclerosis, diabetic retinopathy, obesity. Of note, neither isopentenyl pyrophosphate nor adenine or adenosine have similar behaviors. Thus, it's the entire molecular structure of iPA responsible for all the biological effects observed.

In melanoma cells AMPK activation can be considered responsible of the arrest of cancer cells growth, autophagy induction and subsequent apoptosis (Fig. 31). In this system, indeed, autophagy is not correlated to cell survival and thus chemoresistence, but it really represents a cell death II type. This aspect can be very useful for the melanoma cancer therapy. Obviously, further experiments will be necessary to validate in animal models these *in vitro* data.

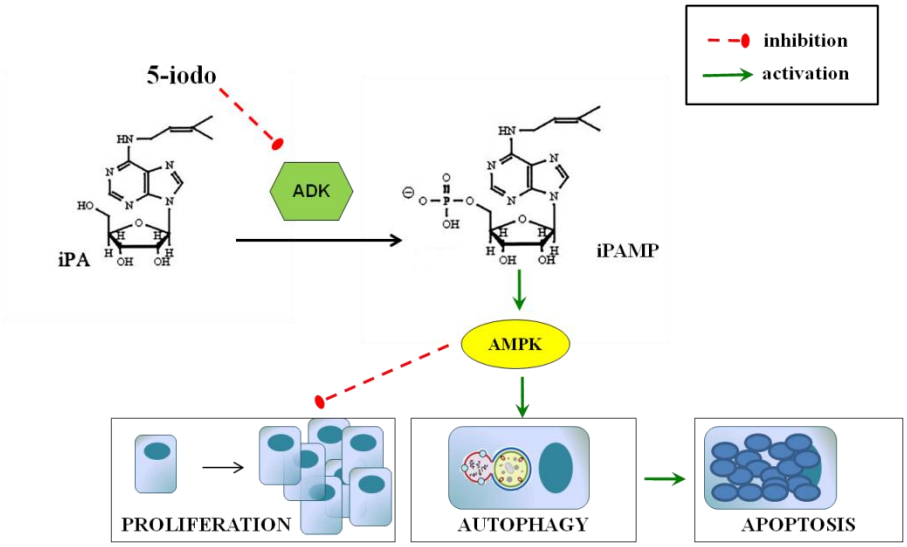

Figure 31. Proposed mechanism of action of iPA in melanoma cells

In the last part of this work an additional piece of evidence of the immune-regulatory function of iPA, at submicrolar concentrations, has been reported. iPA was able, indeed, to stimulate directly the proliferation of NK cells, activating their potential cytotoxicity against tumor cells. The molecular mechanism by which iPA exerts its effects could be related to the activation of Ras (Ras-GTP), responsible then for the activation of MAPK signaling. It was reported also an activation of FDPS, probably involved into the activation and functionality of Ras through its isoprenylation (Fig. 32).

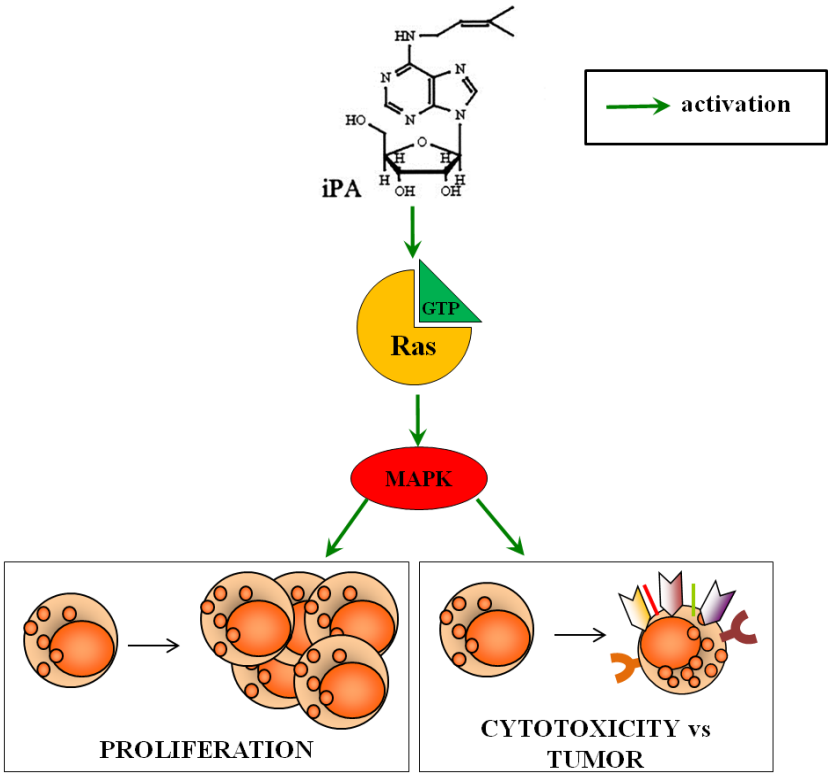

Figure 32. Proposed mechanism of action of iPA in Natural Killer cells

The novel and intriguing insights of this study highlight pleiotropic effects of this isoprenoid derivative, making iPA an interesting lead compound for a new class of antitumoral drugs. Indeed, while the anticancer effects *in vitro* are well-documented, iPA efficacy *in vivo* is limited by its pharmokinetic properties, since when administered intraperitoneally in mice it is quickly catabolized in plasma (Colombo et al., 2009). Of note, when administered subcutaneously, iPA is able to inhibit cancer growth of tumor xenografts, even at lower doses (Laezza et al., 2006). Among the possible enzymes responsible for the inactivation of iPA, adenosine deaminase doesn't seem to be involved, since iPA is not a substrate of this enzyme as we have shown (Fig. 12). Among the enzymes involved in catabolism of iPA, purine nucleoside phosphorylase could be responsible.

New iPA derivatives are necessary to identify a compound with better pharmacokinetic profile and enhanced *in vivo* antitumor activity.

In the light of overall results, iPA is an attractive pharmacological tool for the anticancer strategy, because of its ability to inhibit cancer growth and proliferation both directly on tumor cells and indirectly, by the inhibition of the angiogenic process indispensable to cancer growth and progression. Moreover, iPA can be useful in immune intervention, in particular in the field of anti-tumor immunity, since it has been proven stimulating and activating directly natural killer cells. In this way a multifactorial and cooperative strategy of attack of the neoplastic mass could be carried out.

7. REFERENCES

Adams RH, Alitalo K. Molecular regulation of angiogenesis and lymphangiogenesis. *Nat Rev Mol Cell Biol*. **2007**;8(6):464-78.

Ahearn IM, Haigis K, Bar-Sagi D, Philips MR. Regulating the regulator: post-translational modification of RAS. *Nat Rev Mol Cell Biol*. **2011**; 13(1), 39-51.

Alexander AA, Maniar A, Cummings JS, Hebbeler AM, Schulze DH, Gastman BR, Pauza CD, Strome SE, Chapoval AI. Isopentenyl pyrophosphateactivated CD56+ {gamma}{delta} T lymphocytes display potent antitumor activity toward human squamous cell carcinoma. *Clin Cancer Res*. **2008**; 14(13), 4232-4240.

Alter G, Malenfant JM, Altfeld M. CD107a as a functional marker for the identification of natural killer cell activity. *J Immunol Methods*. **2004**; 294(1-2), 15–22.

Arap W, Kolonin MG, Trepel M, Lahdenranta J, Cardó-Vila M, Giordano RJ, Mintz PJ, Ardelt PU, Yao VJ, Vidal CI, Chen L, Flamm A, Valtanen H, Weavind LM, Hicks ME, Pollock RE, Botz GH, Bucana CD, Koivunen E, Cahill D, Troncoso P, Baggerly KA, Pentz RD, Do KA, Logothetis CJ, Pasqualini R. Steps toward mapping the human vasculature by phage display. *Nat Med*. **2002**;8(2):121-7.

Astot C, Dolezal K, Nordström A, Wang Q, Kunkel T, Moritz T, Chua NH, Sandberg G. An alternative cytokinin biosynthesis pathway. *Proc Natl Acad Sci U S A*. **2000**;97(26):14778-83.

Auchampach JA. Adenosine receptors and angiogenesis. *Circ Res*. **2007**;101(11):1075-7.

Awasthi A, Samarakoon A, Chu H, Kamalakannan R, Quilliam LA, Chrzanowska- Wodnicka M, White 2nd GC, Malarkannan S. Rap1b

facilitates NK cell functions via IQGAP1-mediated signalosomes. *J Exp Med*. **2010**; 207(9), 1923-1938.

Balch CM, Gershenwald JE, Soong SJ, Thompson JF, Atkins MB, Byrd DR, Buzaid AC, Cochran AJ, Coit DG, Ding S, Eggermont AM, Flaherty KT, Gimotty PA, Kirkwood JM, McMasters KM, Mihm MC Jr, Morton DL, Ross MI, Sober AJ, Sondak VK. Final version of 2009 AJCC melanoma staging and classification. *J Clin Oncol*. **2009**;27(36):6199-206.

Bifulco M, Malfitano AM, Proto MC, Santoro A, Caruso MG, Laezza C. Biological and pharmacological roles of N6-isopentenyladenosine: an emerging anticancer drug. *Anticancer Agents Med Chem*. **2008**;8(2):200-4.

Bifulco M, D'Alessandro A, Paladino S, Malfitano AM, Notarnicola M, Caruso MG, Laezza C. N6-isopentenyladenosine improves nuclear shape in fibroblasts from humans with progeroid syndromes by inhibiting the farnesylation of prelamin A. *FEBS J.* **2013**;280(23):6223-32.

Blad CC, von Frijtag Drabbe Künzel JK, de Vries H, Mulder-Krieger T, Bar-Yehuda S, Fishman P, Ijzerman AP. Putative role of the adenosine A(3) receptor in the antiproliferative action of N (6)-(2-isopentenyl)adenosine. *Purinergic Signal*. **2011**;7(4):453-62.

Bonauer A, Boon RA, Dimmeler S. Vascular microRNAs. *Curr. Drug Targets*. **2010**;11: 943–949.

Brandt CS, Baratin M, Yi EC, Kennedy J, Gao Z, Fox B, Haldeman B, Ostrander CD, Kaifu T, Chabannon C, Moretta A, West R, Xu W, Vivier E, Levin SD. The B7 family member B7-H6 is a tumor cell ligand for the activating natural killer cell receptor NKp30 in humans. *J Exp Med*. **2009**; 206(7), 1495-503.

Burke S, Lakshmikanth T, Colucci F, Carbone E. New views on natural killer cell-based immunotherapy for melanoma treatment. *Trends Immunol*. **2010**;31(9):339-45.

Burns DM, Rodi CP, Agris PF. Natural occurrence of an inhibitor of mammalian cell growth in human and mouse cells of normal and tumor origin. *Cancer Biochem Biophys*. **1976**;1(6):269-80.

Carmeliet P. Angiogenesis in health and disease. *Nat Med*. **2003**;9(6):653-60.

Carrega P, Pezzino G, Queirolo P, Bonaccorsi I, Falco M, Vita G, Pende D, Misefari A, Moretta A, Mingari MC, Moretta L, Ferlazzo G. Susceptibility of human melanoma cells to autologous natural killer (NK) cell killing: HLA-related effector mechanisms and role of unlicensed NK cells. *PLoS One.* **2009**;4(12):e8132.

Castiglioni S, Casati S, Ottria R, Ciuffreda P, Maier JA. N6-isopentenyladenosine and its analogue N6-benzyladenosine induce cell cycle arrest and apoptosis in bladder carcinoma T24 cells. *Anticancer Agents Med Chem*. **2013**;13(4):672-8.

Chen MB, Shen WX, Yang Y, Wu XY, Gu JH, Lu PH. Activation of AMP-activated protein kinase is involved in vincristine-induced cell apoptosis in B16 melanoma cell. *J Cell Physiol*. **2011**;226(7):1915-25.

Chiosson L, Vitale C, Cottalasso F, Moretti S, Azzarone B, Moretta L, Mingari MC. Molecular analysis of the methylprednisolone-mediated inhibition of NK-cell function: evidence for different susceptibility of IL-2- versus IL-15-activated NK cells. *Blood.* **2007**; 109(9), 3767-3775.

Ciaglia E, Pisanti S, Picardi P, Laezza C, Malfitano AM, D'Alessandro A, Gazzerro P, Vitale M, Carbone E, Bifulco M. N6-isopentenyladenosine, an endogenous isoprenoid end product, directly affects cytotoxic and regulatory functions of human NK cells through FDPS modulation. *J Leukoc Biol.* **2013**; 94:1207-19.

Clapp C, Thebault S, Jeziorski MC, Martínez De La Escalera G. Peptide hormone regulation of angiogenesis. *Physiol Rev.* **2009**;89(4):1177-215.

Codogno P, Meijer AJ. Autophagy and signaling: their role in cell survival

and cell death. *Cell Death Differ*.**2005**; 12(Suppl2):1509–1518.

Colombo F, Falvella FS, De Cecco L, Tortoreto M, Pratesi G, Ciuffreda P, Ottria R, Santaniello E, Cicatiello L, Weisz A, Dragani TA. Pharmacogenomics and analogues of the antitumour agent N6-isopentenyladenosine. *Int J Cancer*. **2009**;124(9):2179-85.

Corton JM, Gillespie JG, Hawley SA, Hardie DG. 5-aminoimidazole-4-carboxamide ribonucleoside. A specific method for activating AMP-activated protein kinase in intact cells? *Eur J Biochem*. **1995**;229(2):558-65.

Cummins DL, Cummins JM, Pantle H, Silverman MA, Leonard AL, Chanmugam A. Cutaneous malignant melanoma. *Mayo Clin Proc*. **2006**;81(4):500-7.

Dandapani M, Hardie DG. AMPK: opposing the metabolic changes in both tumour cells and inflammatory cells? *Biochem Soc Trans*. **2013**;41(2):687-93.

De Maria A, Bozzano F, Cantoni C, Moretta L. Revisiting human natural killer cell subset function revealed cytolytic CD56(dim)CD16+ NK cells as rapid producers of abundant IFN-gamma on activation. *Proc Natl Acad Sci U S A*. **2011**; 108(2), 728-32.

Decensi A, Puntoni M, Goodwin P, Cazzaniga M, Gennari A, Bonanni B, Gandini S. Metformin and cancer risk in diabetic patients: a systematic review and meta-analysis. *Cancer Prev Res (Phila).* **2010**;3(11):1451-61.

Dieli F, Vermijlen D, Fulfaro F, Caccamo N, Meraviglia S, Cicero G, Roberts A, Buccheri S, D'Asaro M, Gebbia N, Salerno A, Eberl M, Hayday AC. Targeting human {gamma}delta} T cells with zoledronate and interleukin-2 for immunotherapy of hormone-refractory prostate cancer. *Cancer Res*. **2007**;67(15):7450-7.

Din FV, Valanciute A, Houde VP, Zibrova D, Green KA, Sakamoto K, Alessi DR, Dunlop MG. Aspirin inhibits mTOR signaling, activates AMP-

activated protein kinase, and induces autophagy in colorectal cancer cells. *Gastroenterology.* **2012**; 142(1504–1515):e1503.

Divekar AY, Slocum HK, Hakala MT. N6-(delta2-isopentenyl)adenosine 5'-monophosphate: formation and effect on purine metabolism in cellular and enzymatic systems. *Mol Pharmacol*. **1974**;10(3):529-43.

Dons'koi BV, Chernyshov VP, Osypchuk DV. Measurement of NK activity in whole blood by the CD69 up-regulation after co-incubation with K562, comparison with NK cytotoxicity assays and CD107a degranulation assay. *J Immunol Methods*. **2011**; 372(1-2), 187-195.

Dunn SE, Youssef S, Goldstein MJ, Prod'homme T, Weber MS, Zamvil SS, Steinman L Isoprenoids determine Th1/Th2 fate in pathogenic T cells, providing a mechanism of modulation of autoimmunity by atorvastatin. *J Exp Med*. **2006**; 203(2), 401-412.

Ewart MA, Kohlhaas CF, Salt IP. Inhibition of tumor necrosis factor alpha-stimulated monocyte adhesion to human aortic endothelial cells by AMP-activated protein kinase. *Arterioscler Thromb Vasc Biol*. **2008**;28(12):2255-7.

Fang S, Salven P. Stem cells in tumor angiogenesis. *J Mol Cell Cardiol*. **2011**;50(2):290-5.

Farkas T, Daugaard M, Jäättelä M. Identification of small molecule inhibitors of phosphatidylinositol 3-kinase and autophagy. *J Biol Chem*. **2011**;286(45):38904-12

Fauriat C, Long EO, Ljunggren HG, Bryceson YT. Regulation of human NK-cell cytokine and chemokine production by target cell recognition. *Blood.* **2010**; 115(11), 2167-2176.

Faust JR, Dice JF. Evidence for isopentenyladenine modification on a cell cycle-regulated protein. *J Biol Chem*. **1991**;266(15):9961-70.

Feoktistov I, Goldstein AE, Ryzhov S, Zeng D, Belardinelli L, Voyno-Yasenetskaya T, Biaggioni I. Differential expression of adenosine receptors in human endothelial cells: role of A2B receptors in angiogenic factor regulation. *Circ Res.* **2002**;90(5):531-8.

Folkman J. Tumor angiogenesis: therapeutic implications. *N Engl J Med*. **1971**;285(21):1182-6.

Folkman J. Successful treatment of an angiogenic disease. *N Engl J Med*. **1989**;320(18):1211-2.

Folkman J, Hanahan D. Switch to the angiogenic phenotype during tumorigenesis. *Princess Takamatsu Symp*. **1991**;22:339-47.

Folkman J. Angiogenesis. *Annu Rev Med.* **2006**;57:1-18.

Folkman J. Angiogenesis: an organizing principle for drug discovery? *Nat Rev Drug Discov.* **2007**;6(4):273-86.

Fong GH, Takeda K. Role and regulation of prolyl hydroxylase domain proteins. *Cell Death Differ*. **2008**;15(4):635-41.

Gallo RC, Whang-Peng J, Perry S. Isopentenyladenosine stimulates and inhibits mitosis of human lymphocytes treated with phytohemagglutinin. *Science*. **1969**;165(3891):400-2.

Galmarini CM, Mackey JR, Dumontet C. Nucleoside analogues and nucleobases in cancer treatment. *Lancet Oncol*. **2002**;3(7):415-24.

Gazzerro P, Proto MC. Gangemi G, Malfitano AM, Ciaglia E, Pisanti S, Santoro A, Laezza C, Bifulco M. Pharmacological actions of statins: a critical appraisal in the management of cancer. *Pharmacol Rev.* **2012**; 64(1), 102-46.

Goel S, Duda DG, Xu L, Munn LL, Boucher Y, Fukumura D, Jain RK. Normalization of the vasculature for treatment of cancer and other diseases. *Physiol. Rev*. **2011**, 91:1071–1121.

Golovko A, Hjälm G, Sitbon F, Nicander B. Cloning of a human tRNA isopentenyl transferase. *Gene.* **2000**;258(1-2):85-93.

Göransson O, McBride A, Hawley SA, Ross FA, Shpiro N, Foretz M, Viollet B, Hardie DG, Sakamoto K. Mechanism of action of A-769662, a valuable tool for activation of AMP activated protein kinase. *J Biol Chem*. **2007**;282(45):32549-60.

Gozuacik D, Kimchi A. Autophagy as a cell death and tumor suppressor mechanism. *Oncogene* **2004**; 23:2891–2906.

Graells J, Vinyals A, Figueras A, Llorens A, Moreno A, Marcoval J, Gonzalez FJ, Fabra A. Overproduction of VEGF concomitantly expressed with its receptors promotes growth and survival of melanoma cells through MAPK and PI3K signaling. *J Invest Dermatol*. **2004**;123(6):1151-61.

Gruenbacher G, Gander H, Nussbaumer O, Nussbaumer W, Rahm A, Thurnher M. IL-2 costimulation enables statin-mediated activation of human NK cells, preferentially through a mechanism involving CD56+ dendritic cells. *Cancer Res*. **2010**;70(23):9611-20.

Hanahan D, Weinberg RA. The hallmarks of cancer. *Cell*. **2000**;100(1):57-70

Hardie DG, Hawley SA, Scott JW. AMP-activated protein kinase--development of the energy sensor concept. *J Physiol*. **2006**;574(Pt 1):7-15.

Hardie DG. AMP-activated protein kinase: an energy sensor that regulates all aspects of cell function. *Genes Dev*. **2011**;25(18):1895-908.

Hardie DG, Ross FA, Hawley SA. AMPK: a nutrient and energy sensor

that maintains energy homeostasis. *Nat Rev Mol Cell Biol*. **2012**;13(4):251-62

Harish A, Hohana G, Fishman P, Arnon O, Bar-Yehuda S. A3 adenosine receptor agonist potentiates natural killer cell activity. *Int J Oncol*. **2003;** 23(4), 1245-1249.

Helfrich I, Schadendorf D. Blood vessel maturation, vascular phenotype and angiogenic potential in malignant melanoma: one step forward for overcoming anti-angiogenic drug resistance? *Mol Oncol.* **2011**;5(2):137-49.

Hofmann UB, Westphal JR, Van Muijen GN, Ruiter DJ. Matrix metalloproteinases in human melanoma. *J Invest Dermatol*. **2000**;115(3):337-44.

Holash J, Davis S, Papadopoulos N, Croll SD, Ho L, Russell M, Boland P, Leidich R, Hylton D, Burova E, Ioffe E, Huang T, Radziejewski C, Bailey K, Fandl JP, Daly T, Wiegand SJ, Yancopoulos GD, Rudge JS. VEGF-Trap: a VEGF blocker with potent antitumor effects. *Proc Natl Acad Sci U S A*. **2002**;99(17):11393-8.

Høyer-Hansen M, Jäättelä M. Connecting endoplasmic reticulum stress to autophagy by unfolded protein response and calcium. *Cell Death Differ*. **2007**;14(9):1576-82.

Hudspeth K, Fogli M, Correia DV, Mikulak J, Roberto A, Della Bella S, Silva- Santos B, Mavilio D. Engagement of NKp30 on Vδ1 T cells induces the production of CCL3, CCL4, and CCL5 and suppresses HIV-1 replication. *Blood*. **2012**; 119(17), 4013-4016.

Huo HZ, Wang B, Qin J, Guo SY, Liu WY, Gu Y. AMP-activated protein kinase (AMPK)/Ulk1-dependent autophagic pathway contributes to C6 ceramide-induced cytotoxic effects in cultured colorectal cancer HT-29 cells. *Mol Cell Biochem*. **2013**;378(1-2):171-81.

Ishii Y, Hori Y, Sakai S, Honma Y. Control of differentiation and apoptosis of human myeloid leukemia cells by cytokinins and cytokinin nucleosides, plant redifferentiation-inducing hormones. *Cell Growth Differ*. **2002**;13(1):19-26.

Ishii Y, Kasukabe T, Honma Y. Induction of CCAAT/enhancer binding protein-delta by cytokinins, but not by retinoic acid, during granulocytic differentiation of human myeloid leukaemia cells. Br J *Haematol*. **2005**;128(4):540-7.

Jain RK. Molecular regulation of vessel maturation. *Nat Med*. **2003**;9(6):685-93.

Joyce MG, Tran P, Zhuravleva MA, Jaw J, Colonna M, Sun PS. Crystal structure of human natural cytotoxicity receptor NKp30 and identification of its ligand binding site. *Proc Natl Acad Sci U S A*.**2011**; 108(15), 6223-8.

King AE, Ackley MA, Cass CE, Young JD, Baldwin SA. Nucleoside transporters: from scavengers to novel therapeutic targets. *Trends Pharmacol Sci*. **2006**;27(8):416-25.p

Kong W, Engel K, Wang J. Mammalian nucleoside transporters. *Curr Drug Metab*. **2004**;5(1):63-84.

Kuma A, Hatano M, Matsui M, Yamamoto A, Nakaya H, Yoshimori T, Ohsumi Y, Tokuhisa T, Mizushima N. The role of autophagy during the early neonatal starvation period. *Nature*. **2004**;432(7020):1032-6.

Laezza C, Migliaro A, Cerbone R, Tedesco I, Santillo M, Garbi C, Bifulco M. N6-isopentenyladenosine affects cAMP-dependent microfilament organization in FRTL-5 thyroid cells. *Exp Cell Res*. **1997**;234(1):178-82.

Laezza C, Notarnicola M, Caruso MG, Messa C, Macchia M, Bertini S, Minutolo F, Portella G, Fiorentino L, Stingo S, Bifulco M. N6-isopentenyladenosine arrests tumor cell proliferation by inhibiting farnesyl

diphosphate synthase and protein prenylation. *FASEB J.* **2006**;20(3):412-8.

Laezza C, Fiorentino L, Pisanti S, Gazzerro P, Caraglia M, Portella G, Vitale M, Bifulco M. Lovastatin induces apoptosis of k-ras-transformed thyroid cells via inhibition of ras farnesylation and by modulating redox state. *J Mol Med (Berl).* **2008**;86(12):1341-51.

Laezza C, Caruso MG, Gentile T, Notarnicola M, Malfitano AM, Di Matola T, Messa C, Gazzerro P, Bifulco M. N6-isopentenyladenosine inhibits cell proliferation and induces apoptosis in a human colon cancer cell line DLD1. *Int J Cancer*. **2009**;124(6):1322-9.

Lai CB, Mager DL. Role of runt-related transcription factor 3 (RUNX3) in transcription regulation of natural cytotoxicity receptor 1 (NCR1/NKp46), an activating natural killer (NK) cell receptor. *J Biol Chem*. **2012**; 287(10):7324-34.

Landman GW, Kleefstra N, van Hateren KJ, Groenier KH, Gans RO, Bilo HJ. Metformin associated with lower cancer mortality in type 2 diabetes: ZODIAC-16. *Diabetes Care.* **2010**;33(2):322-6.

Lanier LL. NK cell recognition. *Annu Rev Immunol*. **2005**;23:225-74.

Laplante M, Sabatini DM. mTOR signaling in growth control and disease. *Cell*. **2012**;149(2):274-93.

Laten HM, Zahareas-Doktor S. Presence and source of free isopentenyladenosine in yeasts. *Proc Natl Acad Sci U S A*. **1985**;82(4):1113-5.

Lavergne E, Combadière C, Iga M, Boissonnas A, Bonduelle O, Maho M, Debré P, Combadiere B. Intratumoral CC chemokine ligand 5 overexpression delays tumor growth and increases tumor cell infiltration. *J Immunol*.**2004**; 173(6), 3755-3762.

Lee CW, Wong LL, Tse EY, Liu HF, Leong VY, Lee JM, Hardie DG, Ng IO, Ching YP. AMPK promotes p53 acetylation via phosphorylation and inactivation of SIRT1 in liver cancer cells. *Cancer Res*. **2012**;72(17):4394-404.

Lee DH, Lee TH, Jung CH, Kim YH. Wogonin induces apoptosis by activating the AMPK and p53 signaling pathways in human glioblastoma cells. *Cell Signal*. **2012**;24(11):2216-25.

Lee SH, Yun S, Lee J, Kim MJ, Piao ZH, Jeong M, Chung JW, Kim TD, Yoon SR, Greenberg PD, Choi I. RasGRP1 is required for human NK cell function. *J Immunol.* **2009**; 183(12), 7931-7938.

Levine B, Yuan J. Autophagy in cell death: an innocent convict? *J Clin Invest*. **2005**; 115:2679–2688.

Li C, Ge B, Nicotra M, Stern JN, Kopcow HD, Chen X, Strominger JL. JNK MAP kinase activation is required for MTOC and granule polarization in NKG2D-mediated NK cell cytotoxicity. *Proc Natl Acad Sci U S A.* **2008**; 105(8), 3017–3022.

Li J, Herold MJ, Kimmel B, Müller I, Rincon-Orozco B, Kunzmann V, Herrmann T. Reduced expression of the mevalonate pathway enzyme farnesyl pyrophosphate synthase unveils recognition of tumor cells by Vgamma9Vdelta2 T cells. *J Immunol*. **2009**;182(12):8118-24.

Liang J, Shao SH, Xu ZX, Hennessy B, Ding Z, Larrea M, Kondo S, Dumont DJ, Gutterman JU, Walker CL, Slingerland JM, Mills GB. The energy sensing LKB1-AMPK pathway regulates p27(kip1) phosphorylation mediating the decision to enter autophagy or apoptosis. *Nat Cell Biol*. **2007**;9(2):218-24.

Lin JX, Li P, Liu D, Jin HT, He J, Ata Ur Rasheed M, Rochman Wang L, Cui K, Liu C, Kelsall BL, Ahmed A, Leonard WJ. Critical Role of STAT5 transcription factor tetramerization for cytokine responses and normal immune function. *Immunity.* **2012**; 36(4), 586-599.

Liu B, Cheng Y, Zhang B, Bian HJ, Bao JK. Polygonatum cyrtonema lectin induces apoptosis and autophagy in human melanoma A375 cells through a mitochondria-mediated ROS-p38-p53 pathway. *Cancer Lett*. **2009**;275(1):54-60.

Liu JL, Mao Z, Gallick GE, Yung WK. AMPK/TSC2/mTOR-signaling intermediates are not necessary for LKB1-mediated nuclear retention of PTEN tumor suppressor. *Neuro Oncol.* **2011**;13(2):184-94.

Liu YQ, Cheng X, Guo LX, Mao C, Chen YJ, Liu HX, Xiao QC, Jiang S, Yao ZJ, Zhou GB. Identification of an annonaceous acetogenin mimetic, AA005, as an AMPK activator and autophagy inducer in colon cancer cells. *PLoS One*. **2012**;7(10):e47049.

Lokshin A, Raskovalova T, Huang X, Zacharia LC, Jackson EK, Gorelik E. Adenosine-mediated inhibition of the cytotoxic activity and cytokine production by activated natural killer cells. *Cancer Res*. **2006**; 66(15), 7758-7765.

Luci C, Reynders A, Ivanov II, Cognet C, Chiche L, Chasson L, Hardwigsen J, Anguiano E, Banchereau J, Chaussabel D, Dalod M, Littman DR, Vivier E, Tomasello E. Influence of the transcription factor RORgammat on the development of NKp46+ cell populations in gut and skin. *Nat Immunol*. **2009**;10(1):75-82.

Maiuri MC, Zalckvar E, Kimchi A, Kroemer G. Self-eating and self-killing: crosstalk between autophagy and apoptosis. *Nat Rev Mol Cell Biol*. **2007**; 8: 741–752.

Makanya AN, Hlushchuk R, Djonov VG. Intussusceptive angiogenesis and its role in vascular morphogenesis, patterning, and remodeling. *Angiogenesis.* **2009**;12(2):113-23.

Malorni W, Quaranta MG, Straface E, Falzano L, Fabbri A, Viora M, Fiorentini C. The Rac-activating toxin cytotoxic necrotizing factor 1 oversees NK cell-mediated activity by regulating the actin/microtubule interplay. *J Immunol*. **2003**; 171(8), 4195-4202.

Maniar A, Zhang X, Lin W, Gastman BR, Pauza CD, Strome SE, Chapoval AI. Human gammadelta T lymphocytes induce robust NK cell-mediated antitumor cytotoxicity through CD137 engagement. *Blood*. **2010**; 116(10),1726-33.

Mazeron R, Azria D, Deutsch E. Angiogenesis inhibitors and radiation therapy: from biology to clinical practice. *Cancer Radiother*. **2009**;13(6-7):568-73.

Meisel H, Günther S, Martin D, Schlimme E. Apoptosis induced by modified ribonucleosides in human cell culture systems. *FEBS Lett*. **1998**;433(3):265-8.

Meisse D, Van de Casteele M, Beauloye C, Hainault I, Kefas BA, Rider MH, Foufelle F, Hue L. Sustained activation of AMP-activated protein kinase induces c-Jun N-terminal kinase activation and apoptosis in liver cells. *FEBS Lett*. **2002**;526(1-3):38-42.

Meley D, Bauvy C, Houben-Weerts JH, Dubbelhuis PF, Helmond MT, Codogno P, Meijer AJ. AMP-activated protein kinase and the regulation of autophagic proteolysis. *J Biol Chem*. **2006**;281(46):34870-9.

Merighi S, Benini A, Mirandola P, Gessi S, Varani K, Leung E, Maclennan S, Borea PA. A3 adenosine receptor activation inhibits cell proliferation via phosphatidylinositol 3-kinase/Akt-dependent inhibition of the extracellular signal-regulated kinase 1/2 phosphorylation in A375 human melanoma cells. *J Biol Chem.* **2005**;280(20):19516-26.

Mittelman A, Evans JT, Chheda GB. Cytokinins as chemotherapeutic agents. *Ann NY Acad Sci.* **1975**;255:225-34.

Mok DW, Mok MC. CYTOKININ METABOLISM AND ACTION. *Annu Rev Plant Physiol Plant Mol Biol*. **2001**;52:89-118.

Mor A., Philips MR.. Compartmentalized Ras/MAPK signaling. *Annu Rev Immunol*. **2006**; 24, 771-800.

Moretta A, Bottino C, Vitale M, Pende D, Cantoni C, Mingari MC, Biassoni R, Moretta, L. Activating receptors and co-receptors involved in human natural killer cell-mediated cytolysis. *Annu Rev Immunol*. **2001**; 19, 197-223.

Morrow VA, Foufelle F, Connell JM, Petrie JR, Gould GW, Salt IP. Direct activation of AMP-activated protein kinase stimulates nitric-oxide synthesis in human aortic endothelial cells. *J Biol Chem*. **2003**;278(34):31629-39.

Moustafa ME, Carlson BA, El-Saadani MA, Kryukov GV, Sun QA, Harney JW, Hill KE, Combs GF, Feigenbaum L, Mansur DB, Burk RF, Berry MJ, Diamond AM, Lee BJ, Gladyshev VN, Hatfield DL. Selective inhibition of selenocysteine tRNA maturation and selenoprotein synthesis in transgenic mice expressing isopentenyladenosine-deficient selenocysteine tRNA. *Mol Cell Biol.* **2001**;21(11):3840-52.

Nagata D, Mogi M, Walsh K. AMP-activated protein kinase (AMPK) signaling in endothelial cells is essential for angiogenesis in response to hypoxic stress. *J Biol Chem*. **2003**;278(33):31000-6.

Nussbaumer O, Gruenbacher G, Gander H, Thurnher M. DC-like cell-dependent activation of human natural killer cells by the bisphosphonate zoledronic acid is regulated by γδ T lymphocytes. *Blood*. **2011**;118(10):2743-51.

Oka A. New insights into cytokinins. *J Plant Res*. **2003**;116(3):217-20.

Orange JS, Ramesh N, Remold-O'Donnell E, Sasahara Y, Koopman L, Byrne M, Bonilla FA, Rosen FS, Geha RS, Strominger JL. Wiskott-Aldrich syndrome protein is required for NK cell cytotoxicity and colocalizes with actin to NK cellactivating immunologic synapses. *Proc Natl Acad Sci U S A*. **2002**; 99(17), 11351-11356.

Ottria R, Casati S, Baldoli E, Maier JA, Ciuffreda P. N^6-Alkyladenosines: Synthesis and evaluation of in vitro anticancer activity. *Bioorg Med Chem.* **2010**;18(23):8396-402.

Persson BC, Esberg B, Olafsson O, Björk GR. Synthesis and function of isopentenyl adenosine derivatives in tRNA. Biochimie. **1994**;76(12):1152-60.

Peyton KJ, Liu XM, Yu Y, Yates B, Durante W. Activation of AMP-activated protein kinase inhibits the proliferation of human endothelial cells. *J Pharmacol Exp Ther*. **2012**;342(3):827-34.

Picardi P, Pisanti S, Ciaglia E, Margarucci L, Ronca R, Giacomini A, Malfitano AM, Casapullo A, Laezza C, Gazzerro P, Bifulco M. Antiangiogenic effects of N6-isopentenyladenosine, an endogenous isoprenoid end product, mediated by AMPK activation. *FASEB J*. **2013** Nov 21. [Epub ahead of print] PubMed PMID: 24265487.

Potente M, Gerhardt H, Carmeliet P. Basic and therapeutic aspects of angiogenesis. *Cell.* **2011**;146(6):873-87.

Pujari R, Nagre NN, Chachadi VB, Inamdar SR, Swamy BM, Shastry P. Rhizoctonia bataticola lectin (RBL) induces mitogenesis and cytokine production in human PBMC via p38 MAPK and STAT-5 signaling pathways. *Biochim Biophys Acta*. **2010**; 1800(12), 1268-1275.

Qing G, Simon MC. Hypoxia inducible factor-2alpha: a critical mediator of aggressive tumor phenotypes. *Curr Opin Genet Dev***. 2009**;19(1):60-6.

Raemer PC, Kohl K, Watzl C. Statins inhibit NK-cell cytotoxicity by interfering with LFA-1-mediated conjugate formation. *Eur J Immunol*. **2009**; 39(6), 1456-65.

Rahimi N. The ubiquitin-proteasome system meets angiogenesis. *Mol Cancer Ther*. **2012**;11(3):538-48.

Rami A. Review: autophagy in neurodegeneration: firefighter and/or incendiarist? *Neuropathol Appl Neurobiol.* **2009**;35(5):449-61.

Ramirez K, Chandler KJ, Spaulding C, Zandi S, Sigvardsson M, Graves

BJ, Kee BL. Gene deregulation and chronic activation in natural killer cells deficient in the transcription factor ETS1. *Immunity*. **2012**; 36(6):921-32.

Reihill JA, Ewart MA, Salt IP. The role of AMP-activated protein kinase in the functional effects of vascular endothelial growth factor-A and -B in human aortic endothelial cells. *Vasc Cell*. **2011**;3:9.

Reynolds LP, Grazul-Bilska AT, Redmer DA. Angiogenesis in the corpus luteum. *Endocrine.* **2000**;12(1):1-9.

Rodriguez-Enriquez S, He L, Lemasters JJ. Role of mitochondrial permeability transition pores in mitochondrial autophagy. *Int J Biochem Cell Biol*. **2004**;36(12):2463-72.

Rosenfeldt MT, Ryan KM. The multiple roles of autophagy in cancer. *Carcinogenesis.* **2011**; 32:955–963.

Salazar M, Carracedo A, Salanueva IJ, Hernández-Tiedra S, Lorente M, Egia A, Vázquez P, Blázquez C, Torres S, García S, Nowak J, Fimia GM, Piacentini M, Cecconi F, Pandolfi PP, González-Feria L, Iovanna JL, Guzmán M, Boya P, Velasco G. Cannabinoid action induces autophagy-mediated cell death through stimulation of ER stress in human glioma cells. *J Clin Invest*. **2009**;119(5):1359-72.

Sanli T, Steinberg GR, Singh G, Tsakiridis T. AMP-activated protein kinase (AMPK) beyond metabolism: A novel genomic stress sensor participating in the DNA damage response pathway. *Cancer Biol Ther*. **2013**;15(2).

Sato K, Tsuchihara K, Fujii S, Sugiyama M, Goya T, Atomi Y, Ueno T, Ochiai A, Esumi H. Autophagy is activated in colorectal cancer cells and contributes to the tolerance to nutrient deprivation. *Cancer Res*. **2007**;67(20):9677-84

Sinclair CJ, Powell AE, Xiong W, LaRivière CG, Baldwin SA, Cass CE, Young JD, Parkinson FE. Nucleoside transporter subtype expression: effects on potency of adenosine kinase inhibitors. *Br J Pharmacol*.

2001;134(5):1037-44.

Skoog F, Strong FM, Miller CO. Cytokinins. *Science*. **1965**;148(3669):532-3.

Spanholtz J, Tordoir M, Eissens D, Preijers F, van der Meer A, Joosten I, Schaap N, de Witte TM, Dolstra H. High log-scale expansion of functional human natural killer cells from umbilical cord blood CD34-positive cells for adoptive cancer immunotherapy. *PLoS One*. **2010**;5(2):e9221.

Spinola M, Galvan A, Pignatiello C, Conti B, Pastorino U, Nicander B, Paroni R, Dragani TA. Identification and functional characterization of the candidate tumor suppressor gene TRIT1 in human lung cancer. *Oncogene*. **2005**;24(35):5502-9.

Spinola M, Colombo F, Falvella FS, Dragani TA. N6-isopentenyladenosine: a potential therapeutic agent for a variety of epithelial cancers. *Int J Cancer*. **2007**;120(12):2744-8.

Stahmann N, Woods A, Spengler K, Heslegrave A, Bauer R, Krause S, Viollet B, Carling D, Heller R. Activation of AMP-activated protein kinase by vascular endothelial growth factor mediates endothelial angiogenesis independently of nitric-oxide synthase. *J Biol Chem*. **2010**;285(14):10638-52.

Strid J, Roberts SJ, Filler RB, Lewis JM, Kwong BY, Schpero W, Kaplan DH, Hayday AC, Girardi M. Acute upregulation of an NKG2D ligand promotes rapid reorganization of a local immune compartment with pleiotropic effects on carcinogenesis. *Nat Immunol.* **2008**;9(2):146-54.

Suk D, Simpson CL, Mihich E. Toxicological and antiproliferative effects of N6-(delta2-isopentenyl) adenosine, a natural component of mammalian transfer RNA. *Cancer Res*. **1970**;30(5):1429-36.

Swift MR, Weinstein BM. Arterial-venous specification during

development. *Circ Res*. **2009**;104(5):576-88.

Taguchi Y, Kondo T, Watanabe M, Miyaji M, Umehara H, Kozutsumi Y, Okazaki T. Interleukin-2–induced survival of natural killer (NK) cells involving phosphatidylinositol-3 kinase–dependent reduction of ceramide through acid sphingomyelinase, sphingomyelin synthase, and glucosylceramide synthase. *Blood*. **2004**; 104(10), 3285-3293.

Thapa M, Welner RS, Pelayo R, Carr DJ. CXCL9 and CXCL10 expression are critical for control of genital herpes simplex virus type 2 infection through mobilization of HSV-specific CTL and NK cells to the nervous system. *J Immunol.* **2008**; 180(2), 1098-1106.

Theodoropoulou S, Brodowska K, Kayama M, Morizane Y, Miller JW, Gragoudas ES, Vavvas DG. Aminoimidazole carboxamide ribonucleotide (AICAR) inhibits the growth of retinoblastoma in vivo by decreasing angiogenesis and inducing apoptosis. *PLoS One*. **2013**;8(1):e52852.

Theodoropoulou S, Kolovou PE, Morizane Y, Kayama M, Nicolaou F, Miller JW, Gragoudas E, Ksander BR, Vavvas DG. Retinoblastoma cells are inhibited by aminoimidazole carboxamide ribonucleotide (AICAR) partially through activation ofAMP-dependent kinase. *FASEB J*. **2010**;24(8):2620-30.

Thurnher M, Nussbaumer O, Gruenbacher G. Novel aspects of mevalonate pathway inhibitors as antitumor agents. *Clin Cancer Res*. **2012**; 18(13), 3524-3531.

Tomic T, Botton T, Cerezo M, Robert G, Luciano F, Puissant A, Gounon P, Allegra M, Bertolotto C, Bereder JM, Tartare-Deckert S, Bahadoran P, Auberger P, Ballotti R, Rocchi S. Metformin inhibits melanoma development through autophagy and apoptosis mechanisms. *Cell Death Dis*. **2011**;2:e199.

Tsao H, Atkins MB, Sober AJ. Management of cutaneous melanoma. *N Engl J Med*. **2004**;351(10):998-1012. Review. Erratum in: *N Engl J Med*. **2004**;351(23):2461.

Vakana E, Altman JK, Glaser H, Donato NJ, Platanias LC. Antileukemic effects of AMPK activators on BCR-ABL-expressing cells. *Blood*. **2011**;118(24):6399-402.

Vara D, Salazar M, Olea-Herrero N, Guzmán M, Velasco G, Díaz-Laviada I. Anti-tumoral action of cannabinoids on hepatocellular carcinoma: role of AMPK-dependent activation of autophagy. *Cell Death Differ*. **2011**;18(7):1099-111. Erratum in: *Cell Death Differ*. **2011**;18(7):1237.

Vivier E, Nunès JA, Vély F. Natural killer cell signaling pathways. *Science*. **2004**;306(5701):1517-9.

Vivier E, Tomasello E, Baratin M, Walzer T, Ugolini S. Functions of natural killer cells. *Nat Immunol.* **2008**;9(5):503-10.

Vold BS, Keith Jr DE, Slavik M. Urine levels of N-[9-(beta-Dribofuranosyl) purin-6-ylcarbamoyl]-L-threonine, N6-(delta 2-isopentenyl)adenosine, and 2'- O-methylguanosine as determined by radioimmunoassay for normal subjects and cancer patients. *Cancer Res*. **1982**; 42(12), 5265-5269.

Wang Q, Liang B, Shirwany NA, Zou MH. 2-Deoxy-D-glucose treatment of endothelial cells induces autophagy by reactive oxygen species-mediated activation of the AMP-activated protein kinase. *PLoS One*. **2011**;6(2):e17234.

Wang C, Lin W, Playa H, Sun S, Cameron K, Buolamwini JK. Dipyridamole analogs as pharmacological inhibitors of equilibrative nucleoside transporters. Identification of novel potent and selective inhibitors of the adenosine transporter function of human equilibrative nucleoside transporter 4 (hENT4). *Biochem Pharmacol.* **2013**;86(11):1531-40.

Wang Y, Qin ZH. Coordination of autophagy with other cellular activities. *Acta Pharmacol Sin*. **2013**;34(5):585-94.

Warner GJ, Berry MJ, Moustafa ME, Carlson BA, Hatfield DL, Faust JR. Inhibition of selenoprotein synthesis by selenocysteine tRNA[Ser]Sec

lacking isopentenyladenosine. J *Biol Chem*. **2000**;275(36):28110-9.

Woodard J, Platanias LC. AMP-activated kinase (AMPK)-generated signals in malignant melanoma cell growth and survival. *Biochem Biophys Res Commun*. **2010**;398(1):135-9.

Xu ZX, Liang J, Haridas V, Gaikwad A, Connolly FP, Mills GB, Gutterman JU. A plant triterpenoid, avicin D, induces autophagy by activation of AMP-activated protein kinase. *Cell Death Differ*. **2007**;14(11):1948-57.

Yang Z, Klionsky DJ. Eaten alive: a history of macroautophagy. *Nat Cell Biol*. **2010**;12(9):814-22.

Yu T, Caudell EG, Smid C, Grimm EA. IL-2 activation of NK cells: involvement of MKK1/2/ERK but not p38 kinase pathway. *J Immunol.* **2000**; 164(12), 6244-6251.

Yung MM, Chan DW, Liu VW, Yao KM, Ngan HY. Activation of AMPK inhibits cervical cancer cell growth through AKT/FOXO3a/FOXM1 signaling cascade. *BMC Cancer*. **2013**;13:327.

Zaki KA, Basu B, Corrie P. The role of angiogenesis inhibitors in the management of melanoma. *Curr Top Med Chem*. **2012**;12(1):32-49.

Zhang L, Jing H, Cui L, Li H, Zhou B, Zhou G, Dai F. 3,4-Dimethoxystilbene, a resveratrol derivative with anti-angiogenic effect, induces both macroautophagy and apoptosis in endothelial cells. *J Cell Biochem*. **2013**;114(3):697-707.

Zhang XD, Wang Y, Wu JC, Lin F, Han R, Han F, Fukunaga K, Qin ZH. Down-regulation of Bcl-2 enhances autophagy activation and cell death induced by mitochondrial dysfunction in rat striatum. *J Neurosci Res.* **2009**;87(16):3600-10.

Zhou G, Myers R, Li Y, Chen Y, Shen X, Fenyk-Melody J, Wu M, Ventre

J, Doebber T, Fujii N, Musi N, Hirshman MF, Goodyear LJ, Moller DE. Role of AMP-activated protein kinase in mechanism of metformin action. *J Clin Invest*. **2001**;108(8):1167-74.

Zou MH, Wu Y. AMP-activated protein kinase activation as a strategy for protecting vascular endothelial function. *Clin Exp Pharmacol Physiol*. **2008**;35(5-6):535-45.

8. ACKNOWLEDGEMENTS

A research project like this is never the work of someone alone. The contribution of many different people, in several ways, have made this possible.

First of all, I would like to express my deepest gratitude and appreciation to Professor Maurizio Bifulco. His enthusiasm and support have been essential for this experience. I am greatly indebted to him as he gave me the opportunity to realize my dream: to sow a little seed in the field of cancer research.

I am very grateful to Dr Simona Pisanti, my mentor, for her support and her friendship during all these years. She has always believed in me more than I did.

A deep thanks goes to Dr Elena Ciaglia for her generosity and encouragement. She was particularly kind allowing me to enforce the last part of this thesis using the data of her own work.

I would like to thank my supervisor, Dr Patrizia Gazzerro: she toughened up my character and she tested my ambitions.

Thanks to Dr Maria Chiara Proto, Dr Antonio Pagano Zottola and Dr Donatella Fiore: thank you for sharing the everyday life of the laboratory. Also thanks to Dr Chiara Laezza, Dr Anna Maria Malfitano and Dr Alba D'Alessandro for making me feel part of the group.

A special thanks to the students Annapia Lodato, Dr Angela Pastore and Dr Angelica Agizza who helped me in the experimental part of this doctorate project.

A beloved thought to Dr Lucia Prota for her kindness, friendship and support: we have shared some of the most important experiences and the distance does not make less intense our feeling.

It would not have been possible to reach this milestone without the help and the support of lovely people around me. So above all, a warm thank to my family..anywhere and my special "number 13" for their personal support, love and great patience, to whom all my words will never suffice to express how grateful I am.